JOURNAL ON

COMMUNICATIONS

VOLUME XLVII MARCH 1996

ATM NETWORKS II.

REGULAR PAPERS

JOURNAL ON COMMUNICATIONS

A PUBLICATION OF THE SCIENTIFIC SOCIETY FOR TELECOMMUNICATIONS, HUNGARY

Editorial office
Budapest XIV. Ungvár u. 64-66.
H-1525 Budapest, P.O. Box 15.
Phone: (361) 251-1163, (361) 201-7471
Fax: (361) 251-9878, (361) 201-7471

Subscription rates
Hungarian subscribers
1 year, 12 issues 5300 HUF, single copies 650 HUF
Hungarian individual subscribers
1 year, 12 issues 860 HUF, single copies 110 HUF
Foreign subscribers
12 issues 150 USD, 6 English issues 90 USD, single copies 24 USD
Transfer should be made to the Hungarian Foreign Trade Bank, Budapest, H-1821, A/C No. MKKB 203-21411

JOURNAL ON COMMUNICATIONS is published monthly, alternately in English and Hungarian by TYPOTEX Ltd. H-1015 Bp. Retek u. 33-35. Phone/Fax: (361) 115-1759. Publisher: Zsuzsa Votisky. Type-setting by TYPOTEX Ltd. Printed by Dabasi Jegyzetnyomda, Dabas, Hungary HUISSN 0866-5583

DIMENSIONING FOR BETTER PERFORMANCE

FAIRNESS AND REVENUE OPTIMIZATION IN MULTI-RATE LOSS NETWORKS*

L. AST, T. CINKLER, V. T. HAI, G. FODOR
DEPAPRTMENT OF TELECOMMUNICATIONS AND TELEMATICS
TECHNICAL UNIVERSITY OF BUDAPEST
H-111 BUDAPEST, SZTOCZEK U. 2, HUNGARY
{ast,cinkler,hai,fodor}@TTT-ATM.TTT.BME.HU

S. BLAABJERG
INSTITUTE OF TELECOMMUNICATIONS
TECHNICAL UNIVERSITY OF DENMARK
DK-2800 LYNGBY, DENMARK
E-MAIL: SBB@IT.DTU.DK

This paper presents an optimization model in which the revenue or carried traffic in a multi-rate loss network is maximized taking into account an important grade of service (GOS) parameter: the call blocking probability on different levels. With these investigations we can study the achieved fairness in a network and its relation to the optimal load sharing parameters and/or the optimal partitioning between bandwidth classes. We also study some mechanisms to improve fairness, and their impact on the realized revenue.

1. INTRODUCTION

Optimization of revenue in traditional telephone networks has a long tradition and a number of significant theoretical results exist [5], [9], making the optimization of even very large networks quite feasible. However, even in these cases it is not straightforward how to treat GOS constraints.

The situation is definitely more complex in heterogeneous broadband networks based on e.g. ATM. Even adopting the assumption that on call scale the ATM network can be modeled as a multi-rate circuit switched network (see e.g. [3]) difficult questions arise like e.g. how much partitioning/sharing between bandwidth classes should be allowed, whether trunk reservation should be used either to level out blocking probabilities or to make alternative routing stable, or both.

Fairness is also a considerably more complicated question in a heterogeneous environment, since even on the same route or link different classes will encounter different blocking probabilities. Therefore, we also have to consider how to define and ensure fairness in this case. Concerning the definition, [3] gives an overview of different possibilities on the link level and presents some ideas concerning the network level.

Fairness is an important issue, since

- on a highly loaded link the throughput of the traffic stream(s) with higher bandwidth demands are reduced (described e.g. in [3]);
- calls offered to an O-D pair in which the distance[1] between the originating and destinating node is big will in general suffer a larger blocking probability than calls offered to an O-D pair where the distance is short.

Beyond the theoretical possibilities it is also important to investigate what we can implement to dimension networks in practice featuring certain resource sharing techniques and fulfilling the requirements of a specific fairness concept. It is also clear that the fairness formulation will influence the success of different resource sharing methods.

In order to solve these questions in a satisfactory way, the study of network optimization models and a large number of numerical experiments are needed.

This paper tries to give a study of a well defined optimization model and the emerging fairness problems. Of course, our scope has limits, such as only call-level modeling, assuming given and fixed physical topology and routes, considering fixed routing and applying only some representatives of the resource sharing possibilities. Nevertheless, due to the complexity of the problem, these initial steps are necessary.

* This work has been supported by Ellemtel Telecommunications System Laboratories and TeleDenmark.

[1] The distance is defined as the number of hops of a shortest path connecting the originating and destinating node.

In Section 2. the optimization model is presented.

In Section 3. some fairness formulations are presented in line with their possible integration in the optimization process.

Finally, in Section 4. we present numerical results which

- investigate fairness in case of complete sharing, complete partitioning and a special kind of trunk reservation;
- compare the effect of different fairness constraints on the optimization process implementing them either in a direct or in an indirect way.

2. OPTIMIZATION MODEL

In this Section we present the applied mathematical network model as well as a brief description of the algorithm utilized to solve the optimization problem.

2.1. Notation and Mathematical Formulation

Consider a fixed physical network with N nodes[2] and K trunk groups (physical links). On top of this physical network a number of (in most cases only one) logical networks are to be carried. The topology of a logical network can in general differ from the topology of the physical network and a logical link may use more than one trunk group. The total number of logical links over all logical networks is denoted by J, and the capacity of logical link j is denoted by C_j.

The incidence of physical and logical links is expressed by a $K \times J$ zero-one incidence matrix $\mathbf{S}$ in which the entries are given by

$$s_{k,j} = \begin{cases} 1 & \text{if physical link } k \text{ is used by logical link } j \\ 0 & \text{otherwise} \end{cases} \quad (1)$$

The constraint that the sum of logical capacities C_j on a physical link cannot exceed the physical capacity is expressed in vector notation as:

$$\mathbf{S}\overrightarrow{C} \leq \overrightarrow{C}^{phy}, \quad (2)$$

where $\overrightarrow{C} = \{C_1, ..., C_J\}$ and $\overrightarrow{C}^{phy} = (C_1^{phy}, ..., C_K^{phy})$.

In order to distinguish calls of different bandwidth demands, I different traffic classes are assumed to be carried in the network. In what follows, v denotes logical networks, p denotes node pairs (origin-destination or O-D pairs) and m denotes traffic types.

A route r is a subset of the set of those logical links that belong to the same logical network. In principle, it can be taken as an arbitrary subset but in this paper they will be simple paths connecting O-D pairs. By convention, each route carries only calls of a single traffic class. That is, if several traffic classes are to be carried, they are represented by parallel routes.[3] The incidence of routes, links and traffic types is expressed by the indicator variables

$$A_{mjr} = \quad (3)$$

$$= \begin{cases} 1 & \text{when route } r \text{ uses link } j \text{ and carries traffic type } m \\ 0 & \text{otherwise} \end{cases}$$

[2] In the most general formulation no assumption on nodes is needed. It is only in order to be able to introduce O-D pairs and a set of allowed routes between O-D pairs later.

[3] This does not increase needlessly the complexity, since these parallel routes will have in general different characteristics at the optimal state.

A_{mjr} is *not* to be interpreted as the amount of bandwidth that route r requires on link j. For that purpose we use other variables: d_{mj} will denote the amount of bandwidth (capacity) that a call belonging to traffic type m requires on link j. By this notation we implicitly assume that all routes that carry a given traffic type m require the same amount of bandwidth on link j. Since the bandwidth requirement is associated with the traffic type, this is not seen as a restriction. On the other hand, we allow the bandwidth requirement of calls on a given route to vary along the links of the route. In fact, this is needed if the concept of effective or equivalent bandwidth [6] is adopted and the involved links have different capacities.

Let ν_r be the offered traffic to route r.

For a given virtual network v, node pair p and traffic class m let $\overrightarrow{s}^{(v,p,m)} = (s_{r_1}^{(v,p,m)}, s_{r_2}^{(v,p,m)}, \ldots)$ denote the *load sharing vector*. The components of $\overrightarrow{s}^{(v,p,m)}$ tell us in what proportion the load is distributed among the routes that carry traffic class m between the O-D pair p. Since the components of each load sharing vector represent the proportion in which the offered traffic is distributed to various routes they are non-negative and traditionally sum up to one, i.e.

$$\sum_{r \in R^{(v,p,m)}} s_r^{(v,p,m)} = 1 \text{ for all } v,\ p \text{ and } m\ . \tag{4}$$

However, we will see later it also makes sense to relax this equality, allowing a certain kind of loss of the offered traffic before it reaches the network.

As a natural choice for an objective function the total *network revenue* is used. According to this approach connections accepted on route r generate revenue at a rate w_r and the total expected network revenue is then

$$W(\overrightarrow{\nu}, \overrightarrow{C}) = \sum_r w_r \nu_r (1 - L_r) = \sum_r w_r \lambda_r\ , \tag{5}$$

where L_r is the end-to-end blocking probability for traffic on route r, and λ_r is the carried traffic on route r. Clearly, this route blocking probability is defined as the probability of the event that at least one link is blocked along the route.

In order to guarantee fairness (possibly through certain GOS constraints) we may have additional (nonlinear) constraints in the model.

To summarize we have the following optimization model

$$\max W(\overrightarrow{\nu}, \overrightarrow{C}) = \sum_r w_r \nu_r (1 - L_r) \tag{6}$$

over $(\overrightarrow{\nu}, \overrightarrow{C})$ subject to (2), (4), and possible additional constraints to ensure fairness (see later). The number of variables is the sum of the number of logical capacities and routes.[4]

2.2. Solution Approach

The optimization model defined in (6) is difficult to solve for three reasons.

- The individual route blocking probabilities appearing in the objective function are difficult to compute.
- The dimension of the problem is in general high.
- The possible nonlinear constraints are difficult to deal with.

Concerning the first problem, so called *link decomposition methods* were utilized (see e.g. [5], specifically the *reduced load* approximation and *Whitt-like* approximations (see e.g. [11], [8], [4], [1]).

Whitt's approximation has an important property assuming homogeneous traffic conditions: it gives a (concave) lower bound of the revenue function, and upper bounds of route blocking probabilities (see [11] and [4]). Utilizing the latter fact *real* GOS guarantees can be given in this special case.

On the link level several multi-rate formulae could be chosen assuming *complete sharing* (see e.g. [3] and [2]).

Applying *complete partitioning* between traffic classes, the blocking probabilities are given by the classical Erlang B formula.

[4] Of course, the number of independent variables is less.

On link j within the logical network supporting traffic class m and supposing link offered traffic ρ_{mj}, the blocking probability will be $B_j = E(\frac{C_j}{d_{mj}}, \frac{\rho_{mj}}{d_{mj}})$ where $E(C, A)$ is the usual Erlang-B function.

At last, in case of *trunk reservation* for link blocking equalization e.g. [3] presents some formulae.

For the purpose of revenue optimization a software tool named CFSQP (which stands for C code for Feasible Sequential Quadratic Programming) was utilized. CFSQP was mainly chosen because of its generality. It can handle the optimization of a finite set of differentiable objective functions over a feasibility set defined by general nonlinear differentiable functions. We refer the interested readers to [10] for details.

3. FAIRNESS

We consider fairness on call level (in contrast to cell level), and assume a strategy to be fair if a call attempt (regardless of its parameters) has the same chance to be accepted as any other.

An "optimally" fair situation (where e.g. all O-D pairs encounter the same relative revenue loss regardless of their traffic class and length) may not be desirable, or even realizable.

Applicable control techniques will depend on the used resource sharing techniques and also on the specific fairness requirements to be fulfilled. Of course, these techniques are also of different computational complexity.

If we simply want to be fair on link level between different traffic classes, a specific kind of trunk reservation can be the optimal choice. It is well known (see e.g. [7]), that if d_M is the bandwidth demand of the traffic class requiring the largest bandwidth on a link, then all traffic classes will experience the same blocking probability on this link if trunk reservation is applied with a reservation parameter $t_r = d_M$. Of course, this technique does not guarantee upper bound on these link blocking probabilities, nor can it help O-D pairs of larger distance.

In order to ensure *explicit loss constraints* on any levels these have to be incorporated into the optimization model, increasing the complexity of the optimization. These can be called *direct methods*.

We could impose upper bound constraints on link blocking probabilities, for all traffic classes. It is theoretically simple, and of great practical importance since in a typical network there are much fewer links than routes yielding an optimization problem with fewer (nonlinear) constraints. Naturally, the disadvantage is that short routes are in a privileged position.

As a more fair, but generally more complex solution we can put constraints on end-to-end blocking probabilities on routes. However, in case of load sharing, it is even more reasonable for each traffic class to put constraints only on the aggregated traffic traversing the O-D pair.

The success of these methods also depends on the resource sharing techniques applied, as it will be demonstrated in the numerical part (Section 4.).

In case of partitioning a possible further simplification could be made by working only with virtual network blocking limits considering average carried traffic of logically separated subnetworks. However, this could lead to unfair situations considering individual O-D pairs.

Of course, other constraints (e.g. average blocking of different classes) can be constructed, as well, and a combination of direct and indirect methods could also be advantageous.

In this paper we will put the main emphasis on an additional indirect technique: the manipulation of revenue factors (w_r). This possibility has been described by Kelly [9]. If we set the revenue factor of one route (or one whole traffic class) to be higher, then its blocking probability will be reduced, comparing to other routes (or traffic classes) of the network when the optimization procedure has been applied.

In order to assess the applied methods well defined fairness measures are needed. to the previous considerations we could measure fairness e.g. between

1. *traffic classes:*

- on the link level;
- on the O-D pair level;
- on the subnetwork level.

2. *routes*
- of different length;
- of a traffic class.

All techniques that improve fairness generally reduce the revenue. Therefore, this value is also important to be measured.

Results and experiences will be discussed in details in the next session.

4. NUMERICAL RESULTS

The numerical activities are divided into three parts. In the first part a table is given presenting a comparison of complete sharing (CS), complete partitioning (CP) and trunk reservation for link blocking equalization (TR). In all cases load sharing has also been employed.

The second part investigates the performance of tuning the revenue parameters (w_r) to balance average bandwidth loss of traffic classes, while the third part studies constraining the end-to-end blocking probability of one specific O-D pair (Fig. 1, Fig. 2, Table 1, Table 2).

Two network topologies have been studied, a four-node fully connected network and a five-node ring, see the Appendix. (These are the same as in [1].)

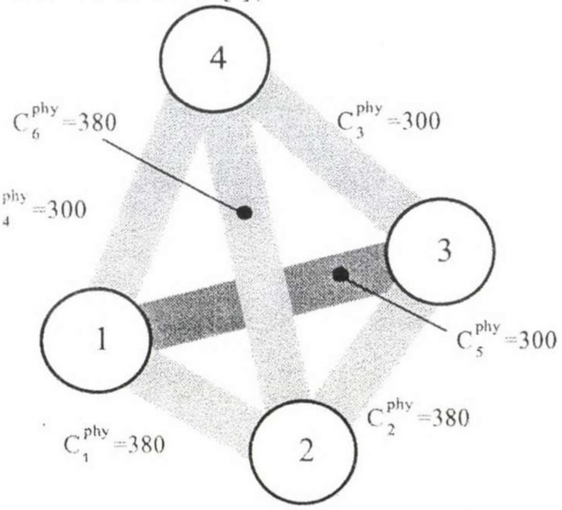

Fig. 1. The four node fully connected network

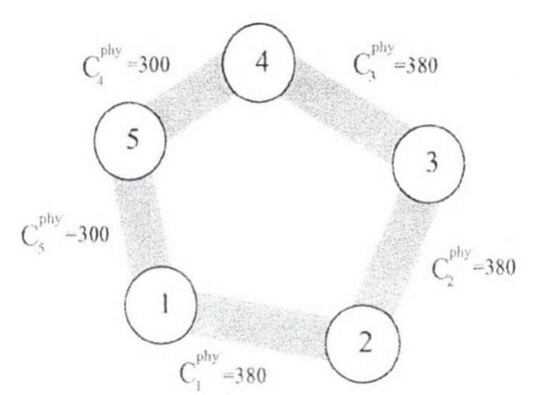

Fig. 2. The five node ring

In all cases there has been two bandwidth classes, a narrow-band class with bandwidth demand 1, and a wideband class with bandwidth demand 10. In case of complete partitioning O-D pairs of different classes are separated into logical networks.

Our traffic streams are symmetric in the sense that we have used all possible O-D pairs. For each O-D pair the two possible routes are utilized in the ring network and the (one-link) direct and the two possible two-link alternatives in the four-node fully connected network. Between these O-D pairs we have both a narrow and a wideband traffic demand.

Table 1. Offered traffic values of the four node network

O-D pair	offered load	
	class 1 (1)	class 2 (10)
1-2	200	20
1-3	75	7.5
1-4	80	8
2-3	180	18
2-4	70	7
3-4	90	9

Table 2. Offered traffic values of the five node network

O-D pair	offered load	
	class 1 (1)	class 2 (10)
1-2	85	8.5
1-3	70	7
1-4	30	3
1-5	25	2.5
2-3	65	6.5
2-4	40	4
2-5	40	4
3-4	35	3.5
3-5	25	2.5
4-5	30	3

However, beyond the topological symmetry neither the physical resources, nor the offered traffic values are completely symmetric in order to ensure nontrivial and reasonable solutions. By this we mean we have load/resource sharing at the (locally) optimal points without excessive blocking on any of the routes.

In the following it is assumed that revenues are always proportional to the bandwidth demands. It means that using unit revenue factors (according to the mentioned "normalization") the carried *bandwidth* of the network is maximized. Since it seems to be a natural objective, this choice of revenue factors is used, unless noted otherwise.

For complete details on the traffic offered between O-D pairs and capacities on links see the Appendix.

For speed reasons Whitt-like approximation was used with normal approximation on the link level [4]. The results were compared with a more refined evaluation of the revenue function at the end of the optimization phases using the reduced load approximation with the Kaufman-Roberts formula on the link level, and also with simulation. The error was less than 1 % even in the worst case, therefore it was justified to use the faster approximations in the optimization process. In case of trunk reservation the approximation given by Tran-Gia and Hübner [7] was utilized with the reduced load assumption.

Since in revenue optimization problems different local optima can be present ([9] and [1]), the best results were chosen given from several random starting points, unless noted otherwise. It is interesting to note that also the local optima were justified by simulation.

The first set of results are summarized in Table 3. The total offered bandwidth was 1390 in the four-node fully connected case and 890 working with the five-node ring. After the revenue (or carried bandwidth due to the special revenue factors) optimization some quantities of interest were evaluated.

The following observations can be made:
- Tolerating the larger blocking probabilities of classes with larger bandwidth requirements (i.e. unfairness) complete sharing gives the best performance (i.e. the maximal carried bandwidth).
- Applying trunk reservation to equalize blocking probabilities of all traffic classes on a link can make the resource allocation more fair. Comparing fairness of traffic classes this method happened to turn out to be almost ideal. However, it is

important to note that it is due to the fact that between every O-D pair we have both a narrow- and a wideband traffic stream with the same offered bandwidth. In a general case this policy can be considerably less fair.

- At last, separation caused notable performance penalty in both cases, but it is the most flexible method of the three investigated ones. (Since applying CP it is possible to realize almost arbitrary fairness ratios with a simple separation of e.g. traffic classes.) Considering fairness, in our examples partition is between the two others, but much closer to TR. With additional constraints it could be noticeably improved. (E.g. constraining the blocking probabilities of the wideband class calls.)

In the second set of numerical investigations tuning the revenue factors of routes that carry wideband traffic was performed and average bandwidth loss of the narrow- and the wideband traffic class was plotted together with the total carried bandwidth of 4 and 5 node networks (Figs. 3 and 4). Here the purpose was to see at which revenue factors the bandwidth losses of the traffic classes are equalized, since there are no closed form expressions in the general case to accomplish this task.

In case of CS this tuning is practically without effect (it also means even *direct* methods are unable to influence blocking probabilities), but we can reject some fraction of the incoming traffic before it is offered to the network and guarantee low blocking of the accepted part. As mentioned before, this possibility can be easily incorporated into our model allowing load sharing parameters not to sum up to one between O-D pairs. (It introduces a new fairness notion, as well, since we have to take into account fairness "outside" and "inside" the network.) In case of complete partitioning of the four-node network (Fig. 3) relaxation of the load sharing constraints did not make any difference.

Table 3. Comparison of CP, CS & TR

	4-node (offered bw = 1390)			5-node (offered bw = 890)		
	CS	CP	TR	CS	CP	TR
carried bw	1371.45	1349.95	1368.94	872.75	854.77	870.411
bw loss [%]	1.33	2.88	1.51	1.94	3.96	2.20
max class loss [%]	2.45	4.30	1.56	3.56	5.91	2.21
min class loss [%]	0.221	1.46	1.46	0.312	2.01	2.18
max/min	11.1	2.94	1.07	11.4	2.94	1.02
max O-D loss [%]	3.94	6.74	2.13	6.86	10.9	3.73
min O-D loss [%]	0.00456	0.111	0.0420	0.0114	0.223	0.133
max/min	862	60.7	50.8	605	48.9	28.2

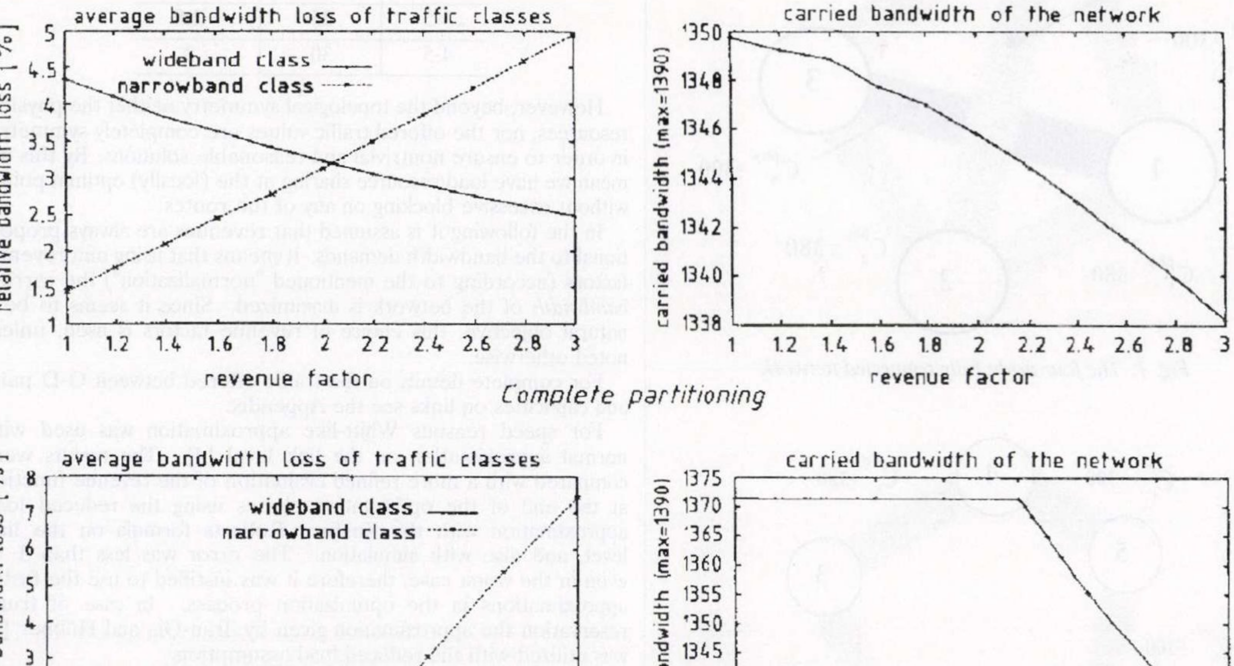

Complete partitioning

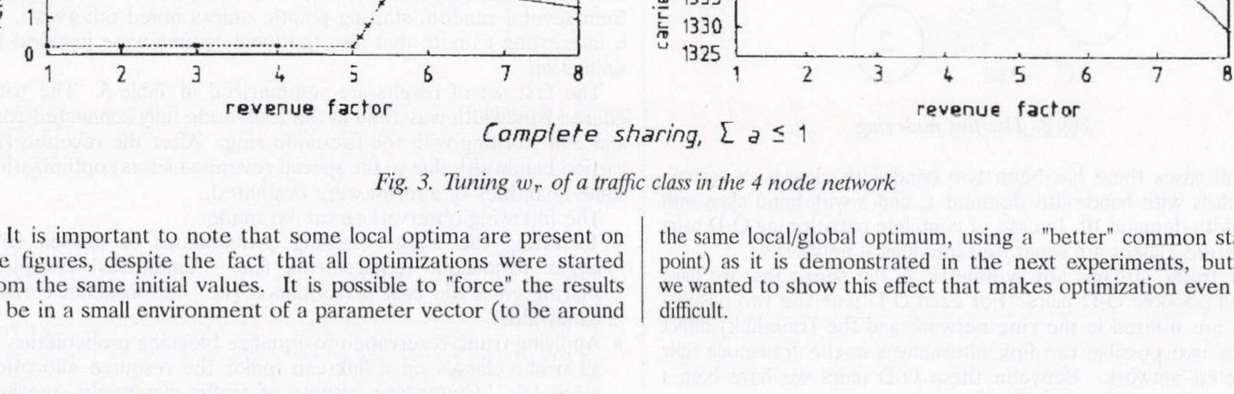

Complete sharing, $\sum a \leq 1$

Fig. 3. Tuning w_r of a traffic class in the 4 node network

It is important to note that some local optima are present on the figures, despite the fact that all optimizations were started from the same initial values. It is possible to "force" the results to be in a small environment of a parameter vector (to be around the same local/global optimum, using a "better" common starting point) as it is demonstrated in the next experiments, but here we wanted to show this effect that makes optimization even more difficult.

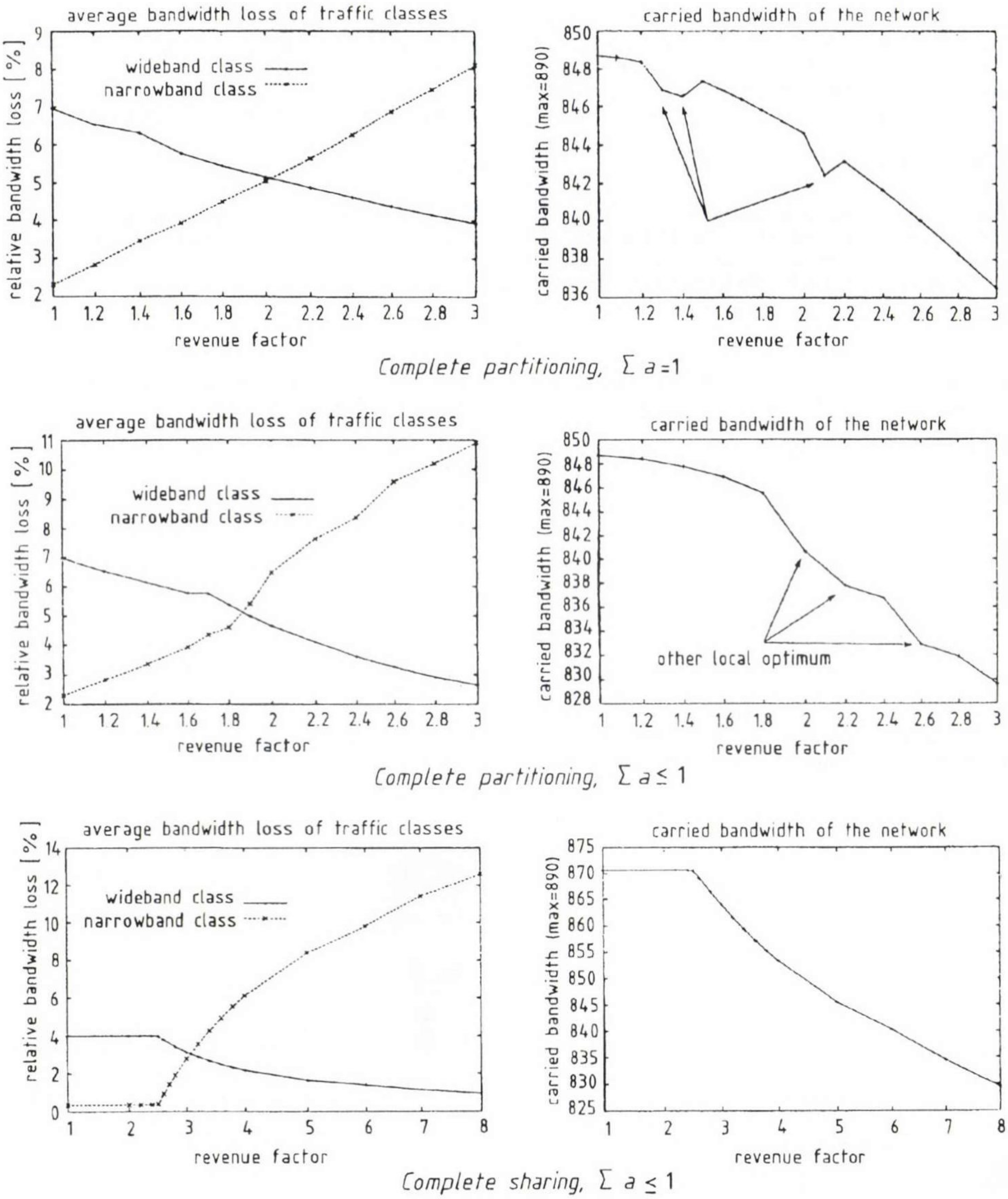

Fig. 4. Tuning w_r of a traffic class in the 5 node network

It is also noteworthy that the plots have somewhat different and slightly nonlinear shape and the "active" region of the revenue factors are also different. (Here the active region means the range where the plots are non-constant.) The revenue factors that were looked for are far from unity [5], and not equal in the examples. The solution depends on the traffic conditions (bandwidth demands, offered traffic values), the resource sharing policy and also on the load sharing constraint (equality or inequality).

5. CONCLUSION

In this paper we have presented an optimization model for multi-rate loss networks.

[5] Do not forget that the revenue factors are normalized, i.e. unit revenue factors correspond to the case when the carried traffic is multiplied by the bandwidth requirement of the class.

A comparison of three resource sharing policies was given demonstrating that the flexible method of complete partitioning is not necessarily the best solution if we simply want to increase fairness in a network.

In the second part it was shown that even though the different losses in a network are generally sensitive to the revenue coefficients w_r, adjusting these only gives an indirect way to obtain fairness in the network. Albeit this method does not increase the complexity of the solution it may be ineffective if the specific w_r values are not known in advance (it is the practical case), since some experimentation is needed to get the appropriate ones.

It was demonstrated that in some cases it is also necessary to make rejection of a fraction of the incoming traffic possible to realize fairness *within* the network.

In more complex cases with a set of GOS constraints it seems to be difficult to apply this indirect method; to accomplish the task treatment of explicit constraints may be necessary. However, due to its simplicity, this method can play a role in network optimization problems assuming e.g. simple and not too strict fairness requirements. Nevertheless, further investigations are needed to assess the value of revenue tuning for dimensioning purposes, and also to seek for possible analytic models that shed more light on the problem.

6. ACKNOWLEDGMENTS

The work has been done as part of the ATM research project between Ellemtel Telecommunication Laboratories, Sweden, and the High Speed Networks Laboratory at the Department of Telecommunications and Telematics, Technical University of Budapest. The authors are grateful to Miklos Boda and his colleagues for their support.

We also would like to thank A. L. Tits for allowing us to use the CFSQP optimization tool.

7. APPENDIX: NETWORKS INVESTIGATED IN THE NUMERICAL PART

Here we give some details about the physical capacities and offered traffic values used in the investigations (both expressed in relative units). The routes are selected according to rules mentioned in the text. After the traffic class identifiers (1 or 2) the corresponding bandwidth demands can be seen in parentheses (also in relative units).

REFERENCES

[1] L. Ast, S. Blaabjerg and T. Cinkler: Approximations for Revenue Optimization in Multi-Rate Loss Networks, to be presented at the *ITC Seminar* in St. Petersburg, 1995.

[2] S.-P. Chung and K. W. Ross: Reduced Load Approximations for Multirate Loss Networks, *ACM/IEEE Trans. on Networking*, 1993, pp. 1222-1231.

[3] Cost 242 Interim Report, M. Ritter and P. Tran-Gia (Ed.): Multi-Rate Models for Dimensioning and Performance Evaluation of ATM Networks, Commission of the European Communities, June 1994.

[4] A. Farago, S. Blaabjerg, L. Ast, G. Gordos and T. Henk: A New Degree of Freedom in ATM Network Dimensioning: Optimizing the Logical Configuration, to appear in *IEEE JSAC, Special Issue on "Advances in the Fundamentals of Networking"*.

[5] A. Girard: *Routing and Dimensioning of Circuit Switched Networks*, Addison-Wesley, 1990.

[6] R. Guérin, H. Ahmadi and M. Naghshineh: Equivalent Capacity and Its Application to Bandwidth Allocation in High Speed Networks, *IEEE JSAC*, September 1991.

[7] F. Hübner and P. Tran-Gia: "An Analysis of Multi-service systems with Trunk Reservation", Cost 242 TD(92) 019.

[8] F. P. Kelly: Blocking Probabilities in Large Circuit-Switched Networks, *Adv. Appl. Prob.*, Vol. 18, 1986, pp. 473-505.

[9] F. P. Kelly: Routing in Circuit-Switched Networks: Optimization, Shadow Prices and Decentralization, *Adv. Appl. Prob.*, Vol. 20, pp. 112-144, 1988.

[10] C. Lawrence, J. L. Zhou and A. L. Tits: "Users Guide for CFSQP version 2.2: A C Code for Solving (Large Scale) Constrained Nonlinear (Minimax) Optimization Problems, Generating Iterates Satisfying All Inequality Constraints", E.E. Department, Institute for System Research, University of Maryland, TR 94-16r1.

[11] W. Whitt: Blocking When Service Is Required From Several Facilities Simultaneously, *AT&T Technical Journal*, Vol. 64, No. 8, pp. 1807-1856, October 1985.

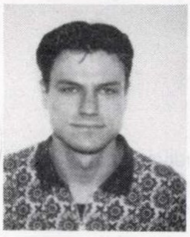

László Ast received the M.Sc. degree in electrical engineering from the Technical University of Budapest, in 1992. He is working toward the Ph.D. degree at the Department of Telecommunications and Telematics, Technical University of Budapest. There he participates in the work of the High-Speed Networks Laboratory. His main fields of interest are call-level modelling and dimensioning of ATM Networks.

Søren Blaabjerg received the M.Sc. degree in mathematics from Aarhus University in 1986. He was first with Electromagnetics Institute, Technical University of Denmark for three years in the RACE Atmospheric project. From 1990 to 1994 he worked for Ellemtel Telecommunication System Laboritories, Lund Sweden and in 1994 he returned to the Technical University of Denmark to work at the Institute of Telecommunications. His main interests include teletraffic analysis and performance evaluation of modern communication networks with special interest in B-ISDN.

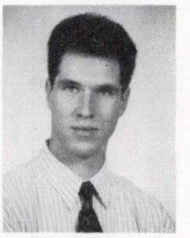

Tibor Cinkler received his M.Sc. degree in electrical engineering from the Technical University of Budapest, in 1994. He is with the High-Speed Networks Laboratory at the Department of Telecommunications and Telematics, Technical University of Budapest, where he is currently working toward the Ph.D. degree in electrical engineering. His research interests are related to the optimisation of broadband (ATM) networks, particularly call-level modelling for dimensioning and performance evaluation, as well as topological design and routing optimisation. He is student member of IEEE and ACM and a member of the Scientific Society for Telecommunications, Hungary.

Hai Vu Thanh received the M.Sc. degree in electrical engineering from the Technical University of Budapest. He is currently working toward the Ph.D. degree in the Department of Telecommunications and Telematics, Technical University of Budapest. His research interests are routing and dimensioning of ATM networks, and survivable network design.

Gábor Fodor received the M. Sc. degree in communication engineering in 1988 from the Technical University of Budapest, faculty of Electrical Engineering. He then worked five years in Sweden at ABB Atom as a software developer for distributed process control systems. In 1993 he joined the Department of Telecommunications and Telematics at the Technical University of Budapest as a graduate student, where he is currently pursuing the Ph.D. degree. His interests include modelling and simulation of B-ISDN and ATM networks.

NEUROCOMPUTING IN LOGICAL PARTITIONING OF ATM NETWORKS

J. BÍRÓ, Z. KORONKAI, T. TRÓN, A. FARAGÓ, T. HENK

DEPT. OF TELECOMMUNICATIONS AND TELEMATICS
TECHNICAL UNIVERSITY OF BUDAPEST
SZTOCZEK U. 2., H-1111 BUDAPEST, HUNGARY

M. BODA

ELLEMTEL TELECOMMUNICATIONS SYSTEMS LABORATORIES
S-12525, ALVSJÖ, SWEDEN

One of the most important things in ATM networks is to satisfy the requirements of different services. An efficient way of providing the quality of service is the logical separation of network resources. It means that on top of the physical network a number of logical (virtual) subnetworks are established in which the logical links share the capacities of physical links. There are several advantages of logical resource separation, such that the network can operate more safely, the management can be simplified and some important structures, e.g. virtual leased networks, are much easier to implement. In this paper we introduce two extensions of Kennedy and Chua's canonical neural circuit which can be applied in algorithms that optimize the logical configuration. We also present analytical results on the stability of these circuts as well as simulation experiences for the validation of both the designed extensions and their usefulness in dimensioning simple ATM network models. The most important practical implication is that the proposed neural structures can operate very fast in a parallel implementation since they solve mathematical programming tasks without computation, thus, forming a good basis of a possible device providing for the network manager with the opportunity of running real-time complex reconfiguration algorithms to enhance network flexibility via improved network intelligence.

1. INTRODUCTION

An important tool in ATM network dimensioning and management is to distribute resources of the physical network among logical subnetworks. There are several reasons why this method of resource separation can serve as a very efficient tool in ATM network configuration. In connection with management functions the main advantage of applying capacity partitioning is that various service classes with similar characteristics can be arranged into groups so that in a subnetwork those of similar properties can be handled together. Here we note that a Virtual Path (VP), a standardized element of ATM network architecture can also be considered as a special logical subnetwork. As another facility, let us assume that large temporary traffic demands have arisen between two or more nodes in the network. To ensure correct network operation with adequate grade of services one can reallocate the logical resources.

As mentioned above, establishing logical subnetworks on top of the given physical network means that the logical links share the physical link capacities. Thus, the optimization task is to operate the whole network optimally, as a family of logical subnetworks according to a given objective function. A reasonable goal is to achieve the maximum revenue, naturally under some fairness issue. The revenue can be formulated as the weighted sum of the carried traffic on each route in the whole network. The algorithms developed for capacity partitioning have the following main features. The input consists of the description of the physical network, the topology of logical subnetworks, the traffic classes and the traffic demands. The algorithms optimize the objective function with respect to variables that are the logical link capacities and load sharing parameters.

As it is well known, artificial neural networks (ANN) contain many simple processing elements connected with each other in some way. Two main properties make them attractive in several applications: the capability of "learning" and the dramatically increased speed when used as parallel computation structures. Neural approaches of optimization problems have also been extensively studied by many researchers. Between the two main types of ANN architectures, feedforward and recurrent, the latter one, which serve the basis of our work, is more suitable for solving optimization tasks.

There has been strong research activity in applying analogue circuits for optimization problems. Pyne presented his concept in 1957 proposing a circuit for solving linear programming tasks [2]. Later Chua and Lin developed a circuit for nonlinear programming problems [3]. The main drawback of this circuit is that it can not solve quadratic programs having negative semi-definite matrices because multiport tranformers are used in realization. One possible way of overcoming this difficulty is to apply negative floating resistors. Hopfield and Tank chose another way [4], they designed a neural circuit in which the decision amplifiers have inverting outputs as well, thus eliminating the necessity of negative resistors. However, the significance of Hopfield and Tank's early papers [4], [5] lies in that the optimization problems appear in a common framework of neural paradigm and analogue circuits (hence the name neural circuits).

The purpose of the paper is to introduce our developments related to the canonical nonlinear programming neural circuits of Kennedy and Chua [7] as well as present an efficient mapping of optimization task rising in logical network partitioning onto such neural networks. Stability analysis is also performed showing that the modified circuits are stable and converge to correct solution. Simulation examples, which are partly presented in the paper, have been made for two reasons such as for validation of the proposed extensions via simple optimization tasks and presenting the usefulness of the modified neural circuits for solving dimensioning problems in logical partitioning of ATM networks.

2. LOGICAL PARTITIONING OF COMMUNICATION NETWORKS

2.1. Emerging the Basic Concept

Resource separation in communication networks means in wide sense that sets of certain physical resources (e.g. transmission link capacities, physical trunk groups, etc.) are divided into subsets and dedicated to groups of users and/or services. It leads to better utilization of available resources, in fact, this is the main objective of the design and the solutions of the dimensioning problem serves the optimal logical configuration.

Recently, a new degree of freedom in ATM network dimensioning, the concept of virtual subnetworks, has been introduced [12]. There are many reasons and possible advantages (as listed above) of making for this way in ATM management. Several algorithms have been developed for dimensioning logical subnetworks that can serve as parts of a powerful management tool. Furthermore, some of these methods have been embedded and tested in an integrated tool for ATM network planning, simulation and management (PLASMA) [13]. In the following section we introduce a quite sophisticated algorithm for logical subnetwork design.

2.2. A Dimensioning Algorithm: Notation and Formulation

In the network model there are M nodes connected by I physical links (trunk groups) in some way. Let the vector C^{phy}, having I elements, comprise the capacity of the physical links.

On top of the given physical network logical networks will be established where the nodes in every subnetwork constitute a subset of the physical nodes and the topology can differ from that of the physical network. Let J denote the total number of logical links of all subnetworks and $C^{\log}$ the vector which contains the logical link capacities. The connection between the physical and logical links is determined by matrix S with entries 0 and 1. The (i, j) entry takes 1 if logical link j uses physical link i, and 0 otherwise. Consequently, the following obvious inequality should be satisfied:

$$SC^{\log} \leq C^{phy}. \tag{1.1}$$

It means that the sum of logical link capacities on the same physical link shouldn't exceed the physical capacity.

Furthermore, let N be the set of logical networks, Ω_l the set of Origin-Destinaton (O-D) pairs and Γ_l the set of traffic classes in logical network l. Now, the notion of *route* can be defined as follows: a route is the concatenation of logical links belonging to the same logical network between an O-D pair, and carrying a certain traffic class. Thereby the set of possible routes over all subnetworks is:

$$R = \bigcup_{l \in N} \bigcup_{\omega \in \Omega_l} \bigcup_{k \in \Gamma_l} R^{(l,\omega,k)} \tag{1.2}$$

The bandwidth demand of a call for route r on logical link j is denoted by $A_{j,r}$ which is sometimes replaced by b_k when the bandwidth demand depends only on the traffic class k.

The Poissonian call arrival rate $\kappa^{(l,\omega,k)}$ offered for each O-D pair ω and traffic class k is assumed to be known. It is distributed among the possible routes resulting in call arrival rate

$$\kappa_r^{(l,\omega,k)} = \kappa^{(l,\omega,k)} a_r^{(l,\omega,k)} \text{ to route } r,$$

where $a_r^{(l,\omega,k)}$ are the load sharing parameters. Evidently, it involves another constraint to the model, namely:

$$\sum_{r \in R^{(l,\omega,k)}} a_r^{(l,\omega,k)} = 1. \tag{1.3}$$

In optimizing the logical network configuration, a reasonable and practical objective is to maximize the total revenue that can be defined, for instance, as a weighted sum of traffic carried in the whole network. Accordingly, the optimization problem can be formulated as follows:

Maximize

$$W(a, C^{\log}) =$$

$$= \sum_{l \in N} \sum_{\omega \in \Omega_l} \sum_{k \in \Gamma_l} \sum_{r \in R^{(l,\omega,k)}} w_r a_r^{(l,\omega,k)} \kappa^{(l,\omega,k)} (1 - L_r)$$

subject to

$$SC^{\log} \leq C^{phy}$$

$$\sum_{r \in R^{(l,\omega,k)}} a_r^{(l,\omega,k)} = 1 \quad \text{for} \quad l \in N,\ \omega \in \Omega_l,\ k \in \Gamma_l$$

$$L_r \leq B_r \quad \text{for all route } r, \tag{1.4}$$

where vector a comprises the load sharing parameters, L_r the actual blocking probability, B_r the largest acceptable blocking probability and w_r the expected revenue gained from an accepted call, all of them for route r.

3. NONLINEAR PROGRAMMING NEURAL CIRCUITS

3.1. The Kennedy and Chua's Circuit

Kennedy and Chua have proposed a circuit called dynamical canonical nonlinear programming circuit which is intended to solve problems formulated as follows [7]:

Minimize $f(x)$

$$\text{subject to } g_j(x) \geq 0, \quad j = 1 \ldots p, \tag{2.1}$$

where $x \in R^n$, $f : R^n \to R$ and $g = [g_1, \ldots, g_p] : R^n \to R^p$ is a p dimensionalvector valued function of n variables. It is assumed that f and g are continuously differentiable functions. The architecture can be seen in Fig. 1 showing the circuit containing controlled voltage and current sources, nonlinear resistors and capacitors. The latter ones realize dynamical behaviour and their voltages represents the decision variables. The left-hand side is responsible for fulfilment of the corresponding constraints, while the required derivatives appear on the right-hand side. It is easy to show that the circuit can be considered as a gradient system and solves the following unconstrained optimization problem derived from the constrained one using penalty function method:

$$\text{Minimize } \{f(x) + cP_2(x)\}, \tag{2.2}$$

where c is a sufficiently large constant and $P_2(.)$ is the second order penalty function defined as

$$P_2(x) = \frac{1}{2} \sum_{j=1}^{p} [g_j^-(x)]^2, \; g_j^-(x) = -\min(0, g_j(x)) \tag{2.3}$$

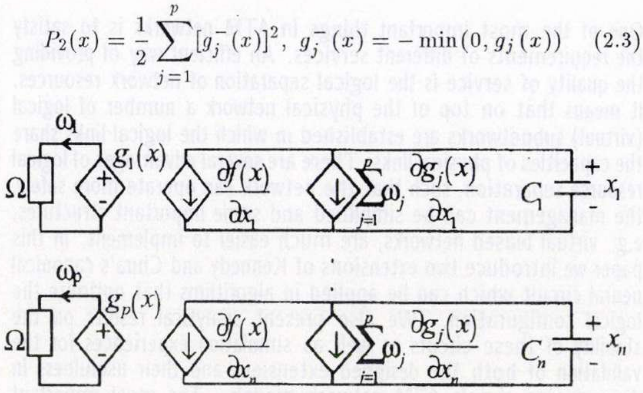

Fig. 1. The canonical nonlinear programming neural circuit of Kennedy and Chua

3.2. First Extension: the Modified Canonical Neural Circuit

The first modification is developed for handling equality constraints in order to make the canonical neural circuit capable of solving more general optimization task formulated in the form of:

Minimize $f(x)$

subject to $g_j(x) \geq 0$, $j = 1 \ldots p$

and $\quad h_i(x) = 0$, $i = 1 \ldots r$. $\quad$ (2.4)

The motivation came from that in the dimensioning task (1.4) the load sharing parameters impose equality constraints. Naturally, there are some obvious ways of taking into account the constraints $h_i(x) = 0$. For example, one of them is considering all equalities as two inequalities, that is $h_i(x) = 0$ is equivalent to $h_i(x) \geq 0$, $h_i(x) \leq 0$. Another possibility is to use simple quadratic penalty terms for equalities and embedding them into $f(x)$ as can be seen in [14]. Hence, in this manner the problem can be transformed to that like in (2.1). Although these approaches are quite simple and applicable, they have some drawbacks, particularly in connection with the possible circuit realization. In the case of the first method the canonical circuit requires 2r additional elements, corresponding pairs of which are responsible for equality constraint fulfilment. It is a prodigal solution, because at most one of the two nonlinearities is active in each pair at any time. In addition, it involves another requirement, the two nonlinearities of each pair should work completely synchronously, otherwise it can occur that both of the inequalities $h_i(x) \geq 0$, $h_i(x) \leq 0$ are considered being violated leading to unnecessary oscillation and pathological behaviour in the circuit. The second approach shoudn't even be preferred, because the neural circuit modified in this manner would lost an attractive feature, i.e. the topologically well-separated treatment of constraints, which exists in the original canonical neural circuit. Preserving this property is very important in obtaining an easily reconfigurable circuit.

Taking into account these facts, we suggest using special nonlinearities which help overcome the difficulties listed above. They are characterized by:

$$\Omega_{jq}(w) =$$

$$= c_j w^{q-1}(-\varepsilon(-w))^{q-2} \quad j = 1 \ldots p,\ q > 0, \text{ integer} \tag{2.5}$$

$$\Lambda_{jq}(x) = d_j w^{q-1}(2\varepsilon(w) - 1)^{q-2} \quad j = 1 \ldots r, \tag{2.6}$$

where c_j, $d_j \in R$ and ε is the Heaviside step function. The *qth order* Ω_{jq} and Λ_{iq} belong to the jth inequality and ith equality constraint, respectively. (Ω and Λ are conductance characteristics as can be seen in Fig. 2). Therefore, in accordance with circuit dynamics, the time evolution of state variables x_k is determined by the following differential equation:

$$\frac{dx_k}{dt} = -\frac{1}{C_k}\left[\frac{\partial f(x)}{\partial x_k} + \right.$$

$$\left. + \sum_{j=1}^{p} c_j \omega_j \frac{\partial g_j(x)}{\partial x_k} + \sum_{i=1}^{r} d_i \lambda_i \frac{\partial h_i(x)}{\partial x_k}\right], \quad k = 1 \ldots n. \quad (2.7)$$

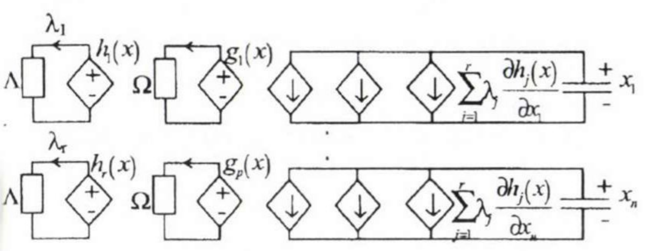

Fig. 2. The modified nonlinear programming circuit

For establishing connection to the optimization task found in (2.4), let us define the unconstrained objective function $\varphi(x)$ as:

$$\varphi(x) = f(x) + P_q(x) + Q_q(x), \quad (2.8)$$

where $P_q(x)$ and $Q_q(x)$ are the *modified qth order* penalty functions:

$$P_q(x) = \frac{1}{q}\sum_{j=1}^{p} c_j [g_j(x)]^q (-\varepsilon(-g_j(x)))^q \; q > 0, \text{ integer} \quad (2.9)$$

$$Q_q(x) = \frac{1}{q}\sum_{j=1}^{r} d_j [h_j(x)]^q (2\varepsilon(h_j(x)) - 1)^q. \quad (2.10)$$

The following theorem makes the relation between the modified canonical circuit and the task in (2.4) more clear.

Theorem 1: *The modified canonical neural circuit with qth order Λ_q and Ω_q nonlinearities solves the unconstrained mathematical programming task having modified qth order penalty terms P_q and Q_q.*

Proof: see Appendix A.

The obvious implication of **Theorem 1** that the modified canonical neural circuit driven by (2.7), with appropriate c and d parameters, converges to a solution which is arbitrarily close to that of the constrained optimization problem in (2.4).

It is also worth noting that the penalty functions used above differ from those usually used in optimization theory [14], [15], hence the adjective modified is used. As it can be seen in (2.9) and (2.10) the members of the constraint functions $h(x)$ and $g(x)$ can be weighted by different scales. One is able to utilize this opportunity efficiently in the modified circuit, for example, to take into account frequently violated constraints with larger weight yielding faster convergence.

3.3. Second Extension: The Stochastic Modified Neural Circuit for Global Optimization

In this subsection, we present a stochastic version of the modified neural circuit which have the ability to overcome the obvious drawback of pure gradient systems, i.e. the lack of global optimization.

For obtaining global optimum in discrete optimization the Simulated Annealing (SA) [19] is a widely used tool. In the neural literature, some powerful deterministic approaches of stochastic global optimization can be found, for example, mean field techniques based on magnetic systems' analogies [11], hardware annealing derived from SA [17], [18] and stochastic Hopfield networks based on the diffusion machine [10]. The attractive feature of these techniques is that they *emulate* the annealing process through deterministic equations providing reasonable convergence time and computational complexity, as opposed to the very time consuming Monte Carlo simulation. These deterministic methods, due to the nature of their governing equations, are suitable for circuit realization.

The SA can be extended for the case of continuous decision variables using the Langevin algorithm [10]. This fact, besides the existence of several local optima of the revenue function W, has motivated us to apply a concept similar to that in [10], that is adding uncorrelated gaussian noises with gradually decreasing amplitudes to the state variables in the modified neural circuit. Then the circuit governing equations derived from the corresponding Ito-type stochastic differential formulas can be expressed as follows:

$$\frac{\partial x_k}{\partial t} = -\frac{1}{C_k}\frac{\partial L(x)}{\partial x_k} + \sqrt{2T}\eta_k(t), \; k = 1 \ldots n, \quad (2.11)$$

where T is the artificial temperature decreasing slowly enough and $\eta_k(t)$ are independent gaussian noises providing quasi-stationarity at a given temperature. If the T-schedule is sufficiently slow (e.g. logarithmic) the network can reach the global optimum with high probability. This approach is also feasible to circuit implementation because of the existence of efficient methods for generating uncorrelated gaussian noises developed for VLSI neural circuits [16].

4. NEURAL APPROACH OF DIMENSIONING LOGICAL SUBNETWORKS

4.1. Mapping the Dimensioning Problem onto the Proposed Neural Structure

Here we present one possible correspondence between the optimization task and the modified canonical circuits. It is obvious that the objective function $f(x)$ to be minimized should be equivalent to the negative of the revenue function, i.e. $-W(a, C^{\log})$. The vector x with respect to which we optimize consists of the load sharing vector a and the logical capacity vector $C^{\log}$. The constraints related to these parameters can be expressed in the form of (2.4). It is more difficult task to handle with end to end route blockings in an exact way. Therefore, it is worth transforming the route blocking constraints to those ones that contain a and $C^{\log}$ instead of the blocking probabilities, yielding the following formula:

$$\sum_{r \in R_j} A_{j,r} \frac{a_r^{(l,\omega,k)}}{\mu_r} \le C_j^{\log} - \beta_j \sqrt{C_j^{\log}} \quad \text{for } j = 1 \ldots J, \quad (3.1)$$

where β_j is a parameter chosen appropriately for obtaining good approximation of (1.4). The definition of $g(x)$ and $h(x)$ obtained from (1.4) and (3.1) can be found in Appendix B.

The derivatives of the revenue function W and the constraint functions g and h with respect to the decision variables play central role in the dynamics of the proposed neural circuits. The required formulas are also presented in Appendix B. Here, we just note that while the constraint derivatives are derived directly, the revenue derivatives can be obtained only in a highly nontrivial way (for details, see [12]) due to the nonlinear recursive relation between capacities and blocking probabilities of the logical links. However, the corresponding formulas are available in [12].

4.2. Simulation Investigations

We have made simulations for two purposes. In the first phase, the proposed neural circuits were tested on simple optimization tasks. The results showed that the modified canonical circuit can converge to correct solutions in accordance with analytical investigations. But what about the performance of the stochastic version is a more exciting question. Although for the time being it has not been supported by rigorous analysis, the simulations indicate its usefulness. Here we show a very simple example which can give an impression of the behaviour of our stochastic neural network. Let us consider Fig. 3 where one of the outputs (one of the decision variables) of the network is plotted. The objective function to be maximized has a local and a global optimum in the feasible region, at 0 and 15, respectively. At the beginning of the operation, two dense range are shaping around 0 and 15. Then, as the artificial temperature becomes low enough, the network output 'gets stuck' at 15, the global maximum.

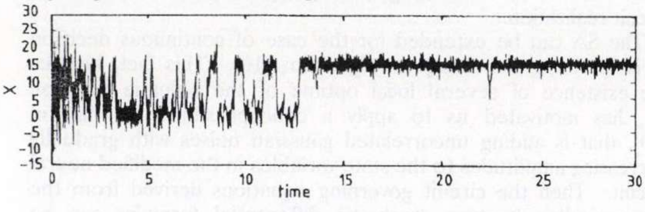

Fig. 3. The output of the stochastic neural circuit

As a communication network dimensioning example, we present a three node case (Fig. 4) with three physical (A-C, A-B, C-B) and eight logical links (1,2, ... 8). Two traffic classes (black and white lines) offer traffic from node A to node B shared between logical link pairs 1-3 and 2-4, respectively. The offered traffic from A to C and from C to B is carried through direct logical links (link 5,6,7,8). The following table summarizes the parameters.

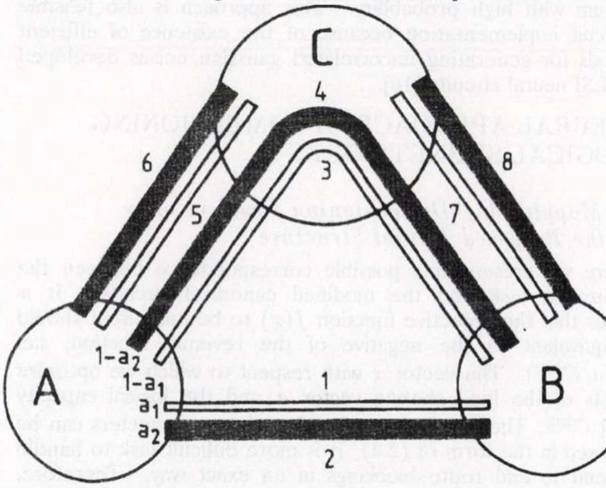

Fig. 4. A three node example for network dimensioning

Table 1. Offered Traffics for Routes

O-D pair	Offered traffic class 1 (Erlang)	Offered traffic class 2 (Erlang)
A-B	270	50
A-C	90	9
B-C	90	9

The ratio of bandwidth demand of traffic class 1 to that of traffic class 2 is 1:10 (as opposed to their offered loads which is 10:1).

The revenue function W has two optima for the above-mentioned parameters. One local optimum is located at $a_1 = 1$ and $a_2 = 0.73$, while the global one can be found at $a_1 = 0$ and $a_2 = 1$. If we don't use the stochastic extension, the rate when the modified canonical neural network can reaches the global optimum with random feasible initial states is 44 % . Using the stochastic neural network the result is much better, more than 99 %.

Although the amount of time required for convergence are relatively large (due to the direct simulation of differential equations), the analogue implementations can work very fast, because the optimization problems are solved *without computation*, at least in traditional sense. Nevertheless, we perform ongoing research in order to find efficient discrete-time algorithms that are based on the presented analogue neural networks and are much faster than those derived from direct approximation of the continuous behaviour.

5. CONCLUSION

In this paper we introduced two extensions of a canonical neural network for nonlinear programming: one of them is related to efficient treatment of equality constraints, the other one is a stochastic extension for global optimization. An ATM network dimensioning problem also presented and solved by the extended neural networks. Analytical investigations and simple simulation examples validated the usefulness of these networks as potential parts of a fast operating network management tool.

6. ACKNOWLEDGMENT

This work has been done in the framework of a joint research between Ellemtel Telecommunication Systems Laboratories and the Department of Telecommunications and Telematics. The authors are grateful to László Ast for helpful discussions. The continuous support of Carl-Gunnar Perntz and Géza Gordos is kindly acknowledged.

7. APPENDIX A

The energy function of the modified canonical neural circuit is:

$$L(x) = f(x) + \sum_{j=1}^{p} \int_0^{g_j(x)} \Omega_{j\,q}(w)dw + \sum_{j=1}^{s} \int_0^{h_j(x)} \Lambda_{j\,q}(w)dw. \tag{A.1}$$

Introducing the variables

$$\omega_j = \Omega(g_j(x)) \quad \text{and} \quad \lambda_j = \Lambda(h_j(x)) \tag{A.2}$$

referring to the conductance characteristics of the applied nonlinearities, the time derivative of $L(x)$ can be expressed as:

$$\frac{\partial L(x)}{dt} = \sum_{k=1}^{n} \frac{\partial f(x)}{\partial x_k}\frac{\partial x_k}{\partial t} + \sum_{j=1}^{p}\sum_{k=1}^{n} c_j \omega_j \frac{\partial g_j(x)}{\partial x_k}\frac{\partial x_k}{\partial t} + \sum_{j=1}^{r}\sum_{k=1}^{n} d_j \lambda_j \frac{\partial h_j(x)}{\partial x_k}\frac{\partial x_k}{\partial t}. \tag{A.3}$$

Substituting governing equation (2.7) into (A.3), we obtain the following more concise form:

$$\sum_{k=1}^{n} \frac{\partial x_k}{\partial t}\left[-C_k \frac{\partial x_k}{\partial t}\right] \tag{A.4}$$

which is evidently less than or equal to zero. Consequently, the system is stable in Lyapunov sense meaning that the dynamical equation (2.7) continuously decreases the energy function $L(x)$ until it reaches its stable equilibrium point.

As the second step, we show that $L(x)$ as a Lyapunov function is equivalent to the objective function $\varphi(x)$ in (2.8). Considering the following identities:

$$\int w^{q-1}(2\varepsilon(w)-1)^{q-2}dw = \frac{1}{q}w^q(2\varepsilon(w)-1)^q \tag{A.5}$$

$$\int w^{q-1}(-\varepsilon(-w))^{q-2}dw = \frac{1}{q}w^q(-\varepsilon(-w))^q \tag{A.6}$$

and substituting them into (A.1) we get the required formula of $\varphi(x)$.

8. APPENDIX B

$$g_i(x) = \tag{B1}$$

$$= \begin{cases} C_i^{phy} - s_i C^{\log} & i \in \{1 \dots I\} \\ C_{i-l}^{\log} - \beta_{i-I}\sqrt{C_{i-I}^{\log}} - \sum\limits_{r \in R_{i-I}} A_{i-I,r} \dfrac{a_r^{(l,\omega,k)}\kappa^{(l,\omega,k)}}{\mu_r} \\ i \in \{I+1 \dots I+J\} \end{cases}$$

where s_j is the jth row in matrix S.

$$h_i(x) = h_i(a) = \sum_{r \in R^{(l,\omega,k)_i}} a_r^{(l,\omega,k)_i} - 1, \tag{B.2}$$

where $(l,\omega,k)_i$ is the ith triplet in the set of possible triplets (l,ω,k).

$$\frac{\partial g_i(x)}{\partial C_j^{\log}} = \begin{cases} s_{i,j} \text{ if } i \in \{1 \dots I\} \\ \delta_{i-I,j}(1 - \beta_{i-I}\frac{1}{2\sqrt{C_{i-I}^{\log}}}) \\ i \in \{I+1 \dots I+J\} \end{cases} \qquad (B.3)$$

$$\frac{\partial g_i(x)}{\partial a_r^{(l,\omega,k)}} = \begin{cases} 0 \text{ if } i \in \{1 \dots I\} \\ \frac{A_{i-I,r}\kappa_r^{(l,\omega,k)}}{\mu_r} \quad \text{if} \quad i \in \{I+1 \dots I+J\} \end{cases} \qquad (B.4)$$

where s_{ij} is the (i,j) entry in matrix S.

$$\frac{\partial h_i(x)}{\partial a_r^{(l,\omega,k)_j}} = 1 \quad \text{for all } r \in R^{(l,\omega,k)_j}. \qquad (B.5)$$

REFERENCES

[1] T. Roska and L. O. Chua : "The CNN Universal Machine: an Analogic Array Computer", *IEEE Trans. on Circuit and Systems*, Vol. CAS-40, pp. 163-173, March, 1993.

[2] I.B. Pyne: "Linear Programming on an Analogue Computer", *Trans. Am. Ins. Ele. Eng.*, Vol. 75, pp. 139-143, May, 1956.

[3] L. O. Chua and G. Lin: "Nonlinear Programming without Computation", *IEEE Trans. on Circuits and Systems*, Vol. CAS-31, No. 2, February, 1984.

[4] J. J. Hopfield and D. W. Tank: "'Neural' Computation on Decisions Optimization Problems", *Biological Cybern.*, Vol. 52, pp. 141-152, 1985.

[5] D. W. Tank and J. J. Hopfield: "Simple 'Neural' Optimization Networks: An A/D Converter, Signal Decision Circuit and a Linear Programming Circuit", *IEEE Trans. on Circuits and Systems*, Vol. CAS-33, No. 5, May, 1986.

[6] M. P. Kennedy and L. O. Chua: "Unifying the Tank and Hopfield Linear Programming Network and the Canonical Nonlinear Programming Circuit of Chua and Lin", *IEEE Trans. on Circuits and Systems*, Vol. CAS-34, No. 2, pp. 210-214, February, 1987.

[7] M. P. Kennedy and L. O. Chua: "Neural Networks for Nonlinear Programming", *IEEE Trans. on Circuits and Systems*, Vol. CAS-35, No 5, pp. 554-562, May, 1988.

[8] W. E. Lillo et. al.: "On Solving Constrained Optimization Problems with Neural Networks: A Penalty Method Approach", *IEEE Trans. on Neural Networks*, Vol. 4, No 6, pp. 931-940, November, 1993.

[9] C. Maa: "Linear and Quadratic Programming Neural Networks Ananlysis", *IEEE Trans. on Neural Networks*, Vol. 3, No. 4, pp. 580-594, July, 1992.

[10] E. Wong: "Stochastic Neural Networks", *Algorithmica*, Vol. 6, No 3, pp. 467-478, 1991.

[11] C. Peterson and B. Söderberg: "A New Method for Mapping Optimization Problems onto Neural Networks", *Int. Journal of Neural Systems*, Vol. 1, No. 1, pp. 3-22, 1989.

[12] A. Faragó et. al.: "A New Degree of Freedom in ATM Network Dimensioning: Optimization of the Logical Configuration", submitted to *IEEE JSAC*, 1994.

[13] Zs. Haraszti et. al.: "PLASMA – An Integrated Tool for ATM Network Operation", *ISS'95*, Berlin, April, 1995.

[14] P. Whittle: *Optimization under Constraints*, Wiley-Interscience, 1971.

[15] V. G. Karmanov: *Mathematical Programming*, Mir Publishers Moscow, 1989.

[16] J. Alspector et. al.: "A VLSI-Efficient Technique for Generating Multiple Uncorrelated Noise Sources and Its Application to Stochastic Neural Networks", *IEEE Trans. on Circuits and Systems*, Vol. 38, No. 1, pp. 109-123, January, 1991.

[17] B. W. Lee and B.J. Shau: "Hardware Annealing in Electronic Neural Networks", *IEEE Trans. on Circuits and Systems*, Vol. 38, No. 1, pp. 134-137, January, 1991.

[18] B. W. Lee and B.J. Shau: "Paralleled Hardware Annealing for Optimal Solutions on Electronic Neural Networks", *IEEE Trans. on Circuits and Systems*, Vol. CAS-40, No. 4, pp. 588-598, July, 1993.

[19] F. Romeo and A. Sangiovanni-Vincentelli: "A Theoretical Framework for Simulated Annealing", *Algorithmica*, Vol. 6, No. 3, pp. 302-345, 1991.

József Bíró received M.Sc. degree in electrical engineering at the Technical University of Budapest in 1993. After graduation he joined to Department of Telecommunications and Telematics (TUB). He is presently working towards his Ph.D. at High Speed Networks Laboratory. His research interest is in neural networks, asynchronous transfer mode networks in general, and neural optimization in particular.

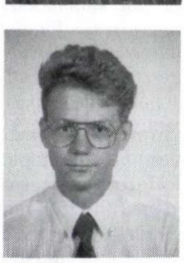

Zoltán Koronkai graduated in Electrical Engineering at the Technical University of Budapest, in 1995. He is presently working on his Ph.D. as a graduate student at the Department of Telecommunications and Telematics at High Speed Network Laboratory (TUB). His fields of interest are neural networks and ATM.

Tibor Trón received the M.Sc.E.E. and Dr. Techn. degrees from the Technical University of Budapest, in 1965 and 1974, respectively, and the Ph.D. degree in network theory from the Hungarian Academy of Sciences in 1987. He is presently an associate professor at the Department of Telecommunications and Telematics (TUB), and teaches network theory and computer aided design. His research interests are in network sensitivities, computer aided analysis of switched-capacitor networks, neural computing and communication system simulation. He is author and co-author of several lecture notes, technical reports and publications.

Miklós Boda graduated in Physics at Eötvös Lorand Univeristy, Budapest. He received his Ph.D. in solid state physics at the University of Uppsala in 1971. Then he joined HAFO (Semiconducter Research Institute) Stockholm. From 1978 he worked as an expert for DATASAAB (now part of Nokia) and from 1980 as manager for Design and Test Center, Philips Elektronik. He joined Ellemtel Telecommunication Systems Laboratories in 1990 as manager of Advanced Technology Research. He is the Chairman of Ericsson Concern Commitee for Artificial Neural Networks and Artificial Intelligence and the founder and president of the Swedish Neuronet Society. He is member of the Industrial Advisory Board of the Research Center for Advanced Communications and Computing, North Carolina, U.S.A. He is a honorary member of the Hungarian Academy of Engineering.

Tamás Henk's biography and photo see on ATM Networks I., page 2.

Tamás Faragó's biography and photo see on ATM Networks I., page 16.

IMPROVING THE PERFORMANCE OF A VIRTUAL PRIVATE NETWORK SERVICE ON THE ATM NETWORK*

T. FIOL COLL

COREP - POLITECNICO DI TORINO
CSO. DUCA DEGLI ABRUZZI 24, 10129 TORINO, ITALY
E-MAIL: SCITFC@PS.UIB.ES

A. TONIETTI

CSELT, CENTRO STUDI E LABORATORI DI TELECOMUNICAZIONI
VIA G.REISS ROMOLI 274, 10148 TORINO, TALY
PHONE: +39-11-2286875, FAX: +39-11-2286862
E-MAIL: TONIETTI@CSELT.STET.IT

This paper presents the results of a simulation study that shows the impact of introducing a B-VPN (Broadband Virtual Private Network) service over an ATM network. The QoS (Quality of Service) is measured separately for the private and the background traffics in terms of cell loss probability and cell delay. As the introduction of the B-VPN service entails a degradation of the QoS provided to the background traffic, even when the global load of the network is not modified, some different traffic shaping strategies have been analyzed. We show that under certain no restrictive conditions an improvement of the service performance can be obtained by operating a two-level shaping strategy on the private traffic.

1. INTRODUCTION

The growing demand for high speed telecommunication services and the interest of telecommunication public operators in the integration of all the services within a single network, have been the basis of the definition of the B-ISDN (*Broadband Integrated Services Digital Network*) as the model for the future telecommunications network. The ATM (*Asynchronous Transfer Mode*) technique has been proposed as the standard for the information transfer in the B-ISDN, because it is a fast and efficient means to transfer heterogeneous traffic. On the other hand, the need for interconnecting computers, which initially resulted in the diffusion of LANs and MANs, is evolving towards establishment of wide area telecommunication services. A useful example of this trend is the demand from some big enterprises of a telecommunication service that permits the interconnection of all their sites, which are usually placed in different cities. The initial solution to such a need was establishing private networks based on dedicated links. This solution, in spite of its technological simplicity, is being given up because of its high costs and low performance. In fact, private networks based on dedicated links have a low flexibility level, are not easily reconfigurable, and an important resource waste exists when the network traffic is "bursty" (which is the normal case in LANs interconnection).

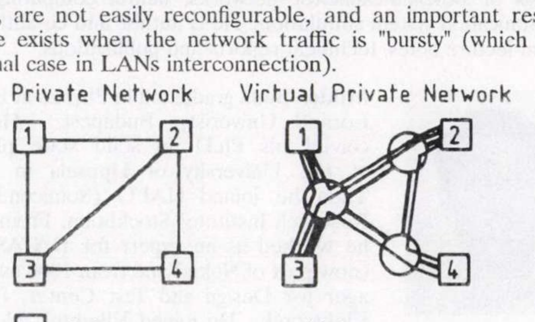

Fig. 1. Implementation of a Virtual Private Network over an ATM network

An important improvement of the performance of private networks can be obtained by using the resources of an existing public network. If the ATM network is used, the private network service can be implemented by offering to the private users a set of semipermanent VCs (*Virtual Connections*), as shown in Fig. 1. Observe that the different sites of the private network are interconnected by the public resources just like if they were interconnected by dedicated links. However, the utilization of public resources permits to make better use of the available bandwidth, due to the statistical multiplexing offered by the ATM technology. The implementation of a Virtual Private Network permits to increment the service flexibility and to reduce its costs because no dedicated link is used. Note that the QoS provided to the B-VPN should be the same of traditional private networks. However, the service would be more efficiently and economically available, and in addition, some complementary services could be offered by the public operator (f.e., management of the private network).

2. OPTIMIZATION OF THE B-VPN RESOURCES

As described in [3], an efficient utilization of the resources allocated to a B-VPN service can be obtained by distinguishing physical and logical connectivity. In this way, every private transmitter-receiver pair is identified by a logical connection identifier (VCI/VPI) but has no allocated bandwidth. The bandwidth is allocated to the *Virtual Paths* (VPs) used by the private connections, and so it can be dynamically shared by all the connections using those VPs. Thus, it is necessary to make an appropriate dimensioning of the bandwidth allocated to each VP, as a function of the medium and peak bandwidths of each logical connection included. By using the mentioned bandwidth optimization technique an important improvement of the VPN service performance can be obtained. However, as any logical connection of the B-VPN has a pre-allocated bandwidth, it is necessary to control the private traffic behaviour, in order to avoid any excess that could damage other users of the ATM infrastructure. The private network requirements must be stated in a service contract with the public operator. Then, some kind of control (UPC, *Usage Parameter Control*) should be used to guarantee that the private traffic meets the characteristics specified in the service contract. This control can be either preventive or repressive. Preventive control is usually called *shaping*, while repressive control is often called *policing*.

Here we present the results of a simulation study that shows the impact of introducing a B-VPN service over an ATM network, and analyze three different traffic shaping strategies to control the private traffic behaviour.

The paper is organized as follows. In the next section we briefly outline the main features of CLASS, the simulator used for this study. Section 4 summarizes the structure of the adopted shaping algorithm. Section 5 describes the scenario of our simulations, while the numerical results are presented in section 6. Finally, section 7 offers some conclusive remarks.

3. CLASS

Simulation results were obtained with a software tool named CLASS (ConnectionLess ATM Services Simulator) [1], developed at Politecnico di Torino, Italy. CLASS is a slotted synchronous simulator, entirely written in standard C language, that aims at the estimation of the performances of connectionless services in ATM networks. The behaviour, the simulation options and the different traffic source models available in CLASS are described in [1]. The traffic pattern used for the experiments is specified in an input file, together with other parameters. At the beginning of the simulation, CLASS calculates the User-to-User traffic matrix that defines the mean level and the destination of the generated traffic. Then, the (static) routing map of the network is computed by operating the following algorithm:

* The work of Mr. T. Fiol Coll was supported with a grant of the program *"Ampliació d'estudis a l'estranger"* of *CAIXA DE BALEARS "SA NOSTRA"*.

WHILE (there is a not-yet-routed connection)

{ 1 - Take the not-yet-routed connection with the highest mean load.

2 - Route it through the sequence of links that permits to maximize (after the routing of the current connection) the not-yet-allocated bandwidth of each single link of the ATM infrastructure. }

The routing table can change from one simulation to another, as a function of the mean-traffic pattern, but it is not modified during a given simulation.

The performance parameters computed with CLASS can be divided into the two following categories:

- *Cell and message loss probabilities.* These parameters are measured considering both the whole network, and individual buffers and VCs. Loss probabilities can be further subdivided in four different constituens due to overflows in the following buffers:
  - users' transmission buffers (the whole message, i.e., all of its cells, are discarded in this case).;
  - buffers associated with links between ATM nodes;
  - buffers associated with the shaping devices;
  - buffers associated with the links connecting the destination node to the final destination (a user).
- *Cell and message delay jitters.* Cell and message delays are made of a constant part and of a variable part. The constant part is due to propagation delays along links and processing delays at nodes. The variable part is due to the waiting time in the users transmission buffer, and to queuing in the buffers associated with links between nodes and/or in the buffers of the shaping devices. Only the variable part is considered and measured. Delay jitters are computed considering the whole network, the individual links and the VCs.

In our work, the preceding parameters are all investigated separately for background traffic and private traffic.

4. THE SHAPING ALGORITHM

Traffic shaping is a preventive traffic control function. Usually, it is performed close to the traffic source, in order to decrease the burstiness of the offered traffic by smoothing the flow of cells, so as to ensure that the traffic crossing the UNI (*User/Network Interface*) meets the characteristics specified during the establishment phase through the CAC (*Call Admission Control*) functions.

Message generations correspond to the request for AAL services from higher layer protocols. In our work, messages are then segmented into cells, and batches of cells corresponding to complete messages are forwarded to the shapers that implement a specified shaping algorithm on the traffic referring to a given group of VCs. When more than one VC belong to a group, it is necessary to multiplex the cells before shaping. VCs can be grouped in any arbitrary way, but a specific performance objective should suggest a grouping of VCs based on some common characteristics.

The shaping policy investigated is an adaptation of the *Generic Cell Rate Algorithm* (GCRA) specified in the CCITT Draft Recommendation I.371 [2] for traffic policing. Our shaping algorithm is specifically designed to suit the connectionless traffic environment where cells are generated in batches, and so, instead of marking or discarding cells (as in [2]), our version delays cells until they comply with the traffic contract.

The GCRA algorithm depends on two key parameters:

- The bandwidth allocated to the group of VCs on which a shaper operates that defines the "increment" for the GCRA; this parameter is specified through its inverse that determines the nominal cell interarrival time and is denoted by T. In the present CLASS implementation, T is an integer number of slots.
- The allowed cell burst length; this parameter defines the "limit" — also called the cell delay variation tolerance — for the GCRA. It is denoted by τ and in the present CLASS implementation it is an integer number of slots.

The goal of our algorithm is to compute the allowed transmission time for an incoming cell, given its theoretical arrival time, and its actual arrival time, where:

- The actual arrival time of cell C_i, Ta_i, is the time at which the cell arrives to the input of the shaping device.
- The theoretical arrival time of cell C_i, TAT_i, is determined as a function of the nominal interarrival time and the actual arrival times of previous cells.
- The allowed transmission time of cell C_i, Tt_i, is the time at which C_i is eligible for transmission.

The GCRA shaper that we used is defined by the following algorithm to be executed at every time slot for each shaper operating on a group of VCs. *TIME* identifies the current slot.

if $Ta_i = TIME$

- if $Ta_i \geq TAT_i$
  then $\quad Tt_i = Ta_i, \quad TAT_{i+1} = Ta_i + T$
- if $TAT_i - \tau \leq Ta_i < TAT_i$
  then $\quad Tt_i = Ta_i, \quad TAT_{i+1} = TAT_i + T$
- if $Ta_i < TAT_i - \tau$
  then $\quad Tt_i = TAT_i - \tau, \quad TAT_{i+1} = TAT_i + T$

Cells arriving at a shaper are tagged with a time stamp equal to their actual arrival time, that is used for shaping and cell delay jitter computation. The allowed transmission time Tt_i for each cell C_i of the VCs in the n-th group is computed by the n-th shaper, which deposits the cells into its output queue, together with the computed value of Tt_i.

As we will show in section 6, this algorithm can also be applied to the whole traffic of each VP used by the private network.

5. THE SIMULATION SCENARIO

In our simulation experiments we have considered the network of Fig. 2, corresponding to a hypothetical Italian ATM network. It contains a total of 10 nodes and 21 users located in the most important cities. The traffic pattern supposed for that network was obtained from realistic considerations on traffic interests and is shown in Table 1. The matrix defines the background traffic load on a node-by-node basis, and the last row gives the total traffic generated by the background users connected to each node. As the nodes located at Roma (RO) and Milano (MI) had a very high load, the network was supplied with a high speed backbone (600 Mbit/s) (MI-RO-FI-BO-MI). The rest of links have a capacity of 150 Mbit/s (300 Mbit/s channels are obtained with two 150 Mbit/s links in parallel). Every link of Fig. 2 represents a bidirectional channel with its relative transmission buffer.

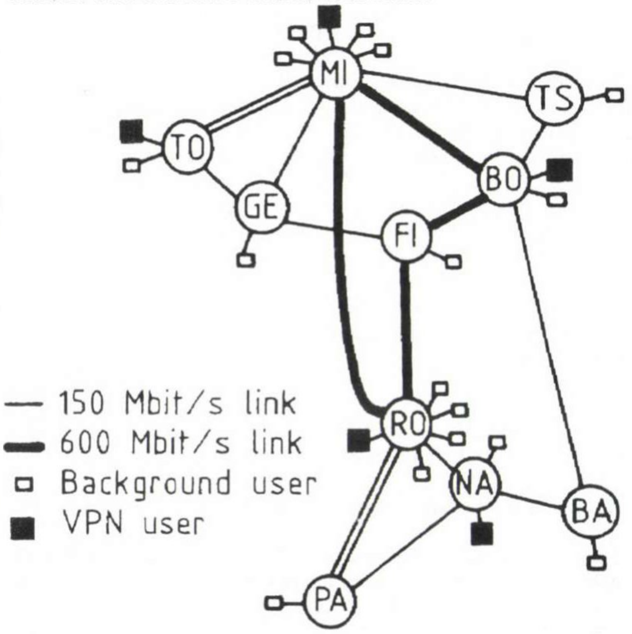

Fig. 2. Topology of the simulated network. The B-VPN users are marked.

For our study, a private network with five users has been overlaid on the ATM network described before. We have assumed a private network belonging to a big industrial plant of Torino (TO) and so we have supposed for the B-VPN the User-to-User traffic pattern shown in Table 2. The matrix defines the private traffic load on a User-to-User basis, and the last row gives the total traffic generated by each private user. It is important to observe that the most important node of the private network (Torino, TO) does not coincide with the two main nodes of the Italian ATM network.

Table 1. Traffic pattern for the background load of the ATM network; the traffic is generated by the node in the column and goes to the node in the row. Relations are expressed in thousandths of the total background traffic.

Node	MI	TO	GE	TS	BO	FI	RO	NA	BA	PA
MI	0	52	20	2	18	35	206	17	2	17
TO	52	0	3	0	3	5	32	3	0	3
GE	20	3	0	0	2	2	12	1	0	1
TS	2	0	0	0	0	0	1	0	0	0
BO	18	3	2	0	0	2	11	1	0	1
FI	35	5	2	0	2	0	22	2	0	2
RO	206	32	12	1	11	22	0	10	1	10
NA	17	3	1	0	1	2	10	0	0	1
BA	2	0	0	0	0	0	1	0	0	0
PA	17	3	1	0	1	2	10	1	0	0
Total	369	101	41	3	38	70	305	35	3	35

Table 2. Traffic pattern for the Virtual Private Network; the traffic is generated by the user in the column and goes to the user in the row. Relations are expressed in thousandths of the private traffic.

User	Mi	TO	BO	RO	NA
MI	0	90	10	50	30
TO	90	0	90	100	90
BO	10	90	0	20	10
RO	50	100	20	0	10
NA	30	90	10	10	0
Total	180	370	130	180	140

The links of the network shown in Fig. 2 were dimensioned to offer a reasonable QoS when the total network load was 1 Gbit/s and no private traffic was present. The objective of our simulation experiments is to maintain the existing QoS without modifying the network topology when the B-VPN service is established over the ATM network. Particularly, we want the performance provided to the background traffic not to be deteriorated when the B-VPN service is introduced without modifying the total network load. It seems to be a reasonable objective since the background users do not have worse behaviour when the private network is introduced.

In the simulation experiments we have also introduced the following hypothesis:

- Both the traffics of the network (Background and Private traffics) are ConnectionLess and not delay sensitive. So, we do not consider real-time traffic.
- The background traffic of each node is uniformly distributed among the background users connected to it. We will refer to the users not belonging to the analyzed B-VPN as background users.
- Users are bursty traffic sources (Poisson message generation with length of the messages distributed according to a truncated geometric law, with average 20 cells, and truncation value 200 cells).
- The destination is randomly selected on a message basis, in agreement with the traffic matrix specifying the users' behaviour.
- Each user has an internal buffer to memorize its own cells waiting for transmission. The buffer's size is 1000 cells, which is enough to guarantee that no losses occur in the user buffer.
- All users are identical, and have transmission and reception peak bandwidths of 150 Mbit/s.
- Each output link of the ATM nodes is supplied with a buffer to memorize the peaks of the output traffic. The buffer's dimension is always equal to 100 cells, and when the buffer is full the overflowing traffic is lost. We will refer to these buffers as "link-buffers".
- Cells from buffers are transmitted in a FIFO order.

6. SIMULATION RESULTS

In this section we present the simulation results obtained for the network described in section 5.

The first set of simulations shows the impact of establishing the described B-VPN service over the ATM network without implementing any control strategy. The traffic of the B-VPN is specified by a percentage of the total traffic in the network, and the results are shown as a function of the total network load and the private network traffic percentage. The matrix of Table 1 gives the whole network traffic pattern when no private traffic is present, while it gives only the background traffic pattern when there is the private network. The private network is considered as a group of users who communicate only between themselves, and in this first study case no control is realized on their traffic.

The results, presented in Fig. 3, show that the introduction of the private network service entails an important degradation of the QoS in the ATM network. As expected, the network performance decreases because the introduction of the B-VPN service changes the traffic pattern for which the ATM network was dimensioned. The performance degradation increases when either the total network load or the private network traffic percentage grow. Note that it is important to deal with the second degradation factor, because it causes a QoS degradation even when the total network load is not modified.

If we observe the cell loss probability, we can see that it degrades for both background and private traffics when the private traffic percentage grows, due to the growing imbalance that exists between network traffic and network resources. Moreover, it can be observed that the cell loss probability of private traffic is always higher than that of background traffic. This is due to the fact that the private traffic always uses links that are also used by the background traffic, while background traffic can use without competition the rest of links of the network (which are in addition less loaded because of the effective reduction of background traffic).

Observing the User-to-User cell delay diagram, we can see two different behaviours for private and background traffics. As expected, the mean delay of private traffic grows when the private traffic percentage is increased, but that of background traffic has an opposite behaviour. Again, this is probably due to the fact that the background traffic can use without competition some of the links of the ATM infrastructure, which become less loaded when the private traffic percentage grows. It is also important to observe that the "NOT-VPN" case (before introducing the VPN) does not follow that trend due to the different routing of connections realized by CLASS when there is or not the B-VPN. The routing map is not later modified when the percentage of private traffic is increased from 5 % to 20 %.

Thus, the introduction of the B-VPN service entails a degradation of the QoS in the ATM network, even when the total network load is not increased. This degradation is not acceptable because it affects also the background users. So, it is necessary to introduce a mechanism to control the behaviour of the private traffic, in order to avoid any damage to the background users.

6.1. Shaping function applied at the private users

The second set of simulations shows the improvement that can be obtained when a traffic shaping mechanism (the control function described in section 4) is operated at the private users side. We have assumed that every private user shapes its generated traffic in a unique group, i.e., the shaping function located at each private user does not distinguish the effective connection to which the cells belong. The bandwidth allocated to each group of VCs (BA_n for the n-th group) defines the nominal cell interarrival time for the shaper (T_n for the n-th group).

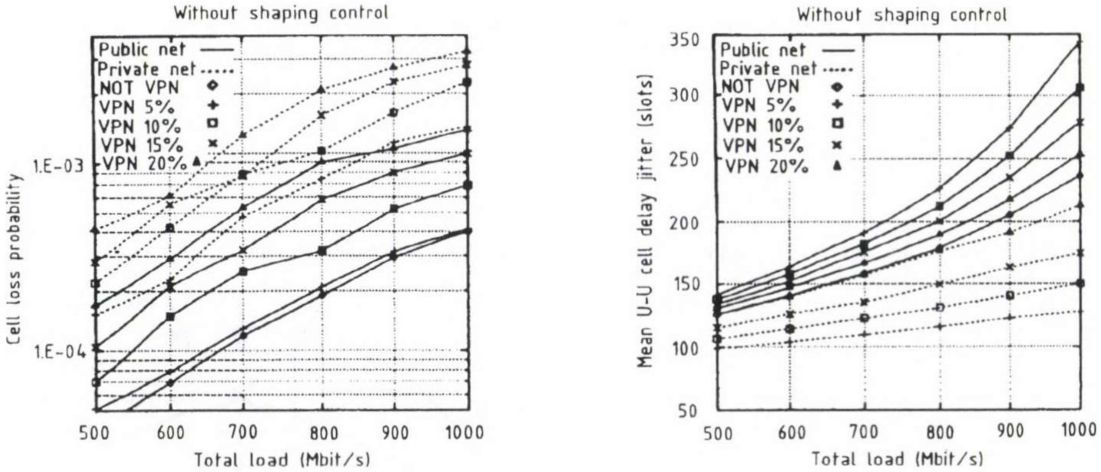

Fig. 3. Diagrams of cell loss probability and End-to-End delay versus total network load and private network load percentage. The figure is referred to the case where no control exists on the private traffic.

If B_{ni} is the average bandwidth of the i-th VC of the n-th group, then the bandwidth allocated to that group is $BA_n = \beta \sum B_{ni}$ where β is the "bandwidth allocation factor", that in our experiments is taken to be constant for all the groups in the network. From BA_n, T_n is obtained as

$$T_n = \max(1, \lfloor C/BA_n \rfloor),$$

where C is the data rate of the output link of the shaper. C is always equal to 150 Mbit/s in the current set of experiments.

Some different values for the bandwidth allocation factor β and the cell delay variation tolerance τ have been considered (note that with $\tau = 0$ all the cells of the n-th group are spaced by at least T_n slots). It is important to observe that the shaping algorithm considered becomes less restrictive (i.e., it permits a faster transmission) when high β and τ values are used.

So, we present the results obtained when the private users operate the described shaping function using some reasonable values of β and τ. The simulated network is the one shown in Fig. 2. We have assumed a total load of 1 Gbit/s and a private network traffic percentage equal to 20 %, which is the worst case analyzed in the previous set of simulations. In addition to the preceding hypothesis, also the following ones have been introduced:

- The shaping function is operated only by the private users (who are responsible for the performance degradation) to reduce the burstiness of their own traffic.
- All the private users use the same β_u and τ_u values, where the subscript u refers to the shaping parameters of the *users*.
- Each private user has an internal buffer to memorize its own traffic waiting to be compliant. The buffer capacity (equal to 1000 cells) is high enough to guarantee that no losses occur at the user buffer.

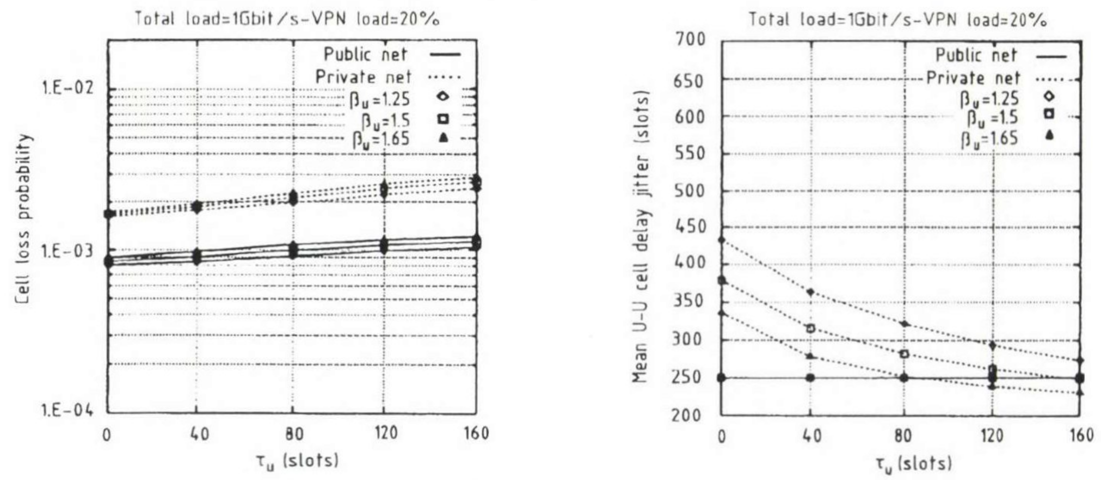

Fig. 4. Diagrams of cell loss probability and End-to-End delay versus β_u and τ_u. The figure is referred to the case where a shaping function is implemented at each private user's premise.

Fig. 4 shows the results of this set of simulations as functions of β_u and τ_u. As expected, the cell loss probability is better than in the preceding scenario, and decreases for small values of β_u and τ_u, due to the transmission restrictions applied to the private traffic, that translate into a minor congestion probability inside the ATM infrastructure. However, the gain obtained (for both background and private traffics) is always low, and considerable restrictions of the VPN's transmission capability translate into small improvements of the cell loss probabilities. As in the preceding scenario, the cell loss probability of private traffic is always higher than that of background traffic, due to the reasons described before. Taking now a look at the User-to-User cell delay diagram, we see that, while the mean End-to-End delay of the background traffic is nearly not modified, the operation of the shaping function causes an important increment of the mean delay of the private cells. As it was observed in [6], that is the price to be paid to reduce the cell loss probability with a shaping function. This is an obvious result, since the burstiness of the private traffic is reduced by delaying the cells. Thus, the operation of a shaping function at the private users side permits to reduce the cell loss probability, but the use of reasonable β_u and τ_u values translates into low QoS improvements. Instead of proposing the use of more restrictive β_u and τ_u values to reach our QoS objectives, which could result in a too drastic shaping function, the possibility of operate the traffic control function inside the ATM infrastructure is analyzed in the next section.

6.2. Shaping function applied inside the ATM network

In this section the traffic shaping function is operated inside the ATM network, and so the control is realized on the whole private traffic instead of on the traffic generated by each single private user. The simulated control strategy is the shaping function described before, but now it acts inside the ATM network, by spacing the private cells (whatever connection they belong to) that share the same Virtual Path (VP). For simplicity, we have considered that all the private cells that share a given link of the network use (in that link) the same VP. So, the private traffic is shaped at every link, whatever private connection it belongs to. The architecture of the shaping mechanism is shown in Fig. 5. The behaviour of the shaping device is the same described in Section 6.1.

The transmission bandwidth is assigned to the VPs, and so it can be dynamically shared by all the VCs that they include. The shaping parameters are calculated as described in section 6.1, but now they are referred to the whole traffic of each private VP inside the ATM network.

We have introduced "shaping devices" in the ATM nodes, with buffers (called "shaper-buffers") to memorize the private traffic waiting to be compliant, as shown in Fig. 5. The dimension of each shaper-buffer (called L_n) has been set to 1000 cells, which guarantees that no cell loss occurs. As the shaping parameters refer to the traffic control function realized inside the *network*, we will refer to them with the subscript n.

If we look at the results of this set of simulations, shown in Fig. 6, we can observe a remarkable improvement of the service performance. We see that the cell loss probability of both background and private traffics decreases when the shaping algorithm becomes more restrictive, i.e., for small β_n and τ_n values. However, it is important to observe that, with a shaping function restrictive enough (but with reasonable values of β_n and τ_n), the cell loss probability of the background traffic reaches the value that it had before the B-VPN service was introduced (4E-4).

On the other hand, the mean private traffic delay grows for small values of β_n and τ_n, while the mean background traffic delay is nearly constant, as observed before.

We conclude therefore that the current shaping strategy could be a possible candidate to meet the service requirements, since it permits to guarantee the network performance when the VPN is established over the ATM network, by operating a shaping function with reasonable β_n and τ_n values.

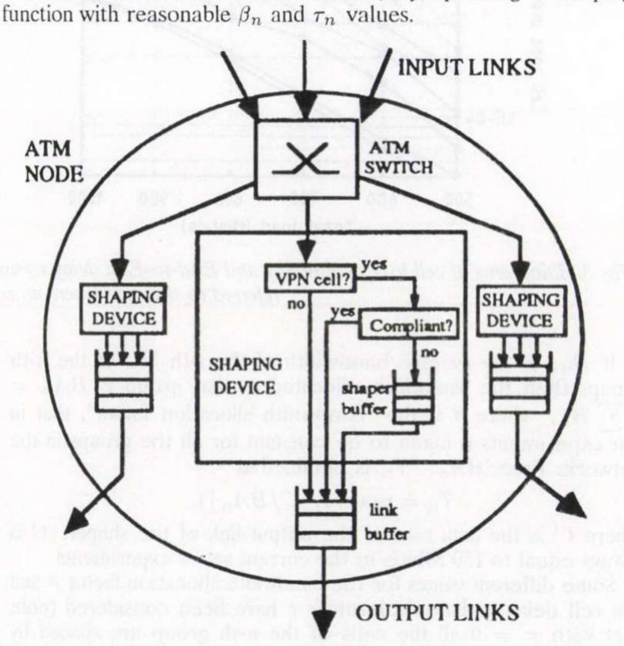

Fig. 5. Architecture of the traffic shaping mechanism implemented inside the ATM network.

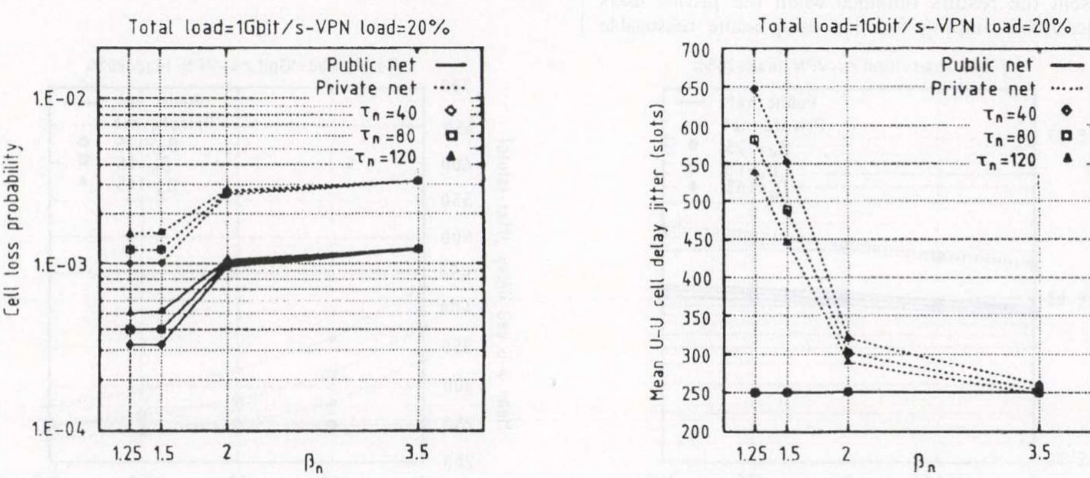

Fig. 6. Diagrams of cell loss probability and End-to-End delay versus β_n and τ_n. The figure is referred to the case where a shaping function is implemented inside the ATM network on the whole traffic of each VP used by the Private Network.

6.3. Shaping function applied both at the private users and inside the ATM network (two-levels)

The strategies previously analyzed are not exclusive and so it is possible to operate them simultaneously. In this way, as the first shaping level (users side) will reduce the burstiness of the traffic generated by each private user, the mechanism of shaping the traffic inside the ATM network (level 2) will work under better conditions, and some kind of improvement will be obtained.

In Fig. 7 we show the simulation results of this *two-level* control strategy. In the current set of simulations, the values $\beta_u = 1.5$ and $\tau_u = 80$ slots have been used. If we compare the diagrams of Fig. 7 with those of Fig. 6, we observe that an additional reduction of the cell loss probability can be obtained by operating at each private user a shaping algorithm *more restrictive* than that applied inside the ATM network. Note that the current strategy is better than the preceding one only when the β_u and τ_u values are more restrictive than the β_n and τ_n ones (otherwise, the increment of technological complexity implicit to the two-level shaping strategy does not translate into a QoS improvement, being so a useless cost). That is due to the fact that two cells generated by the same user are introduced in the ATM network being compliant to the user's parameters, and so, only in the mentioned case they are also compliant to the network ones.

On the other hand, the mean cell delay of the private traffic is lightly higher than that of the preceding strategy, while the mean delay of the background traffic is nearly not modified.

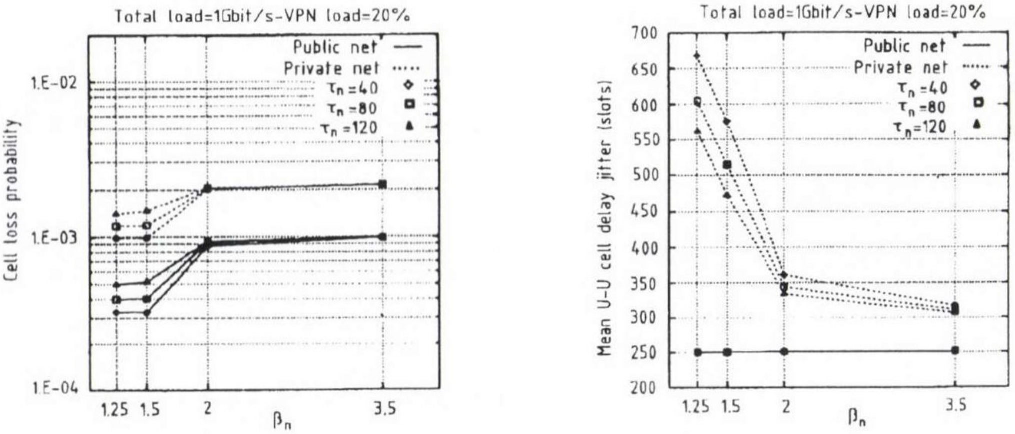

Fig. 7. Diagrams of cell loss probability and End-to-End delay versus β_n and τ_n. The figure is referred to the case where a two-levels (users and network) shaping function is implemented on the private traffic.

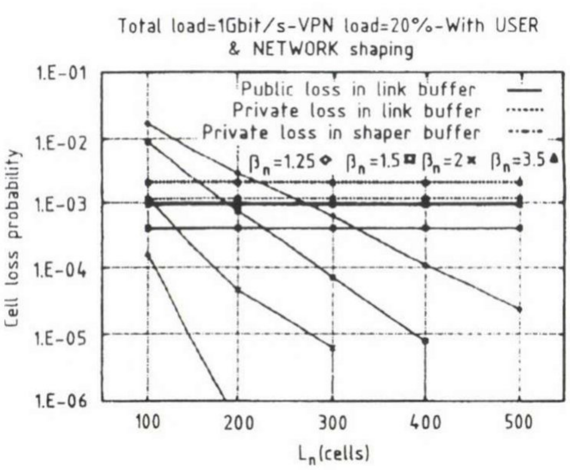

Fig. 8. Diagram of cell loss probability versus L_n and β_n. The figure shows separately the losses at the link-buffers and that at the shaper-buffers, and is referred to the case where a two-level (users and network) shaping function is operated on the private traffic.

A further step in our simulation study was to find an appropriate dimension for the shaper-buffers. In the preceding simulations we used the value $L_n = 1000$ cells in order to guarantee that no losses occur at the shaper-buffers. Now we want to see how the L_n value influences the performance of the shaping strategy. In Fig. 8 we show separately the cell loss probability at both the link-buffers and the shaper-buffers as a function of β_n and L_n, being τ_n equal to 80 slots. We can first observe that the cell loss probability at the link-buffers does not depend on the L_n value, but it depends only on then β_n value. Instead, the cell loss probability at the shaper-buffers decreases exponentially as a function of L_n. It is important to observe that for low L_n values the dominant cell loss probability is the one of the shaper-buffers, while for high L_n values it is the one of the link-buffers. In order to obtain a low overall cell loss probability, it is necessary to use "big" shaper-buffers and "small" β_n values. In this way, the losses at the link-buffers decrease (because of the high transmission restrictions applied to the private traffic) and the losses at the shaper-buffers are low because there is space enough in the buffers to memorize the not compliant cells.

An adequate dimension for the shaper-buffers can be set at the point where the losses at the shaper-buffers are about one order of magnitude smaller than that at the link-buffers. In fact, in Fig. 9 we show the overall cell loss probability and the cell delay diagrams as functions of L_n and β_n, only for small β_n values. It can be observed that all the figures have an asymptotic behaviour when considered as functions of L_n.

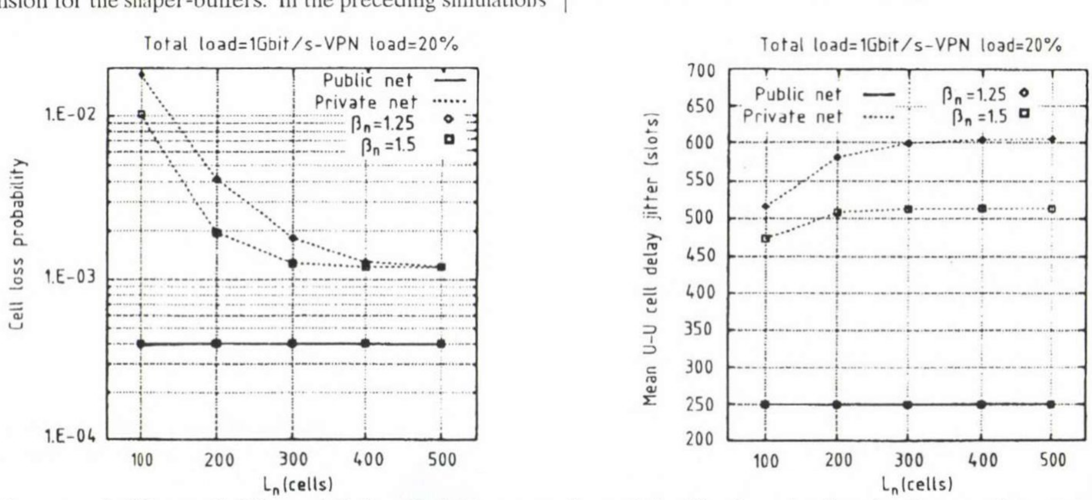

Fig. 9. Diagrams of cell loss probability and End-to-End delay versus L_n and β_n. The figure is referred to the case where a two-level (users and network) shaping function is implemented on the private traffic.

The asymptote value is reached in our simulation experiments for L_n nearly equal to 400 cells, which is a reasonable buffer capacity (observe that for L_n equal to 400 cells, the cell loss probability of the shaper-buffers is nearly one order of magnitude smaller than that of the link-buffers). The use of a higher shaper-buffer capacity (500 cells) does not improve the service performance because the overall quality is now determined by the cell loss probability at the link-buffers, which does not depend on the L_n value, as observed. So, an asymptotic behaviour is reached.

6.4. Comparison of the traffic shaping strategies

The last figure that we present (see Fig. 10) shows the improvement obtained with the three different traffic shaping strategies in a low load scenario. The total load of the network was set to 500 Mbit/s, and the percentage of traffic assigned to the B-VPN was 20 %. From Fig. 10 we can observe how the cell loss probability is degraded when the B-VPN service is introduced. The implementation of a shaping function at the private users side (S-U) permits to reduce the cell loss probability, but the implementation of the shaping function inside the ATM network (S-N) permits to improve that performance. Finally, the two-level shaping strategy (S-2) gives to the private users the best QoS without degrading the initial performance provided to the existing background traffic. The shaping parameters used in this simulation are $\beta_u = 1.25$, $\tau_u = 80$, $\beta_n = 1.5$, $\tau_n = 80$ and $L_n = 1000$.

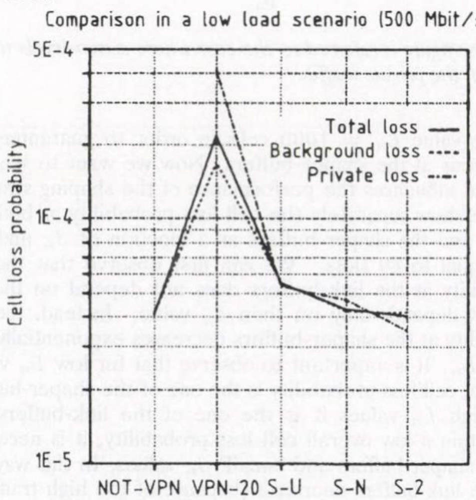

Fig. 10. Diagram of the improvement obtained in a low load scenario with the different traffic shaping strategies.

7. CONCLUSIONS

In this paper we have presented the results of a simulation study that shows the impact of introducing a Virtual Private Network service over an ATM network. As the network performance was degraded, some possible traffic shaping strategies were analyzed. The first strategy was the application of an adaptation of the GCRA algorithm to the traffic generated by each private user. As it was not sufficient to guarantee to the background users the maintenance of the QoS, we analyzed a second strategy that applied the shaping algorithm to each private VP inside the ATM network. That strategy permitted to improve the network performance. Finally, a two-level (users and network) shaping strategy was simulated, and a further improvement of the B-VPN service performance was obtained. The main conclusions of this work are the following ones:

- When a B-VPN is established over an ATM network, the public operator must control the private traffic behaviour in order to avoid any degradation of the performance provided to the background users.
- A useful way to realize that control is to implement inside the ATM network a shaping algorithm on the whole traffic of each VP used by the Virtual Private Network.
- Each shaping device must use a buffer big enough to allow a cell loss probability about one order of magnitude smaller than that existing at the link-buffers of the ATM infrastructure.
- The cell loss probability of the Virtual Private Network can be further reduced if each private user shapes its own traffic. The shaping function operated at the private users side must be more restrictive than that applied inside the ATM network.
- The price to be paid to reduce the cell loss probability using a shaping algorithm is always an increment of the End-to-End cell delay.

REFERENCES

[1] M. Ajmone Marsan, R. Lo Cigno, M. Munafò and A. Tonietti: "Simulation of ATM Computer Networks with CLASS", *Proc. of the 7th International Conference on Modeling Techniques and Tools for Computer Performance Evaluation*, Vienna, Austria, May 1994.

[2] CCITT Recommendation I.371, "Traffic Control and Congestion Control in B-ISDN", Geneva, Switzerland, 1992.

[3] S. M. Walters and M. Ahmed: "Broadband Private Networks and their evolution", *International Switching Symposium ISS'92*, Yokohama, Japan, October 1992.

[4] A. Ciccardi, P. Coppo, M. D'Ambrosio and V. Vercellone: "Broadband Virtual Private Networks on ATM networks", Technical report CSELT RR 93384, in Italian.

[5] P. Coppo, M. D'Ambrosio and V. Vercellone: "The A-VPN Server: a solution for ATM Virtual Private Networks", *Proc. of ICCS'94*, Singapore, November 1994.

[6] M. Ajmone Marsan, T. V. Do, L. Jereb, R. Lo Cigno and A. Tonietti: "Some simulation results on the performances of traffic shaping algorithms in ATM networks", *Proc. of the 2nd IFIP Workshop on Performance Modeling and Evaluation of ATM networks*, Bradford, U.K., July 1994.

Tomeu Fiol Coll received the Telecommunication Engineering degree from the Universitat Politècnica de Catalunya, Barcelona, Spain, in 1993 and the Master degree in Telecommunication and Computer Science from the Politecnico di Torino, Turin, Italy, in 1995. Since February 1995 he co-operates in some research projects at the Universitat de les Illes Balears, Mallorca, Spain. His research interests are High Speed Networking and Protocols.

Alberto Tonietti graduated in Electrical Engineering at the Politecnico di Torino, Turin, Italy, in 1965. He joined CSELT in 1967. Since 1969 his primary concern has been with teletraffic and network dimensioning problems. He is currently working on performance evaluation and dimensioning of ATM networks. He has participated in several European research projects and is currently member of the Management Committee of the project COST 242. He is also Associated Reporter of Question 17/2 of ITU-TSS.

CALL ADMISSION CONTROL OF ATM NETWORKS BASED ON MODULATING MARKOV CHAINS

J. LEVENDOVSZKY, S. IMRE, L. PAP, B. VARGA

DEPARTMENT OF TELECOMMUNICATIONS
TECHNICAL UNIVERSITY OF BUDAPEST
H-1111 BUDAPEST, SZTOCZEK U. 2., HUNGARY
E-MAIL: LEVENDOW@HIT.BME.HU

E. C. VAN DER MEULEN

DEPARTMENT OF MATHEMATICS
UNIVERSITEIT LEUVEN
ELESTIJNENLAAN 200B,
B-3000 LEUVEN (HEVERLEE), BELGIUM
E-MAIL: ECVDM@GAUSS.WIS.KULEUVEN.AC.BE

Efficient Call Admission Control (CAC) is one of the most important research issues in multi-access systems (like ATM networks) [1]. Its importance is due to the need for optimizing network utilization and providing a smooth flow of traffic. This task is achieved by limiting the number of users getting access to the system in order to prevent congestion. To implement an efficient CAC, however, the tail distribution of the aggregate traffic must be estimated, in the form of $P(\sum_j X_j > C) < e^{-\gamma}$ (where X_j represents the load presented by the jth user and C and γ stand for the node capacity and quality of service, respectively). This inequality can be relatively easily calculated when the users are regarded to be independent and memoryless (zero buffer approximation [5], [6], [7]). In the case of users with memory, the tail of the stationary queue distribution is of interest. If q denotes the stationary queue length formed by the unserved cells and L is the buffer length, then the cell loss probability $P(q > L)$ must be calculated by estimating the tail of q. The evaluation of the stationary queue distribution, however, hardly lends itself to tractable analysis, which makes the study of Markovian users a considerably more difficult case. Consequently, the paper is chiefly concerned with different estimations of the tail of the stationary queue length distribution. The novel approach to CAC lies in the methods, proposed to circumvent the cumbersome calculation of the stationary queue distribution (through the inverse z transform of the moment generating function). The exclusion of inverse z transform is achieved by pole estimation and statistical inequalities, which are based on the stationary moment generating function derived by the modulating Markov chain technique [2], [5]. The concluding numerical analysis compares the efficiency of the different estimation techniques used for CAC.

1. INTRODUCTION

The traffic situation at an ATM node can be modeled in the following way [2]:

There is a stream of cells emitted by the users (being subject to a modulating Markov process), which is loaded into a buffer with length L. A single server serves one cell in each time slot (the content of the buffer is decreased by one in each slot). As a result, the length of the queue formed by the waiting cells at time instant n (denoted by q_n) fulfils the following stochastic differentia equation:

$$q_{n+1} = q_n - \Delta_{q_n} + a_{n+1}, \tag{1}$$

where

$$\Delta_{q_n} = \begin{cases} 1 & \text{if } q_n > 0 \\ 0 & \text{if } q_n = 0 \end{cases}$$

and a_{n+1} is the generated load in the $n+1$st time instant. Since a_n is a modulating Markov chain, it can be characterized by the probabilities $P(S_{n+1} = j, a_{n+1} = k \mid S_n = i)$, where S_n refers to the inner state of the users, which is a homogeneous finite-state, aperiodic Markov chain. Our basic concern is to derive the stationary queue length distribution, defined as $\pi_k^{(i)} = \lim_{n\to\infty} P(q_n = k, S_n = i)$ characterizing the network in the state of equilibrium. The tail distribution of the stationary queue length

$$P(q_{stationary} > L) = \sum_i \sum_{k>L} \pi_k^{(i)} \tag{2}$$

is of special interest, as it relates to the cell loss probability. Based on the tail, the call admission can be performed as accepting or rejecting users to enforce the fulfillment of the following inequality

$$P(q_{stationer} > L) = \sum_i \sum_{k>L} \pi_k^{(i)} \le e^{-\gamma}, \tag{3}$$

where γ is a given constant, often referred to as Quality of Service (QOS). For example, if a new user wants to be admitted to the network, then the tail of the aggregate traffic must be evaluated and the new call can only be accepted if inequality (3) holds, otherwise it should be rejected.

As it was pointed out in the literature [3], [4], to calculate the the tail distribution is an extremely hard problem, which proves to be rather infeasible with restricted computational power. Therefore, we attempt to estimate the tail by using two different approaches:

- Obtaining the z transform of the stationary distribution through the Pollacek-Khintchin equation [1] and then applying some statistical bounds.
- Using the pole estimation technique related to the Perron-Frobenious eigenvalue of the underlying chain.

It is noteworthy, that the latter approach is similar to the work of Sohraby [2], where the full characterization of the tail distribution (the coefficents of the Perron-Frobenious eigenvalue) is omitted, though.

2. HOW TO ESTIMATE THE TAIL IF THE STATIONARY MOMENT GENERATING FUNCTION IS GIVEN?

Let us tentatively assume that the z transform of the stationary queue length distribution

$$Q(z) := \lim_{n\to\infty} \sum_{i=0}^{\infty} P(q_n = i) z^i$$

is given. Instead of calculating the tail distribution directly by performing an inverse z transform, we are going to estimate $P(\lim_{n\to\infty} q_n > L)$ based on the knowledge of $Q(z)$, in order to circumvent the cumbersome computations of the direct method. It must be parenthetically remarked, though, that the evaluation of $Q(z)$ is not a trivial task by any means (see the next section).

The first option to estimate the tail is given by the Markov inequality. Taking into account that $Q'(1) = Eq$, the following estimation can be used for the cell loss probability

$$P(q_{stationary} > L) \le \frac{Q'(1)}{L}.$$

The inequality above has the advantage that there is no need for the full knowledge of $Q(z)$ to evaluate the tail.

In order to get a sharper estimation, one can use the Chernoff bound in the following fashion:

$$P(q_{stationary} > L) \leq \frac{Q(z)\mid_{z=r}}{r^L},$$

where the parameter r is optimized as

$$r_{opt}: \quad \frac{d \log Q(r)}{dr} = Lr^{-1} \tag{4}$$

It is obvious that there is a trade off for the tighter bound, which appears in the fact that the whole $Q(z)$ must be known and equation (4) must be solved, as well. This makes the Chernoff bound rather impractical for CAC.

Another method to avoid the full evaluation of $Q(z)$, is based on the algebraic properties of the moment generating function. In this case, one can exploit the fact that $Q(z)$ is given as a division of two polynomials $Q(z) = A(z)/B(z)$, $A(z) = \sum_{j=1} a_j z^j$ and $B(z) = \sum_{i=1} b_i z^i$. To obtain the stationary queue length distribution from $Q(z)$, the invers z transform has to be performed through the residuum method

$$P(q = i) = \sum_k \frac{A(\beta_k)}{B'(\beta_k)} \beta_k^i,$$

where $\beta_k : \mid \beta_k \mid < 1$, $\forall k$ denotes the roots of polynomial $B(z)$ and $B'(z) = \frac{dB(z)}{dz}$. To derive an upper bound, one can choose the largest pole (the closest one to the unit circle) and obtain

$$P(q = i) = \sum_k \frac{A(\beta_k)}{B'(\beta_k)} \beta_k^i \leq \alpha\beta^i, \tag{5}$$

where $\alpha := N \max_k \frac{A(\beta_k)}{B'(\beta_k)}$ and $\beta := \max_k \beta_k$. Hence, that tail distribution can be estimated in the form of

$$P(q = i) \approx \alpha\beta^i. \tag{6}$$

From this expression, the CAC can be directly performed as accepting only those users, whose aggregate traffic fulfills the following inequality

$$P(q > L) = \sum_{i > L} \alpha\beta^i = \frac{\alpha\beta^L}{1 - \beta} < e^{-\gamma}. \tag{7}$$

It is worthwhile to notice that in this case only the maximal pole and its coefficient must be known instead of the whole $Q(z)$.

3. DERIVING THE MOMENT GENERATING FUNCTION OF THE STATIONARY QUEUE LENGTH DISTRIBUTION

After clarifying how to use $Q(z)$ for tail distribution estimation and consequently for CAC, let us embark on its calculation. To obtain $Q(z)$, first the aggregate traffic must be modeled by the means of modulating Markov chains, which gives ground to the description of $q(k)$ as a modulating chain, as well.

The aggregate traffic (or load) is described by the transition probabilities $P(S_{n+1} = j, a_{n+1} = k \mid S_n = i)$, which express the change in the statistical nature of the load when a state transition occurs from $S_n = i$ to $S_{n+1} = j$. From these probabilities one can build up a generator matrix $\mathbf{A}(z)$, the elements of which are defined as

$$a_{ij}(z) := \sum_k P(S_{n+1} = j, a_{n+1} = k \mid S_n = i) z^k. \tag{8}$$

(It is easy to see that $\mathbf{A}(1) = \mathbf{P}$ where $\mathbf{P}$ denotes the stochastic matrix of the underlying chain S_n.) Thus, the stochastic matrix of the doublet (q_n, S_n) (denoted by $\mathbf{R}$) can be written into the following form:

$$\mathbf{R} = \begin{bmatrix} \mathbf{A_0} & \mathbf{A_1} & \mathbf{A_2} & \mathbf{A_3} & \cdots \\ \mathbf{A_0} & \mathbf{A_1} & \mathbf{A_2} & \mathbf{A_3} & \cdots \\ 0 & \mathbf{A_0} & \mathbf{A_1} & \mathbf{A_2} & \cdots \\ 0 & 0 & \mathbf{A_0} & \mathbf{A_1} & \cdots \\ \vdots & \vdots & \vdots & \vdots & \ddots \end{bmatrix}, \tag{9}$$

where $\mathbf{A_i}$ is the ith coefficient in the corresponding Laurent expansion of $\mathbf{A}(z)$

$$\mathbf{A}(z) = \sum_{i=0}^{\infty} \mathbf{A_i} z^i.$$

Since we are interested in the stationary distribution only, our aim is to obtain the following z transforms:

$$Q_j(z) := \lim_{n \to \infty} \sum_{i=0}^{\infty} P(q_n = i, S_n = j) z^i \quad \forall j,$$

which can be arranged into a vector

$$\mathbf{Q}(z) := \begin{pmatrix} Q_1(z) \\ Q_2(z) \\ Q_3(z) \\ \vdots \end{pmatrix}$$

with respect to index j. Similarly to the derivation of the Pollaczek-Khinchin equations [2], [4] $\mathbf{Q}(z)$ fulfills the following expression

$$\mathbf{Q}^\mathrm{T}(z)(z\mathbf{I} - \mathbf{A}(z)) = (z - 1)\mathbf{Q}^\mathrm{T}(0)\mathbf{A}(z). \tag{10}$$

Here $\mathbf{I}$ denotes the identity matrix and the boundary vector $\mathbf{Q}(0)$ is uniquely determined by the zeros of the determinant $det(z\mathbf{I} - \mathbf{A}(z))$ and by the equation $\mathbf{Q}^\mathrm{T}(0)e = 1 - \varrho$ (where ϱ is the utilization of the mutiplexer). By rearranging equation (10), $\mathbf{Q}(z)$ is obtained as

$$\mathbf{Q}^\mathrm{T}(z) = (z - 1)\mathbf{Q}^\mathrm{T}(0)\mathbf{A}(z)(z\mathbf{I} - \mathbf{A}(z))^{-1}, \tag{11}$$

which could now pave the way to the application of Chernoff bound to estimate the tail distribution. In this case, the tail estimation is done in the following fashion

$$P(q_{stationary} > L) \leq Y,$$

where

$$Y := \max_i \frac{Q(z)|_{z=r_i}}{r_i^L} \quad r_i : \frac{d \log Q_i(r)}{dr} = Lr_i^{-1}.$$

The analitical evaluation of $\mathbf{Q(z)}$, however, is extremely difficult if not impossible. Thus we focus our attention on the application of Markov inequality and pole estimation technique, which do not need the full knowledge of $\mathbf{Q(z)}$.

3.1. *CAC by Markov inequality*

When applying the Markov inequality, we are only concerned with the calculation of the expected value of the stationary distribution. This can be evaluated by using the first derivative of the moment generating function, in the form of $\mathbf{Q}'(1) = E[q]$. It can be easily proven that the following equation holds if the pole $z = 1$ is excluded

$$\mathbf{Q}^\mathrm{T}(z)|_{z=1} = (z - 1)\mathbf{Q}^\mathrm{T}(0)\mathbf{A}(z)(z\mathbf{I} - \mathbf{A}(z))^{-1}|_{z=1} = \mathbf{0}^\mathrm{T}. \tag{12}$$

Thus, by differentiating both sides of equation (10), we obtain

$$\mathbf{Q}'^\mathrm{T}(z)(z\mathbf{I} - \mathbf{A}(z)) + \mathbf{Q}^\mathrm{T}(z)(z\mathbf{I} - \mathbf{A}(z))' = \\ = \mathbf{Q}^\mathrm{T}(0)\mathbf{A}(z) + (z - 1)\mathbf{Q}^\mathrm{T}(0)\mathbf{A}'(z).$$

Substituting $z = 1$ and recalling (12) yields

$$\mathbf{Q}'^\mathrm{T}(1) = (\mathbf{I} - \mathbf{A}(1))^{-1}\mathbf{Q}^\mathrm{T}(0)\mathbf{A}(1). \tag{13}$$

Equation (13) can now be numerically evaluated since, $\mathbf{A}(1)$ is available from the corresponding traffic situation. To account for the most pessimistic situation, one can choose

$$E_{worst}q := \max_i Q_i'(1),$$

from which the tail of the stationary distribution can be estimated as

$$P(q > L) \leq \frac{\max_i Q_i'(1)}{L}. \tag{14}$$

Thus CAC can be performed by accepting those users, whose aggregate traffic satisfies the following inequality:

$$\frac{\max_i Q_i'(1)}{L} < e^{-\gamma}. \tag{15}$$

3.2. Call admission with pole estimation

Investigating equation (11), it is clear that the poles of the expression

$$(z\mathbf{I} - \mathbf{A}(z))^{-1}(z-1)\mathbf{Q}^{\mathrm{T}}(0)\mathbf{A}(z)$$

occur when $det(z\mathbf{I} - \mathbf{A}(z))$ becomes zero. If the eigenvalues of $\mathbf{A}(z)$ are denoted by $\lambda_i(z) \quad i = 1, 2, \ldots$ then (after a diagonal transformation) the poles are determined by the following equation:

$$\beta : \quad det(\beta\mathbf{I} - \mathbf{A}(\beta)) = \prod_i (\beta - \lambda_i(\beta)) = 0. \tag{16}$$

Instead of solving all equations, $(\beta - \lambda_i(\beta)) = 0 \quad \forall i$, simultaneously we are only concerned with estimating the eigenvalue $\Lambda(\beta)$, which lies closest to the unit circle, often referred to as Perron-Frobenious (PF) eigenvalue. With the PF eigenvalue one can calculate the largest pole β, by solving the following equation

$$\beta : \quad \Lambda(\beta) = \beta. \tag{17}$$

This pole plays the central role in the estimation of the stationary tail, yielding the approximation

$$\pi_i \approx N\alpha\beta^i.$$

Consequently, to find the maximal pole, the PF eigenvalue must be calculated which does not lend itself to tractable analysis, though. Nevertheless, one can solve equation (17) approximately, by using the the Laurent series expansion of $\Lambda(z)$ and truncating it after the second derivative

$$\beta = 1 + \varrho(\beta - 1) + \frac{\Lambda''(1)}{2}(\beta - 1)^2 + O(\beta - 1)^3.$$

The fact that the expansion is made around $z = 1$ is explained by the heavy traffic assumption [2] when the tail is supposed to be long, therefore z is close to one. It is also noteworthy that $\Lambda'(1) = \varrho$ is the total utilization of the multiplexer. Hence the calculation of β reduces to solving the following equation

$$\beta = 1 + \frac{2(1-\varrho)}{\Lambda''(1)}. \tag{18}$$

To our satisfication, expression (18) turns out to be a tractable numerical problem, since the second derivative of PF eigenvalue can be numerically calculated from the matrix $\mathbf{A}(z)$.

In this paper, the exact calculation of β is carried out for the case of *On/Off* sources, i.e. the users are either emitting cells at a certain rate or 'being silent' (not emitting at all). The duration of the *On* period (in number of slots) is denoted by t_{on}, whereas the duration of *Off* periods is denoted by t_{off}. The statistical characterization of *On* and *Off* periods are as follows:

$$P(t_{on} = i) := \kappa_i \quad P(t_{off} = i) := \theta_i.$$

The Markovian behaviour of the sources is taken into account by the following definitions:

$$x_i := P(t_{on} > i | t_{on} > i-1) = 1 - \frac{\kappa_i}{1 - \sum_{j=1}^{i-1} \kappa_j} \quad i \geq 1$$

$$y_i := P(t_{off} > i | t_{off} > i-1) = 1 - \frac{\theta_i}{1 - \sum_{j=1}^{i-1} \theta_j} \quad i \geq 1.$$

If the maximum duration of *On* (*Off*) periods is denoted by T_{on} (T_{off}), then the On/Off sources can be represented as a T_{on} state random process. Furthermore, the global state of the source can be described by the doublet (j, i), where $j = 1$ stands for the source being in the state *On* (if $j = 0$ then the source is in *Off* state) and i indicates the duration already spent in the indicated state. It is easy to conclude that the doublet (i, j) forms a Markov chain whose $\mathbf{A}(z)$ matrix (in the case of $T_{on} = T_{off} = 4$) can be given as

$$\mathbf{A}(z) = \begin{pmatrix} 0 & y_1 & 0 & 0 & (1-y_1)z & 0 & 0 & 0 \\ 0 & 0 & y_2 & 0 & (1-y_2)z & 0 & 0 & 0 \\ 0 & 0 & 0 & y_3 & (1-y_3)z & 0 & 0 & 0 \\ 0 & 0 & 0 & 0 & z & 0 & 0 & 0 \\ 1-x_1 & 0 & 0 & 0 & 0 & x_1 z & 0 & 0 \\ 1-x_2 & 0 & 0 & 0 & 0 & 0 & x_2 z & 0 \\ 1-x_3 & 0 & 0 & 0 & 0 & 0 & 0 & x_3 z \\ 1 & 0 & 0 & 0 & 0 & 0 & 0 & 0 \end{pmatrix}$$

From this matrix, one can calculate the second derivative of the PF eigenvalue as

$$\Lambda''(1) = \left(\frac{E\,t_{on}^2}{E\,t_{on}^2} + \frac{E\,t_{off}^2}{E\,t_{off}^2} - 2\right) \frac{E\,t_{on}}{E\,t_{on} + E\,t_{off}} \left(1 - \frac{E\,t_{on}}{E\,t_{on} + E\,t_{off}}\right)^2 E\,t_{on} - \frac{E\,t_{on}}{E\,t_{on} + E\,t_{off}} \left(1 - \frac{E\,t_{on}}{E\,t_{on} + E\,t_{off}}\right).$$

Since the above expression needs only the knowledge of the first and second order moments of t_{on} and t_{off}, these parameters are to be declared by the users when logging in to the network. As a result, the key equation to obtain β is

$$\beta \approx 1 + 2(1-\varrho) / \left\{ \left(\frac{E\,t_{on}^2}{E\,t_{on}^2} + \frac{E\,t_{off}^2}{E\,t_{off}^2} - 2\right) \frac{E\,t_{on}}{E\,t_{on} + E\,t_{off}} \left(1 - \frac{E\,t_{on}}{E\,t_{on} + E\,t_{off}}\right)^2 E\,t_{on} - \right.$$
$$\left. - \frac{E\,t_{on}}{E\,t_{on} + E\,t_{off}} \left(1 - \frac{E\,t_{on}}{E\,t_{on} + E\,t_{off}}\right) \right\}. \tag{19}$$

Going through similar calculations, equation (19) can be easily extended to the case of heterogeneous sources (the moments of t_{on} and t_{off} are different from source to source labeled by superindex i)

$$\beta \approx 1 + 2(1-\varrho) / \left\{ \sum_i \left(E\,t_{on}^{i^2} E\,t_{on}^{i^2} + \frac{E\,t_{off}^{i^2}}{E\,t_{off}^{i^2}} - 2 \right) \frac{E\,t_{on}^i}{E\,t_{on}^i + E\,t_{off}^i} \left(1 - \frac{E\,t_{on}^i}{E\,t_{on}^i + E\,t_{off}^i}\right)^2 E\,t_{on}^i - \right.$$
$$\left. - \frac{E\,t_{on}^i}{E\,t_{on}^i + E\,t_{off}^i} \left(1 - \frac{E\,t_{on}^i}{E\,t_{on}^i + E\,t_{off}^i}\right) \right\}, \tag{20}$$

which conludes the procedure for estimating the largest pole.

For the tail estimation, the coefficient α must also be evaluated. Unfortunately, it does not lend itself to analytical methods. Thus, in the lack of profound theoretical methods, one can utilize the common approach suggested in the literature, taking $\alpha = \varrho$ [5]. A more elaborated choice, providing a tighter bound on the tail, can emerge from extensive simulation (see the next section), where $alpha$ is set as $\alpha = \varrho/2$. This choice of α is verified by only simulation, though.

4. NUMERICAL RESULTS

In this section a comparative analysis of different tail distribution estimators is presented in the case of *On/Off* sources. The estimates are obtained as follows:

- Estimating the stationary tail by a histogram (performing the stochastic recursion (1) until it reaches its equilibrium). This method is accurate enough but impractical, it can only serve as a basis for comparison. (It is referred to as *Tail hist.* in the tables.)
- The largest pole is evaluated and the tail estimation is given as $\alpha\beta^L/(1-\beta)$. (It is referred to as *Tail pole est.* in the tables.)
- Using the pole estimation technique but the coefficient α is set to $\varrho/2$ and $\beta^{L-E\,q_{stationary}}$ instead of β^L, assuming that $\sum_{i>E\,q_{stationary}} \pi_i^{(j)} < 0.5$. This assumption was well established by simulations. (This estimation is referred to as *Tail pole' est.* in the tables.)
- The expected value of Eq is calculated and the Markov inequality used as a tail estimator. (It is referred to as *Tail Markov* in the tables.)

The results (obtained by setting the utilization of the multiplexer as $\varrho = 0.9639$, $\varrho = 0.8978$, $\varrho = 0.8716$ and $\varrho = 0.8317$, respectively) are summarized in the following tables.

$\varrho = 0.9639$			
L	7	12	17
Tail hist.	0.2558	0.0594	0.0106
Tail pole est.	0.5663	0.3873	0.2649
Tail pole' est.	0.4140	0.2831	0.1936
Tail Markov	0.9360	0.5460	0.3854

$\varrho = 0.8978$			
L	4	7	10
Tail hist.	0.2243	0.0389	0.0050
Tail pole est.	0.3594	0.1809	0.0911
Tail pole' est.	0.2840	0.1430	0.0720
Tail Markov	0.9961	0.5691	0.3984

$\varrho = 0.8716$			
L	7	12	17
Tail hist.	0.1542	0.0215	0.0017
Tail pole est.	0.2662	0.1094	0.0449
Tail pole' est.	0.2408	0.0989	0.0406
Tail Markov	0.8902	0.5087	0.3561

$\varrho = 0.8317$			
L	3	5	7
Tail hist.	0.1755	0.0410	0.0069
Tail pole est.	0.2501	0.1122	0.0504
Tail pole' est.	0.1866	0.0838	0.0376
Tail Markov	1.0000	0.6087	0.4348

As can be seen, the pole estimation methods always give better results than the Markov inequality.

In accordance with our expectation, the approximation provided by the pole estimation is tighter in the case of $\varrho = 0.9639$ which is close to one (heavy traffic assumption when the related Laurent series is expanded around $z = 1$).

5. CONCLUSION

In the paper, different methods were used to estimate the tail of aggergate traffic in the case of Markovian users. The obtained estimates were based on the Markov inequality and the estimation of the PF eigenvalue. Both methods can directly be applied to call admission in ATM networks, in the fashion that CAC can only accept those users whose estimated tail of traffic will not exceed a given threshold, parametrized by the QoS.

The developed estimates lent themselves to tractable calculations and were compared with each other in different traffic situations. As was expected, the estimate based on the PF eigenvalue provided tighter bound on the tail, threfore its application to CAC seems to be more favourable.

6. ACKNOWLEDGEMENT

The research reported here was partly supported by the Hungarian Scientific Research Foundation, Project No. F 014456 and the European Union, Project No. Copernicus 579.

REFERENCES

[1] de Prycker, M.: "*Asynchronous Transfer Mode Solution for Broadband ISDN*, Ellis Harwood Ltd. 1991.

[2] Sohraby, K.: "Flow Admission Control of ON-OFF Sources in High Speed Networks", *IEEE, GLOBECOM, San Francisco, 1994.*

[4] Eckberg, A., Dashi, B. and Zoccolilla, R.: "Controlling congestion in B-ISDN/ATM: Issues and Startegies", *IEEE Communication Magazine*, Vol. 29, No. 9, pp. 64-70, September 1991.

[3] Hui, J.: "Resource Allocation for Broadband Networks", *IEEE Journal on Selected Area of Communications*, Vol. 6, No. 9, pp. 1598-1608, December 1988.

[5] Hui, J.: *Switching and Traffic Theory for Integrated Broadband Networks*, Kluwer Academic Publishers, 1990.

[6] Yasuhiro, M.: "A Dimensioning Scheme in ATM networks", *Networks'92*, pp. 171-176, May 1992.

[7] Hiramatsu, A.: "ATM Traffic Control Using Neural Networks", *Neural Networks in Telecommunications*, edited by Yuhas, B. and Ansari, N., Kluwer Academic Publishers, 1994.

János Levendovszky graduated from the Technical University of Budapest in 1986, obtaining a summa cum laude degree in Communication Engineering. From 1986 to 1989 he was granted a research scholarship by the Hungarian Academy of Sciences for a Ph.D. He obtained his Ph.D. (Candidate of Science) in 1989 in the field of adaptive signal processing and stochastic approximation. From 1989 to 1990 he researched on neural networks and their optical implementation at the University of Oxford, sponsored by a Soros Fellowship. From 1990 to 1993 by the invitation of the Department of Mathemtics at the Catholic University of Leuven (Belgium) he filled to position of Free Researcher working on the mathematical foundations of neural network theory and statistical signal processing. From 1993 he is an associative professor at the Department of Telecommunications (TUB). His current interest lies in statistical traffic modelling and call admission theory of multi-user systems. He published numerous papers in the above mentioned fields and is involved in international projects related to ATM networks and stochastic control.

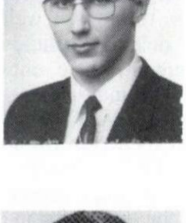

Sándor Imre graduated from the Technical University of Budapest in 1993. He is a third year Ph.D. student on the Department of Telecommunications at the Technical Univeristy of Budapest. His present interests are in the field of Call Admittion Control problem of ATM networks.

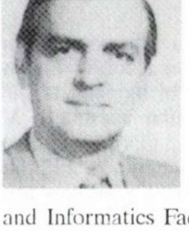

László Pap graduated from the Technical University of Budapest at the Telecommunication Branch of the Electrical Engineering Faculty in 1967. He received the candidate of sciences and the Academy doctor of sciences degrees in 1980 and 1992, respectively. Since 1992, he is a full university professor and head of the Department of Telecommunications, and since 1994, dean of the Electrical Engineering and Informatics Faculty. His main interests include communication theory, encoding, modulation, synchronization, further mobile communications and the theory of modern telecommunications sytems.

Edward C. van der Meulen received the B.S. degree in mathematics and physics and the M.S. degree in mathematics from the University of Leiden, Netherlands, and the Ph.D. degree in statistics from the University of California, Berkeley, in 1958, 1962, and 1968, respectively. From 1968 to 1975, he served on the faculty of the Department of Statistics at the Univeristy of Rochester, Rochester, NY. From 1972 to 1974, he was on leave at the Mathematical Center in Amsterdam. He has been a Professor of Mathematics at the Katholieke Universiteit Leuven, Belgium, since 1975. From 1975 to 1991, he was for short periods Visiting Professor or Visiting Scientist at the Stanford University, Ohio State University, Syracuse University, and the Technical University of Budapest. In 1985, he spent one month at South China Institute of Technology, Gaungzhou, in the framework of the Chinese University Development Project. His research interests include multi-user information theory and information-theoretic statistical inference. In 1983, he organized the Fourth Benelux Symposium on Information Theory, Haasrode, Belgium. Van der Meulen is a member of ASA, IMS, ISI, MAA, INNS, the Dutch Society for Statistics, and Sigma Xi. He is also a Member of the Editorial Board of the American Journal of Mathematical and Management Sciences. Currently he is Chairman of the Information Theory Chapter in the Benelux Section of IEEE.

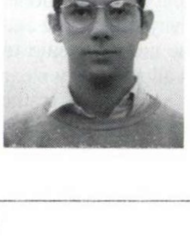

Balázs Varga graduated from the Technical University of Budapest in 1993. He is a third year Ph.D. student on the Department of Telecommunications at the Technical Univeristy of Budapest. His present interests are in the field of Call Admittion Control problem of ATM networks.

COMPARISON OF THREE CONTROL LAWS FOR STATISTICAL MULTIPLEXING IN ATM

N. M. MITROU and K. P. KONTOVASILIS

NATIONAL TECHNICAL UNIVERSITY OF ATHENS
COMPUTER SCIENCE DIVISION
HEROON POLYTECHNEIOU 9, ZOGRAPHOU,
GR-15773, ATHENS, GREECE E-MAIL: MITROU@PHGASOS.SOFTLAB.NTUA.GR

Three approximate formulae, relating the effective rate of an ATM ON/OFF stream with its main parameters, the system's dimensions and the desired Quality of Service in a statistical multiplexing environment, are presented and compared in terms of the achieved multiplexing gain and the associated computational complexity. The formulae can be solved for the main traffic parameters involved, and used in traffic shaping and control functions, thereby referred to as control laws.

1. INTRODUCTION

Statistical multiplexing of traffic addresses the sharing of a resource among many statistically varying sources, where the cumulative peak demand may exceed the available resource capacity. Such a peak, however, should occur with only a small probability, in order to maintain an affordable performance. The statistical multiplexing is quantified by means of the *multiplexing gain*, defined as the ratio of the resource utilization with statistical multiplexing to the resource utilization with peak demand allocation to each source.

Exploitation of the statistical multiplexing gain is of prime importance for a successful introduction of the ATM networks [1], because it is the only way to obtain a cost-effective operation under significant and diverse traffic demands. An ATM multiplexer is equipped with two resources: the *output link capacity* and *the buffer space*. One component of the multiplexing gain springs from the mutual compensation of the instantaneous rates of the input sources, so that their aggregate peak rate rarely exceeds the link capacity, and a second component is obtained from buffering the information that overflows the link, so that losses actually occur with an even smaller probability.

As a consequence of the law of large numbers, the component of the multiplexing gain arising from the rate compensation can only be significant when a large number of statistically varying streams are serviced by a high link capacity. There is no doubt that this is the case with the ATM link capacity being of the order of some hundred Mb/s or even Gb/s. Regarding the other multiplexing gain component, due to buffering, an endless debate has been being maintained for years about the appropriate buffer sizes for the ATM multiplexers and switches. Initially, the prominent position was in favour of small buffers, just adequate to absorb the congestion arising from the instantaneous arrivals of cells (cell-level congestion). As the time passes, however, more and more people support the idea of using larger buffers in order to get a gain also from buffering. The ABR service proposed in various fora (ATM Forum is one of them) is based on this idea [2].

To take advantage of the burstiness of the information sources and exploit the gain out of their statistical multiplexing, appropriate traffic models and control mechanisms become necessary. The traffic engineer, when confronted by a choice over a class of models, is usually faced with a trade-off between simplicity and accuracy. One traffic model that combines simplicity of the associated analysis and control procedures with the ability to describe features that are important to statistical multiplexing, like burstiness, is the fluid ON/OFF model. In a fluid setting, non-bursty sources are conveniently represented by a constant rate, equal to their mean rate. The simplest non-trivial bursty fluid model comprises two states, corresponding to two activity rates, low and high. When the low rate is taken to be null, the model is said to characterise an ON/OFF source. These models allow a very clear representation of burstiness, with a minimum number of traffic parameters; this feature, together with their increased tractability, has made Markovian ON/OFF models very popular for the description of bursty traffic. In some instances, sources that exhibit a more complex rate-fluctuations pattern can be modelled as the superposition of a number of ON/OFF sources. But even more important is the fact that shaping, when it is allowed , can be used to enforce a simple ON/OFF pattern.

Towards this end, three approximate, closed-form formulae, derived for Markovian fluid ON/OFF models, are presented in this paper and compared to each other. The comparison is performed in terms of the multiplexing gain achieved and the computational complexity associated with the formulae application in solving traffic control problems. Following this introduction, the rest of the paper is organized as follows: Section 2 gives some background information and the basic assumptions for the traffic models under consideration. It also defines the *Effective Rate* as an alternative way of quantifying the statistical multiplexing, and introduces the main traffic control problems in such an environment. Section 3 presents the approximate control formulas and compares them with respect to the two aspects mentioned above. Finally, section 4 gives some concluding remarks.

2. PRELIMINARIES AND ASSUMPTIONS

The basic assumption stated hereafter is that a great deal of applications in the future B-ISDN are expected to be able to afford some transfer delay, in order to make use of cheep transport services over ATM, featuring an increased utilization of network resources through statistical multiplexing. All data-exchange applications surely belong to this category. Even some real-time applications, however, like MPEG-coded live video exchange, could be developed to survive in such an environment.

Following the basic assumption stated above and the more general argumentation presented in the introduction, some further assumptions and requirements are:

A1. Buffers large enough to support statistical multiplexing are available at the multiplexers and switches of the network;

A2. The network can implement Connection Admission Control (CAC) and Usage Parameter Control (UPC) based on statistical traffic profiles;

A3. The sources are able to shape the generated traffic streams in order to enforce the contracted profiles.

With respect to A1 above, the dimensioning of the buffers will be based on the type of traffic expected to pass through as well as on the target QoS figures (e.g. maximum delay percentiles or cell-loss rates). A2 is an obvious requirement, since only statistical types of control can cope with statistical multiplexing. Finally, by virtue of A3, the terminals are assumed to be able to produce traffic streams that, on the one hand fit their own traffic generation features, on the other hand they could be modelled, monitored and controlled in an easy way. As one step further, the terminals are assumed to be able to change the traffic shaping parameters adaptively, according to congestion feedbacks issued by the network.

The configuration considered here is shown schematically in Fig. 1. Each of the sources of Fig. 1(a) produces a traffic stream of the ON/OFF type, being also able to control its main traffic parameters, namely the peak rate c, the mean burst size V (measured by the number of cells produced in an ON period) and the burstiness B, defined as the ratio between peak rate and the mean rate r. Although mean values of statistical quantities are difficult to control, we assume that short-term averages (over a window) can in principle be enforced.

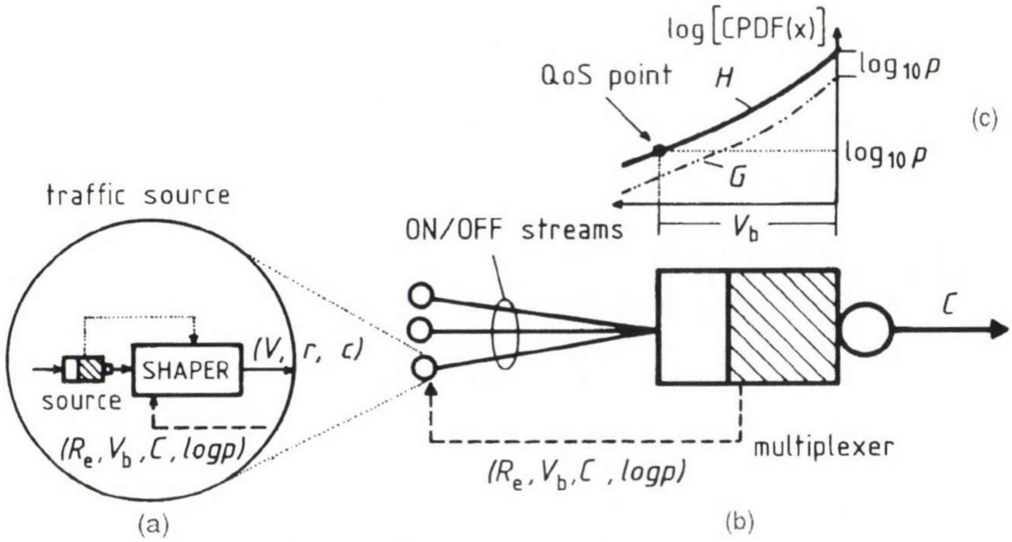

Fig. 1. An ATM statistical multiplexing environment.
(a) traffic sources with adaptive shaping capabilities; (b) multiplexer; (c) complementary distribution of buffer occupancy

We further assume that the produced streams can be approximately modelled as two-state Markovian fluid streams, i.e. as continuous flows of information at a constant rate in the ON state, with exponentially distributed ON and OFF duration. In that case, the three-parameter vector $[V, r, c]$ uniquely describes each stream. Due to the large-buffer assumption, cell-level congestion, which cannot be modelled by the fluid flow approximation method, is insignificant in our setting.

In conclusion, the two-state Markovian fluid modelling is appropriate for the case at hand, it can cope with statistical multiplexing and, most importantly, it can offer a manageable solution to the main traffic control problems, as we will see in a later section. In the remaining of this section some important performance measures of a statistical multiplexer, as the one of Fig. 1(c), will be presented and the effective rate consumed by a stream in such an environment will be defined.

2.1. Performance measures

Considering a single ATM multiplexing stage, as in Fig. 1, the performance measure that can yield useful engineering figures (e.g. cell-loss probability bounds or cell-delay percentiles) is the buffer occupancy distribution in a complementary form (CPDF), i.e.

$$CPDF(x) \equiv G(x) = \Pr\{buffer\_content > x\}. \quad (1)$$

For general Markovian fluid models, in particular, $G(x)$ is expressed as a sum of exponential terms:

$$G(x) = \sum_i \alpha_i e^{z_i x}, \quad (2)$$

where z_i are eigenvalues of an associated eigenvalue problem and α_i are coefficients obtained by enforcing appropriate boundary conditions. In an infinite buffer setting only negative z_i eigenvalues participate. On the other hand, a fixed buffer size (say V_b), results in engaging both positive and negative z_i; in addition, the coefficients α_i change and are derived by a more complicated and less stable system of equations (see e.g. [5]). The changes are required to allow for a probability mass accumulated at $x = V_b$, which is absent in the infinite buffer setting.

When the system is engineered for a low probability of overflow, however, then $G(x)$, $\forall x < V_b$, as computed by the infinite buffer assumption, is a tight upper bound to the probability of exceeding threshold x at the respective finite-buffer model of size V_b [5], [6]. In particular, $G(V_b)$ is a tight upper bound to the probability of overflow. The claim for upper bound is justified since in the infinite buffer configuration information is always stored and never rejected; in result, a certain buffer threshold is exceeded in the infinite buffer configuration with higher probability than in the finite buffer case. The claim for tightness becomes clear when it is realized that, since the threshold V_b is 'hit' with a very low probability, the extra boundary condition present at the finite buffer configuration does not have a significant effect on the performance metrics of interest.

In this paper we are always interested in small probabilities of overflow. We will, therefore, justifiably use infinite buffer models and substitute the probability $G(V_b)$ of exceeding threshold V_b for the probability of overflow in a real system of buffer size V_b.

One further point that usually escapes the attention of the traffic analyst is the following: *for bursty traffic, the buffer occupancy observed at a random instance is different from what is seen by the arriving cells; and it is the latter that actually determines the desired performance figures.* Let $H(.)$ denote the complementary buffer occupancy distribution seen by the arriving cells. For Markovian fluid models and an infinite buffer setting a Little's like formula relating $G(.)$ and $H(.)$ has been proven in [6]:

$$H(x) = \frac{G(x)}{\rho} \forall x \geq 0, \quad (3)$$

where ρ is the normalized load or the utilization of the output link. In a logarithmic scale, the G and H curves have a constant distance equal to $\log_{10} \rho$, as shown in Fig. 1(c). Under high utilization conditions, however, ρ is close to 1 and this distance is small.

As for $G(x)$, in a real system, with a finite buffer of size V_b, $H(x)$ provides an upper bound to both the delay percentile (at any $x < V_b$) and the cell-loss probability (calculated at $x = V_b$). The larger the buffer size, the tighter these bounds become.

2.2. Traffic control problems and Effective Rate definition

Consider the multiplexer of Fig. 1 fed by N independent input streams. The multiplexer is serviced by a link rate C and has an available buffer capacity V_b. By fixing a QoS point (V_b, $\log p \equiv \log_{10} p$), as shown in Fig. 1(c), one can find a value for the link capacity such that $H(V_b) = p$ (in [6] it was shown that for Markovian fluid streams, $H(x)$ is uniformly continuous with respect to all the parameters involved for any $x > 0$, so that a unique value for C always exists). This is the *Bandwidth Allocation problem*. Inversely, for a given link capacity, C, the *Connection Admission Control problem* consists in finding the maximum number N of streams (this is for identical streams or *homogeneous traffic*; for heterogeneous traffic the problem is to find whether a new stream can be added to an already established set) such that $H(V_b) \leq p$. The *Traffic Shaping problem*, finally, consists in finding and enforcing in appropriate traffic profiles on the multiplexed streams in order to respect the given QoS criterion.

To facilitate solving the control problems outlined above, a notional parameter called *Effective Rate or Effective Bandwidth* should be defined for each stream expressing the rate effectively spent by the stream in the given environment. Ideally, this parameter would be given by a relationship of the type

$$R_e = f([traffic\ profile]C, V_b, \log p) \qquad (4)$$

solvable for any of the parameters involved. However, in the general case of heterogeneous traffic, this problem is not well-defined. But even if we succeeded in defining and solving it, the dependence of R_e on the characteristics of the other traffic streams multiplexed together would deprive it of the generality and flexibility that is actually needed for traffic control.

Two main approaches to bypassing the above drawback can be found in the literature. The first one defines the Effective Rate in a homogeneous multiplexing environment, where such a definition is conceptually simple. For the sake of completeness, we quote this definition from [7]:

Definition 1: Given that N traffic streams of a certain class are multiplexed together, there can be found a unique output rate C_N, such that $\Pr\{\text{queue} > V_b\} = p$ (specified). Then, the *effective rate* required by each stream within this multiplexing environment is defined as $R_e = C/N$. Calculating the R_e as a function of N and making a suitable interpolation between the discrete points $(C_N, C_N/N)$, $N = 2, 3, \ldots$ (a linear interpolation is sufficient in the context of this work), a continuous curve is derived allowing the definition of R_e for a fixed output rate (instead of fixing the number of multiplexed streams). The continuous alternative permits, in principle, an extension to cases where heterogeneous streams share a common output link.

However, the effective rate thus defined is not summable in heterogeneous settings, i.e. the cumulative bandwidth required by an heterogeneous mix exceeds the sum of the effective rates of the participating streams. It has been found experimentally, however, that the effective rate thus defined can be safely used also in heterogeneous environments, as far as no strong differences appear among the stream parameters.

The second approach consists in considering each stream alone and using asymptotic upper bounds to the respective $H(x)$, e.g. the dominant-eigenvalue approximation of (3) (see [9] and relevant work cited there). This approach is conservative compared to the first one, because it takes into account the gain only from buffering. On the other hand, it leads to some nice properties, like the *summability* of effective rates (which is very desirable in heterogeneous traffic environments) and the simplicity of the respective computations, compared to the first approach.

In the sequel, we will confine ourselves to similar ON/OFF Markovian traffic streams, in which case each stream is described by the triplet $[V, r, c]$ (the mean burst size, the mean rate and the peak rate) and the relationship (4) is further refined as

$$R_e = f([V, r, c], C, V_b, \log p). \qquad (5)$$

Relationships in the form (5), which can be solved for the traffic, resource and QoS parameters involved, are referred here as *control laws*.

3. THREE APPROXIMATE CONTROL LAWS AND THEIR PERFORMANCE

In this section three control laws in the form (5) will be derived and compared to each other with respect to the multiplexing gain achieved and the respective computational complexity when used in traffic control problems. The first two are directly based on the effective rate definitions outlined in the previous paragraph, while the third one is a further processed approximation. The comparison reveals ranges of parameter values where the three laws converge to each other.

The first control law takes into account both multiplexing and buffering gains. As elaborated in the Appendix, for large output capacity values, the effective rate exhibits a square-root dependence on the link capacity, in the fashion of Eq. (6a) below. Taking this as a starting point, we enforced this particular functional form by suitable fitting of data (so as to ensure conservative approximations over the parameter range of interest). The data were obtained by a fluid-flow based multiplexing analysis tool which, given a number N of homogeneous ON/OFF streams, the stream parameters $[V, r, c]$, the buffer size V_b and a desired probability of overflow p, yields the smallest link capacity C_N, with which the buffer content does not exceed V_b with probability greater than p. This fitting results in approximate functional relationships shown in the equations below and displayed in Fig. 2–5. Thus, from Fig. 2 we get:

$$H_1: \qquad \frac{c - R_e}{R_e - r} = \alpha\sqrt{\frac{C}{c}} + b\,, \qquad (6a)$$

from Fig. 3:

$$a \cong a_a B + b_a, \quad b \cong a_b B + b_b;$$

from Fig. 4:

$$\begin{cases} \ln(a_a - a_0) \cong a_{aa}\frac{V_b}{V} + b_{aa} \\ a_b \cong a_{ab}\frac{V_b}{V} + b_{ab}, \; b_b \cong a_{bb}\frac{V_b}{V} + b_{bb}, \end{cases}$$

and from Fig. 5:

$$\begin{cases} \ln(a_0 - k_1) \cong k_2 \log_{10} p + k_3 \\ \ln(a_{ab} - k_4) \cong k_5 \log_{10} p + k_6 \\ \ln(a_{bb} - k_7) \cong k_8 \log_{10} p + k_9 \end{cases}$$

while the rest of the parameters involved $(b_a, a_{aa}, b_{aa}, b_{ab}, b_{bb})$ are approximately constant.

Optimizing the fitting in the Least-Squares sense over the range

$$20 < \frac{V_b}{V} < 200, \quad 5 < B < 100, \quad -3 < \log_{10} pM < -9$$

we get the expressions for the parameters a and b in (6a):

$$a \cong [0.075 + e^{0.4\log_{10} p - 0.7186} + e^{-0.03\frac{V_b}{b} - 1.3}]\frac{c}{r} + 0.3,$$

$$b \cong [(0.035 + e^{0.3321\log_{10} p - 1.28})\frac{V_b}{V} - 1.1]\frac{c}{r} + \qquad (6b)$$

$$+ (0.043 + e^{0.281\log_{10} p - 1.247})\frac{V_b}{V} - 1.7$$

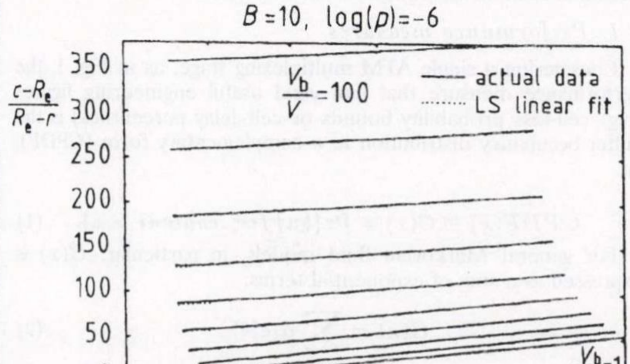

Fig. 2. Effective rate versus output capacity

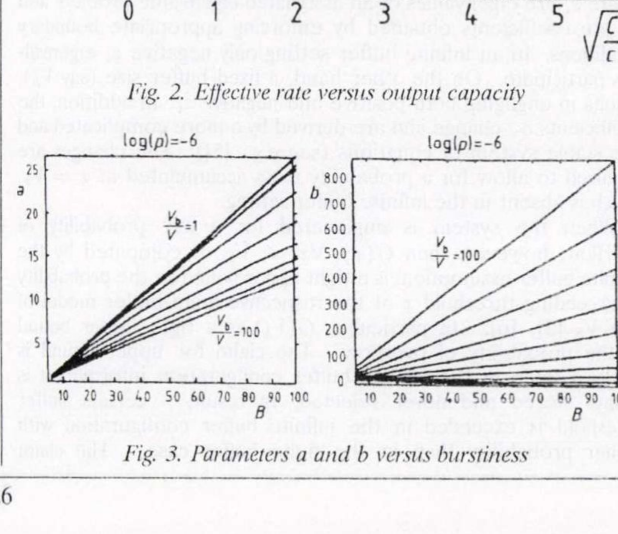

Fig. 3. Parameters a and b versus burstiness

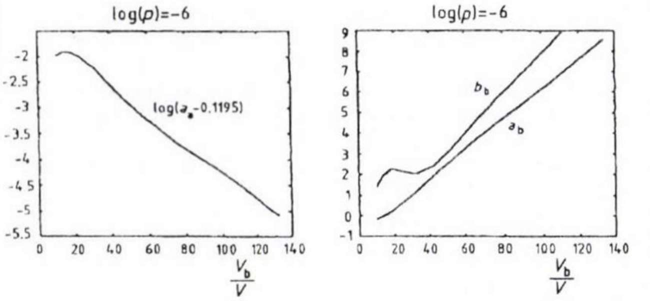

Fig. 4. Parameters a_a, a_b, b_b versus mean volume of bursts

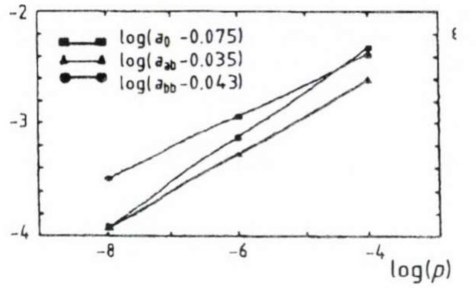

Fig. 5. Parameter variation with overflow probability

Since this control law takes into account the gain from multiplexing, it yields the most efficient (i.e. the smallest) values for R_e. As already mentioned, however, these effective rates are not summable in heterogeneous multiplexing environments. As a result, H_1 is to be used in environments where the multiplexed streams do not have great differences in their traffic descriptors.

The second control law takes into account only the gain from buffering, while it ignores the multiplexing gain arising from rate cancellations. As fully explained in [8], this is equivalent to making the conservative approximation $H(x) = e^{-z_0 x}$, where we have kept only the asymptotically dominant component in (2) and replaced with the maximum possible coefficient. Such conservative effective rates for general Markovian fluids are discussed in [9]. We now specialise these results for the ON/OFF case at hand; each ON/OFF stream with parameter vector $[V, r, c]$ must be attributed an effective rate so that $H(V_b) = e^{-z_0 V_b} = p$ i.e.

$$z_0 = -\ln p/V_b. \tag{7}$$

The value of R_e acts as the output capacity of a fictitious queuing element loaded simply by this ON/OFF stream. Then [3], z_0 is given as:

$$z_0 = -\frac{c}{c-r} V \frac{1 - r/R_e}{1 - R_e/c}. \tag{8}$$

Combining (7) and (8), the equation yielding the effective rate is

$$\mathrm{H}_2: \qquad \frac{\log_{10} p}{\log_{10} e} = -\frac{c}{c-r}\frac{1 - r/R_e}{1 - R_e/c}\frac{V_b}{V}. \tag{9}$$

Note that since the multiplexing gain is not taken into account, R_e does not depend on the link capacity C any more. Further, this effective rate is both conservative and summable [8], [9]. Unlike the first control law, it can be used in a heterogeneous environment, in which case the cumulative bandwidth required by a number of (generally heterogeneous) streams is simply the sum of the respective effective rates.

The third law is derived as the limit of (9) by letting the peak rate c to take arbitrarily high values. This corresponds to batch arrivals of ATM cells into the buffer, providing crude but useful approximations in cases where the peak rate of the multiplexed streams is either not known or difficult to control. By letting $c \to \infty$ but maintaining a fixed mean rate r (9) gives H3:

$$\mathrm{H}_3: \qquad \frac{\log_{10} p}{\log_{10} e} = -(1 - \frac{r}{R_e})\frac{V_b}{V}. \tag{10}$$

An alternative way to arrive to (10) is to solve the quadratic arising from (9) for R_e (it always yields a unique positive solution, satisfying $r < R_e < c$), replace c by its equivalent rB and let $B \to +\infty$. The limit yields the value of R_e satisfying (10). It has to be noted that this third control law cannot be used unconditionally; the buffer size has to be adequately large. Specifically, by observing that $0 < 1 - r/R_e < 1$, (10) immediately yields the relevant condition, viz.

$$\frac{-\log_{10} p}{\log_{10} e}\frac{V}{V_b} < 1. \tag{10a}$$

Since the third control law results from a limiting operation on the second law, it retains the summability property.

Fig. 6 gives us a first feeling of how the three formulae behave. They have been solved for $\log p \equiv \log_{10} p$ (H_1 numerically, the other two directly) and drawn against V_b, along with the actual $H(.)$. We should remind the reader once again that $H(.)$ is by itself an approximation of the real system behaviour, due to the fluid flow modelling and the infinite-buffer boundary condition used for the solution. We can see from Fig. 6 that H_1 is the most accurate, while H_3 the crudest one of the three. Although all of them are in closed form, the balance between accuracy and computational complexity, when applied in traffic control problems, may be in favour of any of the three. Thus, even the very simple and crude H_3, may be appropriate in some settings.

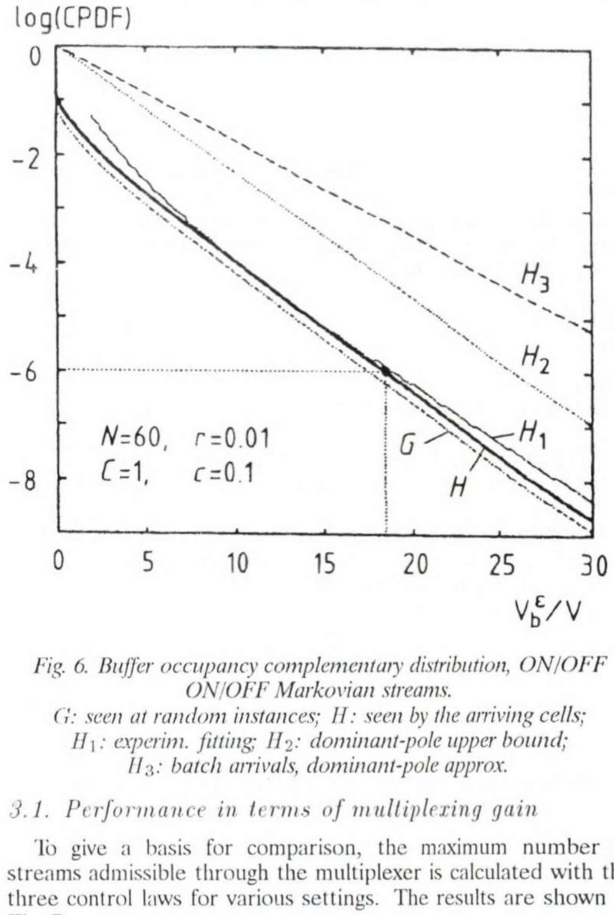

Fig. 6. Buffer occupancy complementary distribution, ON/OFF ON/OFF Markovian streams.
G: seen at random instances; H: seen by the arriving cells;
H_1: experim. fitting; H_2: dominant-pole upper bound;
H_3: batch arrivals, dominant-pole approx.

3.1. Performance in terms of multiplexing gain

To give a basis for comparison, the maximum number of streams admissible through the multiplexer is calculated with the three control laws for various settings. The results are shown in Fig. 7.

In Fig. 7(a) the three curves are drawn with a varying peak rate, keeping the rest of the parameters fixed. We can see that the three curves converge for large values of the peak rate, while diverge significantly for smaller values (note that the horizontal axis displays the ratio of the link over peak rate). Naturally, the number of admissible connections calculated by the third law is not affected at all by the changes in the peak rate, since the latter is not involved in (10) (it has been assumed infinitely high). The other two curves maintain a rather constant distance for small values of c.

Fig. 7(b) gives the three curves with varying target overflow probability, logp. They diverge for smaller ordinate values, but H_1 and H_2 tend to keep a constant distance.

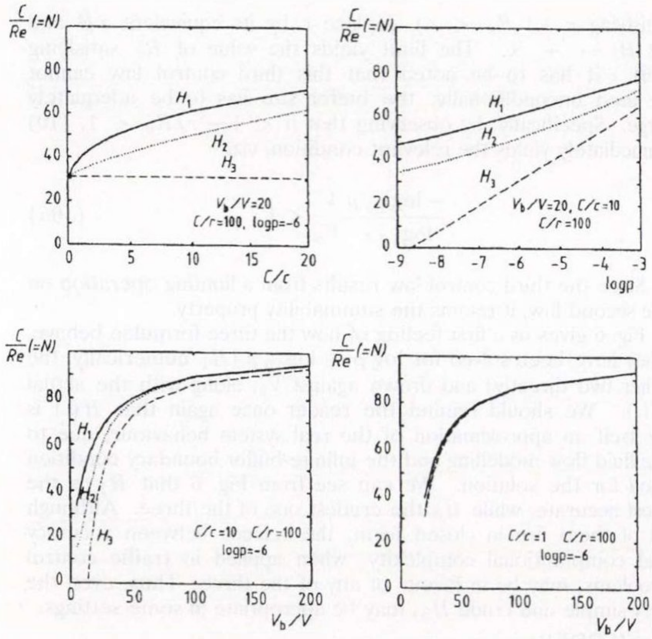

Fig. 7. Maximum number of admissible connections with the three control laws.
(a) versus peak rate; (b) versus overflow probability;
(c), (d) versus buffer size

Fig. 7(c) plots the three curves against the ratio V_b/V, i.e. the buffer capacity normalized with respect to the mean burst size of the multiplexed streams. The larger this ratio, the smaller the distance between the curves. Figs. 7(b) and 7(c) have been drawn for a peak rate equal to one tenth of the link rate. Fig 7(c) is repeated in 7(d) for $c = C$. For such a high peak rate we can see that the three curves become indistinguishable for relatively large buffers.

To conclude:

- The three control laws converge to each other for
  - large peak rate values (Fig. 7(a)) and/or;
  - large ratios V_b/V, for constant logp (Fig. 7(c)) and/or;
  - large buffer overflow probabilities, for constant V_b/V (Fig. 7(b)).
- The three laws are quite close already with $c = C$ (the full link speed) as shown in Fig. 7(d). Thus the simplest of them, H_3, can be efficiently used when cell emission is performed at full speed and the buffer size is adequately large compared to the mean burst size of the multiplexed streams.

An obvious, yet quite important observation regarding the above three laws is that they *depend only on normalized values of rates (e.g. over the output link capacity) and burst volumes (over the buffer capacity)*, and not on the respective absolute values. This implies that the results are absolutely scalable to any system dimensions (link capacity and buffer capacity), as far as all respective quantities are also scaled appropriately.

3.2. Computational complexity

The second criterion for comparing the three laws is with respect to the computational complexity implied in solving the main traffic control problems outlined in section 2. As expected, of course, there is a trade-off between complexity and accuracy.

Regarding the CAC problem, all the three laws are first-order equations with respect to N (or R_e). For bandwidth allocation, one must solve for C, i.e. a third-order equation for H_1, a second-order equation for H_2, and a first-order one for H_3. For shaping, finally, we may use peak-rate shaping, solving for c, or mean rate shaping, solving for r. In the first case one has to solve a third-order equation for H_1, a second-order equation for H_2, while H_3 cannot be used for peak-rate shaping, since this parameter is not involved in H_3. In the case of mean-rate shaping, r is calculated by solving a second-order equation through H_1, and a first-order one through H_2 or H_3.

It is important to emphasise the simplicity of H_3 and its usefulness when the multiplexing conditions allow an affordable approximation through it. Such cases can be found in an ABR service environment [2], where large buffers (compared to the bursts of the multiplexed streams) and relatively large threshold-overflow probabilities may be allowed. Then, according to the curves of Fig. 7, H_3 may be not too far from the other two laws and its usage greatly simplifies calculations. It has to be kept in mind, however, that condition (10a) must hold before H_3 may be used.

4. CONCLUSION

The fluid flow approximation provides tight upper bounds to the performance of an ATM multiplexer when it is equipped with a large buffer size compared to the mean burst size of the streams multiplexed through. The ON/OFF fluid model, in particular, is a good compromise between the model's ability to exploit the gain from statistical multiplexing of bursty streams and the simplicity of the associated analysis and control procedures.

Three approximate closed-form formulae, quantifying the statistical multiplexing of fluid ON/OFF streams, have been presented in this paper and compared to each other. Each of them represents a different solution of R_e the trade off between simplicity and accuracy. There have been identified, however, ranges of parameter values where the three formulae converge to each other, in which cases the simplest of them, H_3, can be used without sacrificing the multiplexing gain. Another important observation was that all of the quantities involved (rates, burst volumes) are normalized over the respective system capacities (link capacity and buffer capacity, respectively). Thus the results are directly scalable to any system dimensions.

5. APPENDIX

Here we give an explanation for the asymptotic square-root dependence of the effective rate according to the first control law, in the fashion of equation (6a). First recall that, asymptotically, the link capacity contributes only to the reduction of R_e due to rate cancellations (the multiplexing gain effect), while a large buffer size contributes to the buffering gain, as explained in describing control laws H_2 & H_3. Consequently, in the asymptotic regime where the link capacity $C \rightarrow \infty$, while the buffer size remains fixed, the important portion of the reduction of R_e comes from the multiplexing gain, and the buffering gain may be neglected. We are thus entitled to proceed on our asymptotic reasoning by considering a bufferless model. Indeed, assume N similar streams are multiplexed; let r be the mean rate and σ^2 the rate-variance of each of these streams. For ON/OFF sources, $\sigma = c/\sqrt{B}$. Now, for each value C in the range (N_r, N_c) and a target overflow probability p, we can find a constant $K(N,p)$ such that the cumulative rate does not exceed

$$C \equiv Nr + \sqrt{N}\sigma K(N,p) \qquad (A1)$$

with probability greater than p. As $N \rightarrow \infty$, by virtue of the central limit theorem $K(N,p) \rightarrow \Phi^{-1}(1-p)$, where $\Phi(.)$ is the standard Gaussian distribution function. We now view (A1) as an equation defining the maximum number of streams N that can be admitted given a link capacity C, so as the overflow probability p is respected. Eq. (A1) becomes

$$Nr + \sqrt{N}\sigma K(C,p) = C, \qquad (A2)$$

where the fact that C is now the independent variable is emphasized. The asymptotic behaviour due to the central limit theorem now translates to

$$\lim_{C \to \infty} K(C,p) = \Phi^{-1}(1-p). \qquad (A3)$$

Since p remains fixed, the dependence of $K()$ on p is henceforth dropped. By recalling that the effective rate is defined as $R_e = C/N$, (A2) becomes

$$R_e = \sqrt{R_e}\sigma \frac{K(C)}{\sqrt{C}} + r.$$

By letting

$$d \equiv \frac{\sigma K(C)}{2\sqrt{C}}, \qquad (A4)$$

this yields a quadratic for R_e with unique solution

$$\sqrt{R_e} = d + \sqrt{d^2 + r},$$

equivalently,

$$R_e - r = \frac{2r}{\sqrt{1 + r/d^2} - 1}. \qquad (A5)$$

With this result,

$$\frac{c - R_e}{R_e - r} = \frac{c - r}{R_e - r} - 1 = (B - 1)\frac{r}{R_e - r} - 1,$$

and, by replacing (A5),

$$\frac{c - R_e}{R_e - r} = \frac{B - 1}{2}\sqrt{\frac{r}{d^2} + 1} - \frac{B + 1}{2}.$$

By substituting d from (A4) and recalling that, for ON/OFF sources $\sigma^2 = c^2/B = rc$, we get

$$\frac{c - R_e}{R_e - r} = \frac{B - 1}{2}\sqrt{\frac{4}{K^2(C)}\frac{C}{c} + 1} - \frac{B + 1}{2} \cong$$

$$\cong \frac{B - 1}{\sqrt{K(C)}}\sqrt{\frac{C}{c}} - \frac{B + 1}{2}, \qquad (A6)$$

for $\frac{C}{c} \gg \frac{K^2(C)}{4}$. Now, since $K(C)$ tends to a bounded limit as $C \to \infty$, we immediately get the functional dependence on (6a). Eq. (A6) also explains the approximate linearity of coefficients a and b in (6a), as a function of the burstiness B.

REFERENCES

[1] ITU-T Recommendation I.311, "B-ISDN General Network Aspects", Geneva, April 1991.

[2] ATM Forum Traffic Management SWG "Baseline performance using PRCA rate-control", *ATM Forum*/94-0597, July 1994.

[3] D. Anick, D. Mitra and M. M. Sondhi: "Stochastic theory of a data-handling system with multiple sources", *Bell Syst. Tech. J.* 61 (1982) 1871-1894.

[4] L. Kosten: "Stochastic theory of data-handling systems with groups of multiple sources," in *Performance of Computer Communication Systems*, H. Rudin and W. Bux, Eds. Amsterdam, The Netherlands: Elsevier, 1984, pp. 321-331.

[5] T. E. Stern and A. I. Elwalid: "Analysis of separable Markov-modulated rate models for information-handling systems", *Advances in Applied Probability*, Vol. 23, 1991, pp. 105-139.

[6] K. P. Kontovasilis and N. M. Mitrou: "Bursty Traffic Modeling and Efficient Analysis Algorithms via Fluid-Flow Models for ATM IBCN", *Annals of Operations Research*, Vol. 49, special issue on Methodologies for High Speed Networks (1994) pp. 279-323.

[7] N. M. Mitrou, K. P. Kontovasilis and E. N. Protonotarios: "A closed-form expression for the Effective Rate of ON/OFF traffic streams and its usage in basic traffic control problems", presented in the *International Teletraffic Seminar*, St. Petersburg, June 1995.

[8] R. Guerin, H. Ahmadi and M. Naghshineh: "Equivalent capacity and its application to bandwidth allocation in high-speed networks", *IEEE JSAC*, Vol. 9, pp. 968-981, 1991.

[9] A. Elwalid and D. Mitra: "Effective bandwidth of general Markovian sources and admission control of high speed networks", *IEEE/ACM Trans. on Networking*, June 1993, pp. 329-343.

Nikolas M. Mitrou received the undergraduate Diploma degree in electrical engineering from the National Technical University of Athens (NTUA) in 1980, the MSc degree in Systems and Control from the UMIST, Manchester, in 1982 and the PhD degree in electrical engineering from the NTUA in 1986. From 1982 to 1985 he was with the Nuclear Research Centre "Demokritos", Athens, where he was involved in signal processing projects. From 1986 to 1988 he worked at the National Defence Research Centre, Athens, for the development of a low-bit-rate voice coding system. In 1988 he joined the NTUA as a senior researcher, where he is currently an assistant professor in the Department of Electrical and Computer Engineering. His research interests are in the areas of digital communication systems and signal processing, with emphasis on the architecture, modeling, performance evaluation and optimization of integrated networks, local area networks and mobile communication systems, digital video and multimedia, having more than 20 publications in the above fields. He has actively participated in several RACE and ESPRIT projects. Dr. Mitrou is a member of the IEEE, and of the Technical Chamber of Greece.

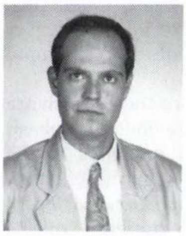

Kimon P. Kontovasilis received the Diploma in Electrical Engineering from the National Technical University of Athens (NTUA), Athens, Greece, the MSc degree in Computer Science from the North Carolina State University (NCSU), Raleigh, NC and the PhD degree in Electrical Engineering from NTUA, in 1987, 1990 and 1993 respectively. From 1987 to 1988 he was with NTUA as a research assistant involved in the analysis of B-ISDN switches. From 1988 to 1990 he was with NCSU, as a teaching/research assistant, involved in research on numerical methods for Markov-Chain problems. Since October 1990 he is with NTUA, involved in research on modelling, analysis and control of Broadband Digital Communication Networks. He has participated in the RACE R1022 project, within Task Group TGIII (the Traffic Group). Currently, he is a senior researcher in the Telecommunications Institute of the Nuclear Research Center "Demokritos". His research interests include modelling, analysis and control of Broadband Communication Networks, Queueing Theory, Numerical Methods for Markov Chain Problems and Numerical Linear Algebra.

TRAFFIC MEASUREMENTS FROM WORKING NETWORKS

L. J. BOTTOMLEY
DUKE UNIVERSITY
DURHAM, NC, USA
E-MAIL: LAURAB@EE.DUKE.EDU

A. NILSSON
NORTH CAROLINA STATE UNIVERSITY
RALEIGH, NC, USA
E-MAIL: NILSSON@ECEYV.NCSU.EDU

The shape and behavior of ATM network traffic, both at the input to the network before adaptation and inside the network after packets have been broken into 53 byte cells, has significant impact on issues ranging from proper connection admission control to switch dimensioning. Peak allocation methods which rely on standardized traffic parameters may allow for guaranteed quality of service but may be grossly wasteful of network resources when the carried traffic is highly bursty. Indeed, these methods may prevent the types of statistical multiplexing gains that ATM was initially conceived to allow. Significant need exists for traffic measurements which can give a clearer picture of real traffic behavior. This paper describes traffic measurements taken from several working networks, including the VISTAnet ATM network, various Ethernet networks and a token ring network. The measurements were collected from both the customer-side of the network, before terminal adaptation, and also from the network side of the terminal adaptor. The Ethernet traffic was measured at a university campus and at the gateway to the Internet from a supercomputing center at MCNC in North Carolina, and the token ring data was taken from a heavily loaded ring at IBM in Research Triangle Park, North Carolina. Each of these data sets consists of packet/cell interarrival times and packet lengths (where appropriate). The measurements were fit to various theoretical traffic models, as was deemed appropriate. The aim was to find mathematically tractable models which would adequately describe both the temporal and amplitude aspects of the measured stochastic process. All of the models examined were chosen for their ability to account for correlation between interarrival times. Careful attention was taken to make sure that any conclusions gleaned from the experiment are statistically justifiable.

1. INTRODUCTION

ATM networks present a great opportunity for networking of heterogeneous applications with a single unifying protocol. But this same opportunity brings a significant number of challenges. Connection admission, policing, monitoring, switch design, routing algorithms and decision points: all are areas where development and study is needed. Each of these diverse research and development topics requires assumptions about traffic behavior.

As ATM networks are assembled and evolve, they will likely receive input from a variety of sources. One class of sources will almost certainly be legacy LANs. Router companies have already demonstrated their recognition of this fact as they begin to offer products designed to route from Ethernet, token ring, etc. networks to ATM. For this reason, characterization of legacy LAN traffic plays an important role in depiction of ATM input traffic.

Few would argue that the best assumptions are those which are verified by measurement. Indeed, to that end, much emphasis has been placed on traffic measurement and modeling in the literature. The earliest studies of data traffic recognized its bursty behavior [7]. Since then work has proceeded along different directions to model traffic with the specific emphasis relying strongly on the area of interest of individual researchers (i.e. whether they are queuing theorists, switch or protocol designers, etc.). Measurements have been taken from lower speed networks such as Ethernet (e.g. [12], [1], [10], etc.) and from higher speed ATM networks, as they have become available [5], [11], [9], [13].

Of the ATM measurements referenced above, the last three deal with data from the VISTAnet network. The ATM data presented in this paper is from the same network. Analysis techniques are the same across all types of data. VISTAnet is a working ATM network whose driving application is Dynamic Radiation Therapy Planning (DRTP) (see Fig. 1). The network essentially operates as a metacomputer allowing a physician to have access to computing capabilities from a medical workstation which far exceed any previously available. The network allows treatment plans to be completed in very short periods of time using multiple sources of data.

The measurements presented here are from the traffic stream sent from the CRAY-YMP supercomputer across the network to the Pixel-Planes 5 machine. This is the network location where the greatest volume of traffic flow takes place. Section 3 presents data from both the user and network sides of the user/network interface (UNI). The authors gratefully acknowledge the assistance of MCNC in the acquisition of the traffic data.

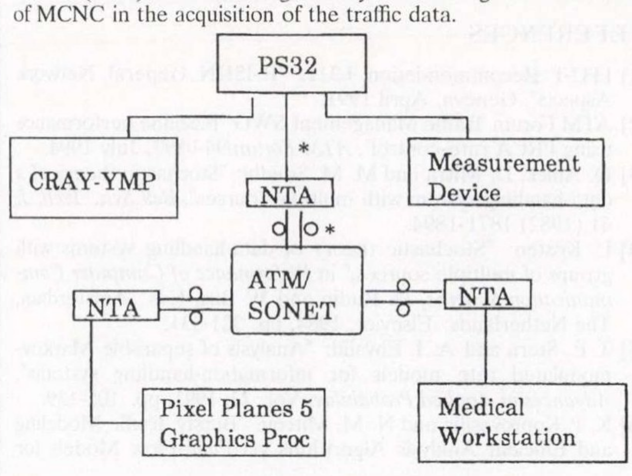

Fig. 1. Traffic Data Collection Sites

The Ethernet data were measured from very busy network segments at North Carolina State University and from MCNC in Research Triangle Park, North Carolina. The University is clearly an academic environment, while the MCNC data includes some academic and some industry traffic.

The token ring data is from an all industry environment at IBM in Research Triangle Park. The assistance of John Bartoles of ISSC is gratefully acknowledged

2. EXPERIMENTAL FRAMEWORK

2.1. Data Collection

Our philosophy of data collection is aimed at acquiring statistically significant samples during known busy periods. This traffic sampling technique is based on the sampling techniques used for many years in the telephony field. Traffic on any communications network is inherently non-stationary, as it is related to work and/or play patterns of human beings. Sampling during known busy periods is done acquire a "worst-case" traffic characterization which can be assumed to be stationary. The statistical techniques used for data analysis are formulated on the basis of stationarity.

Data traffic is recorded by a network analysis device as a series of interarrival times and packet lengths (where appropriate). The data recorded from the pre-UNI side (i.e. before terminal adaptation) of the VISTAnet network were collected by a network analysis device designed by MCNC called HILDA. This device collects data from a 800 Mbps parallel HIPPI interface. The pre-UNI data consists of both interarrival times and packet lengths. Post-UNI data was collected from VISTAnet using a data collection system custom designed by Bell South to record cell interarrival times at the OC-12 rate [TALM94]. During the collection period all arrivals were recorded.

Token ring data were recorded using a network sniffer, and Ethernet data with an Excelan EX5000 Series LANalyzer.

Experimental interarrival time density functions were calculated from the data by binning all interarrival times between 0 and 1 ms long, between 1 and 2 ms long, etc. Then serial correlation coefficients (sometimes called autocorrelation coefficients) were calculated from the data for a number of lags less than or equal to the square root of the number of packets/cells recorded [4]. This view of the data separates out the two aspects of a stochastic process in terms of amplitude and temporal variation to allow us to (theoretically) look at how each aspect affects network behavior.

2.2. Stochastic Models

After the experimental data have been processed, the data are fit to theoretical stochastic models. Many types of models exist, and the choices for candidate models are dictated by the uses to which the resultant models are to be put. Analytical queuing solutions and real-time monitoring algorithms versus complex network simulations may allow for quite different models in terms of complexity.

The candidate model initially considered for the data described in this paper is a three-state Markovian arrival process. The process description has been slightly modified to reduce the number of parameters in the model to six. Previous work with Ethernet data has shown that four parameter models, such as a two-state MMPP or two-state MAP, are unable to characterize correlation found in the data [2]. It was hoped that the increased number of parameters would allow for an adequate representation of correlation.

A three state MAP process generates arrivals according to the state of an underlying continuous time Markov chain. In each of the three states, arrivals are generated according to a Poisson process with an arrival rate i. Movement between states is not tied to arrivals. Thus, the Markov chain could change states multiple times between arrivals or not at all. The process is then described by two matrices, $\mathbf{D}_0$ and $\mathbf{P}$.

$$\mathbf{D}_0 = \begin{bmatrix} -\lambda_1 & 0 & 0 \\ 0 & -\lambda_2 & 0 \\ 0 & 0 & -\lambda_3 \end{bmatrix}$$

$$\mathbf{P} = \begin{bmatrix} p_{11} & p_{12} & p_{13} \\ p_{21} & p_{22} & p_{23} \\ p_{31} & p_{32} & p_{33} \end{bmatrix}$$

where $\mathbf{D}_0$ is the matrix of arrival rates and $\mathbf{P}$ is the transition probability matrix of the discrete time Markov chain embedded at arrival epochs. The unconditional probability density function of interarrival times, x, can be derived to be hyperexponential:

$$f(x) = p_1 \cdot \lambda_1 \cdot e^{-\lambda_1 x} + p_2 \cdot \lambda_2 \cdot e^{-\lambda_2 x} + p_3 \cdot \lambda_3 \cdot e^{-\lambda_3 x},$$

where the p_i and λ_i obtained from the usual $\mathbf{pP} = \mathbf{p}$ and $\mathbf{pe} = 1$. The serial correlation coefficients for the three state MAP are derived in [14]. A six parameter fit was obtained by restricting movement in the continuous time Markov chain to states of higher number (i.e. the transition from state 1 to state 2 was disallowed, etc.).

For a model to be sufficient, both dimensions of a stochastic process must be fit simultaneously. This can be accomplished by a variety of fitting techniques. Moment matches that include either a combination of interarrival moments and correlation coefficients and/or moments of the counting process can account for temporal and amplitude variation. Other techniques aim to extract parameters from some function of the arrival process such as entropy [6] or work [8]. The technique used for this paper is to fit the experimental interarrival density function and serial correlation coefficients to the equations for the theoretical model to determine the six model parameters.

We chose the equation fitting technique for a variety of reasons. We are very interested in how different aspects of an arrival process affect the behavior of a network. There is some evidence that the shape of the interarrival density function plays an important role in queuing behavior [3]. In addition, work is in progress to demonstrate the role of correlation in queuing behavior. Preliminary results indicate that an inaccurate representation of degree of correlation can drastically affect queuing losses and/or delays for simple queuing models [15] and ATM switch models [11]. One of the uses we hope to make of the current traffic measurements is to explore how correlation extending across many lags versus correlation of large magnitude affect various aspects of network behavior.

3. TRAFFIC DATA

Four types of data are presented in this paper: one set of data was collected from the user side of the user/network interface of the VISTAnet network and one set from the network side of the same interface. The different sets of data were taken when the same application was running on the network, but not simultaneously.

Two sets of Ethernet data and one set of token ring data are also described. The data are presented in the form of packet/cell interarrival time density functions, serial correlation coefficients, and packet length distributions, as appropriate.

3.1. User-side ATM Data

Seven different sets of data were recorded each containing in the vicinity of 10,000 packets. Fig. 2 shows an example of a packet interarrival density function from the user-side of the network interface. The speed of the HIPPI interface where data were recorded is 800 Mbps.

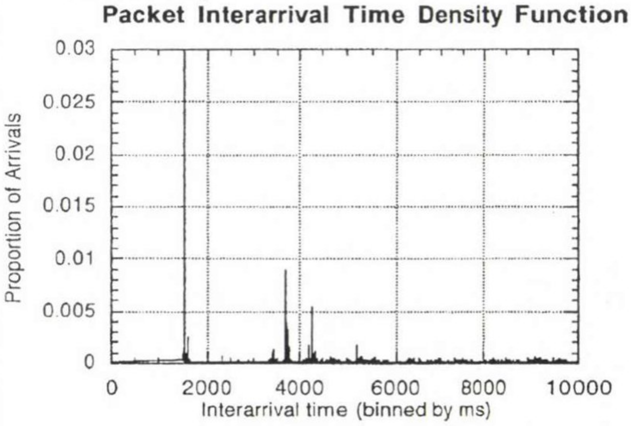

Fig. 2. Packet Interarrival Time Density Function

Each of the data sets exhibit a similar form for their interarrival time density functions. Keeping in mind that these are single application measurements, the structure is interesting. Essentially, most of the energy in the density function is placed at a few likely interarrival times.

Serial correlation coefficients for the same data set are pictured in Fig. 3. Recall that serial correlation coefficients are defined as:

$$\rho(k) = \frac{E[(X_i - E(x)) \cdot (X_{i+k} - E(X))]}{\sigma_x^2},$$

where X_i is the ith interarrival time and σ_x^2 is the variance of interarrival times.

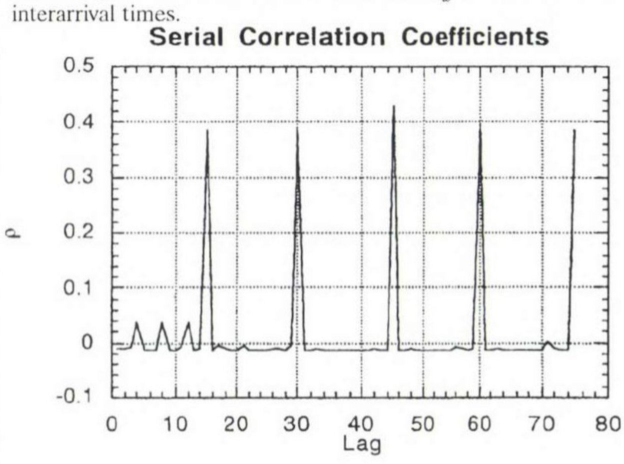

Fig. 3. Serial Correlation Coefficients

The periodic nature of the graph is believed to be due to the way the Cray buffers data for output. Clearly, single application data is heavily dependent on its platform. Nevertheless, significant correlation is observed of a degree much higher than that seen in previous Ethernet data [2].

The data clearly do not fit any of the Markovian models (which all have some form of hyperexponential interarrival density function). However, these data may be represented by a much simpler process which is more deterministic.

The packet length distribution for the same data is depicted in Fig. 4.

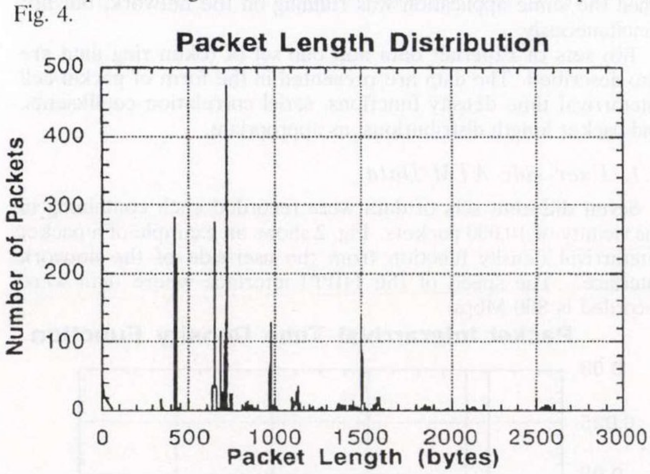

Fig. 4. Packet Length Distribution

3.2. Network-side Data

Numerous data were collected from the network side of the ATM adapter. (The data files are available by anonymous ftp from kira.mcnc.org under pub/vista.net.) Traffic at this point in the network has been broken into 53 byte ATM cells, and the link is inherently slotted. The link speed is at the OC-12c rate. Because packet lengths are much greater than 53 bytes and the adaptation of the packets is done in real time, cells tended to arrive in large bursts. The cell interarrival distribution is thus heavily weighted toward a large proportion of very short interarrival times (i.e. 99 % are below 1 ms). We thus calculated a burst interarrival density function, an example of which is shown in Fig. 5.

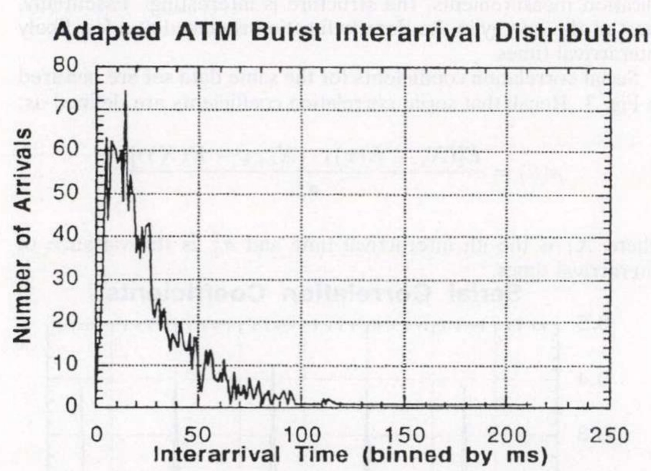

Fig. 5. Adapted ATM Burst Interarrival Distribution

The burst length distribution is shown in Fig. 6. (Note that, although the graph may seem to indicate that all burst lengths occurred at least once, this is deceiving. There were lengths that did not occur.)

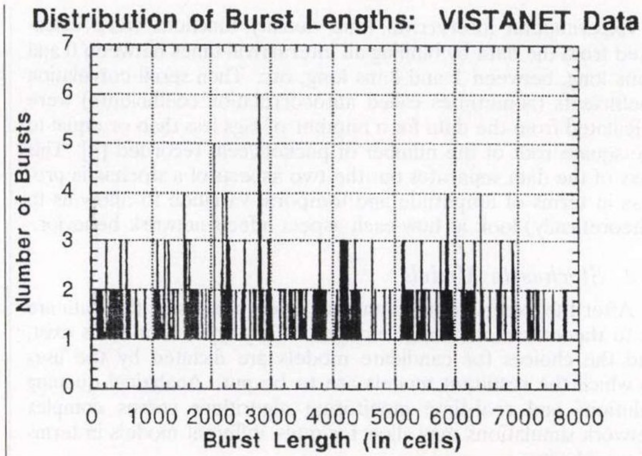

Fig. 6. Distribution of Burst Lengths: VISTANET Data

A burst is defined as a series of contiguous cells. The first empty slot marks the end of a burst, and the next cell to arrive marks the beginning of the next burst. The distribution of burst lengths is surprisingly uniform.

The burst interarrival density function was fit to a MAP-3 model. The resulting fit is quite poor. The MAP-3 interarrival density function has the form of a sum of three exponentials. (The MAP-3 interarrival density function was fit by fitting the distribution equation directly to the data histogram using simulated annealing to solve the overdetermined system of equations.) Instead, a lognormal density function was found to be an excellent fit; see Fig. 7.

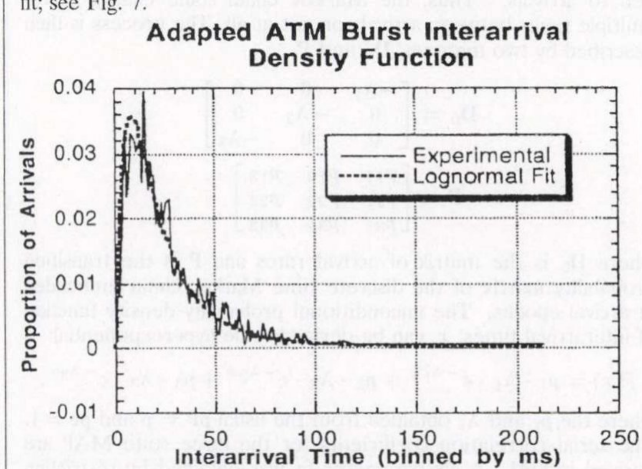

Fig. 7. Adapted ATM Burst Interarrival Density Function

The serial correlation coefficients for burst interarrival times are pictured in Fig. 8.

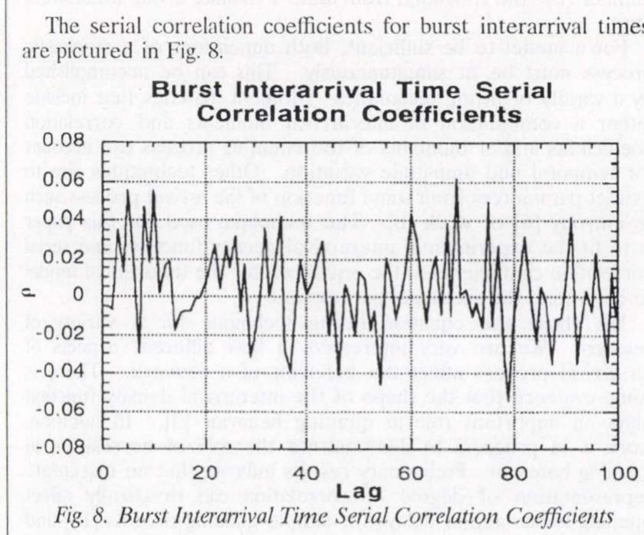

Fig. 8. Burst Interarrival Time Serial Correlation Coefficients

A significance test for the data indicates a value of ρ over 0.05 is significant [4]. This implies that correlation between burst interarrival times is not significant. Correlation at the cell level is, on the contrary, as high as 0.9 at small lags. This is due to the tendency of cells to arrive in relatively large bursts.

The shape of the burst interarrival density function and the results for cell and burst correlation imply that a simple two-state burst arrival renewal process may adequately represent this data. It also means, of course, that the Markovian-based models such as MAP and MMPP are not good fits for this data.

3.3. Ethernet Data

Two sets of Ethernet data are presented: one from North Carolina State University and one from MCNC. Each interarrival density function was fit to a MAP-3 model. The resulting fits are shown in Figs. 9 and 10. Both networks operate at 10 Mbps.

Serial correlation coefficients for the two data sets are shown in Table 1.

Table 1. Correlation coefficients corresponding to Figs. 9. and 10.

Lag	NCSU	MCNC
1	0.05	-0.09
2	0.07	0.16
3	0.03	0.06
4	0.05	0.08
5	0.04	0.05
6	0.03	0.08
7	0.05	0.05
8	0.02	0.08
9	0.003	0.04
10	0.04	0.06
5 % Significance Level	0.07	0.09

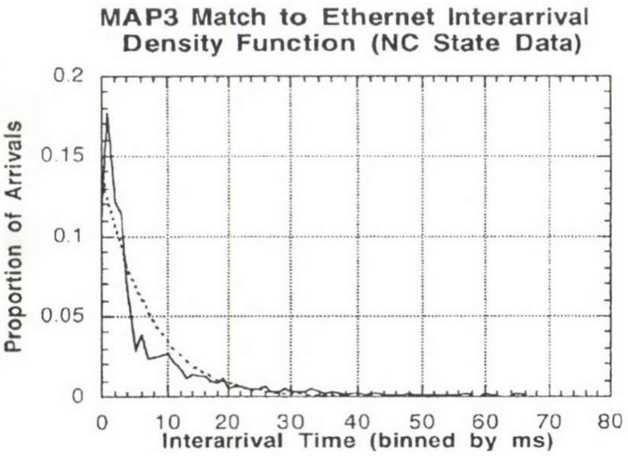

Fig. 9. MAP3 Match to Ethernet Interarrival Density Function (NC State Data)

Clearly, the Ethernet data present much less degree of correlation than the ATM data. Initial fits of interarrival density function simultaneous with correlation coefficients indicate that the MAP-3 process can fit up to the first ten correlation coefficients while maintaining a good interarrival density fit. This should be adequate to model this data, since lags with significant correlation are included.

Packet length distributions for the Ethernet data are strictly bimodal.

3.4. Token Ring Network Data

The token ring data was recorded from a network under approximately 64 % utilization. The accuracy of the time stamps is somewhat less than desirable at only 1 ms. Each of the other data sets was recorded with at least 1 microsecond accuracy. The speed of the token ring network was 16 Mbps. Fig. 11 shows the experimental token ring packet interarrival density function fit to a MAP-3 interarrival density function.

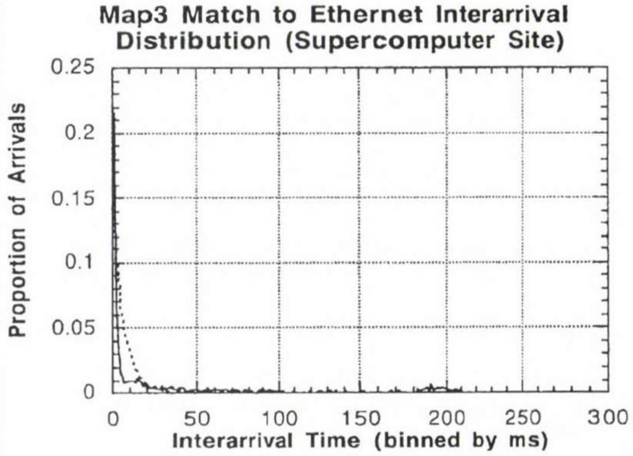

Fig. 10. MAP3 Match to Ethernet Interarrival Distribution (Supercomputer Site)

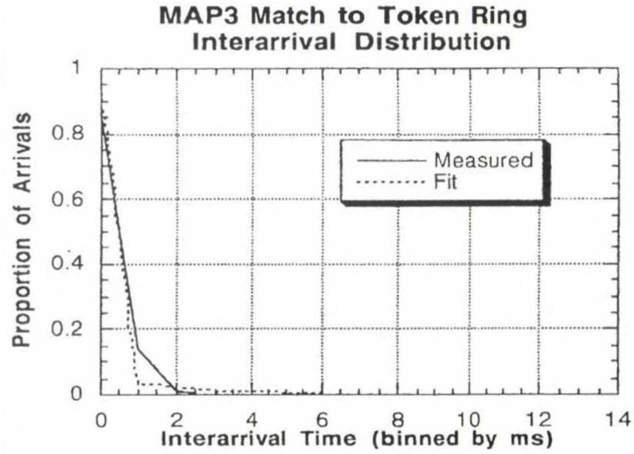

Fig. 11. MAP3 Match to Token Ring Interarrival Distribution

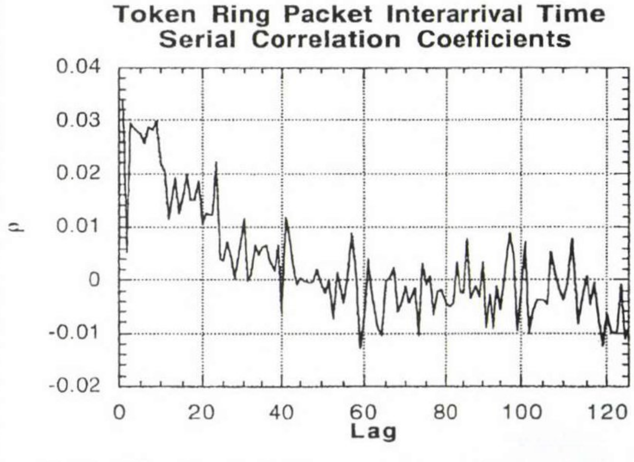

Fig. 12. Token Ring Packet Interarrival Time Serial Correlation Coefficients

Fig. 12 shows the serial correlation coefficients calculated for this data. The simple significance test gives a threshold of 0.01 for this data. The nearly exponential decline is typical of Markovian arrival processes.

4. CONCLUSIONS AND FUTURE WORK

The data collected from the VISTAnet network are from a single metacomputing application. Single application traffic has a tendency to be less well behaved from a modeling perspective, so we are encouraged to see the results from these measurements.

For the cases where "significant" correlation is observed, we seek an answer to the question, "How much correlation is significant from a network perspective?" As a result, in parallel with future measurement work, we are continuing experiments to identify how both degree and persistence of correlation affect various network protocols/policies, switch designs, etc. Preliminary results indicate that correlation can play an important role.

The data that we have discussed does not appear to display the type of long-term dependency that would indicate self-similarity. The manner in which the traffic was sampled may or may not inhibit any such conclusion. Measurements were taken using the busy hour concept introduced by Erlang. Traffic was measured during peak times of utilization on the networks for statistically significant intervals that were still short enough to permit an assumption of stationarity over the observation period. For this reason and for the reason that we expect models gleaned from this data to be used for simulation and design of network protocols such as policing, admission control, buffer sizing, etc., we are interested in traffic characterizations that will give good accuracy for busy time unit concepts and not as much with models that may have longer time scales.

REFERENCES

[1] Bottomley, L. J., Nilsson, A. A. and Blatecky, A. J.: "Traffic Measurements on a Working Wide Area Network", ITC13, Copenhagen, June 1991.

[2] L. J. Bottomley: "Traffic Measurements on a Working Wide Area Network", PhD Dissertation, North Carolina State University, February 1992.

[3] Bux, W.: "Single Server Queues with General Interarrivals and Phase-Type Service Times, ITC9, Torremolinos, 1979.

[4] Cox, D. R. and Lewis, P.: *The Statistical Analysis of Series of Events*, John Wiley and Sons Inc., 1966.

[5] Crosby, Simon, et. al., "Bypassin Modelling: an Investigation of Entropy as a Traffic Descriptor in the Fairisle ATM Network", *Proc. of the l2th IEE UK Teletraffic Symposium*, Old Winsor, March 1995.

[6] Duffield, J. T., et. al.: "Issues Raised by the Bellcore Data", *Proc. of the 11th IEE UK Teletraffic Symposium*, Cambridge, March 1994.

[7] Fuchs, E. and Jackson, P.: "Estimates of Distributions of Random Variables for Certain Computer Communications Traffic Models", *Comm. of the ACM*, Vol. 13, 1970.

[8] Gibbens, R. J. and F. P. Kelly: "A Decision-Theoretic Approach to Call Admission Control in ATM Networks", *IEEE Journal on Selected Areas of Communications*, 1995.

[9] Holtsinger, D.: "Analysis of VISTAnet Traffic Measurements", CCSP Internal Report, North Carolina State University, 1993.

[9a] F. Jou and A. Nilsson: "ATM Traffic Measurement and Congestion Control Issues from VISTAnet Testbed", to be published, 1995.

[10] Leland, W. et. al.: "On the Self Similar Nature of Ethernet Traffic", *Proc. of SIGCOMM*, 1993.

[11] Rindos, A., Woolet, S., Viniotis I. and Trivedi, K.: "Exact Methods for the Transient Analysis of Nonhomogeneous Continuous-Time Markov Chains", *2nd International Workshop on the Numerical Solution of Markov Chains*, Raleigh, NC, 1995.

[12] Shoch, J. F. and J. A. Hupp: "Measured Performance of an Ethernet Local Network", *Comm. of the ACM*, Dec. 1980.

[13] Talman, K.: "Asynchronous Transfer Mode Traffic Characterization on the VISTAnet Gigabit Network", Masters Thesis, Georgia Tech, April 1994.

[14] Wang, C. Y.: "Some Problems in Design and Analysis of ATM Networks", Masters Thesis, Duke University, October 1995.

[15] Zhi, Chi, private conversation, January 1992.

Laura J. Bottomley received her M.S. in Electrical Engineering from Virginia Polytechnic Institute and State University in 1985 and her Ph.D. from North Carolina State University in 1992. From 1985 to 1987, she was a Member of Technical Staff at AT & T Bell Laboratories. From 1987 to 1989, she was an instructor at North Carolina State University, where she completed her dissertation work in the area of computer communications networks traffic measurement and modelling. Since 1991 she has been a Research Assistant Professor or Adjunct Assistant Professor at Duke University. She is currently working with the industry/government/university cooperative research center which now includes both Duke and N. C. State, the Center for Advanced Computing and Communications (formerly the Center for Communications and Signal Processing).

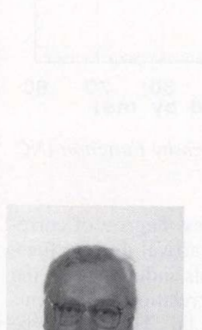

Arne A. Nilsson received the M.S. and Ph.D. degrees from Lund Institute of Technology, Lund, Sweden in 1968 and 1976, respectively. From 1973 to 1978 he was an Assistant Professor in the Department of Electrical Engineering at Lund Institute of Technology. In 1978 he moved to the Department of Electrical and Computer Engineering at North Carolina State University, Raleigh, North Carolina, where he is now a Professor. Since 1982 he has been the Program Manager for the Networking area in the Industry/University Center for Advanced Computing and Communications at NCSU. In 1988 he became Director of this research center and he is now, as Technical Director, responsible for the research program in the Center. From 1986 to 1987 he held the position of Professor at the Royal Institute of Technology, Stockholm, Sweden. He has published more than 90 papers in technical journals and conferences and has consulted for many government agencies and corporations.

LAN ACCESS TO ATM NETWORKS

I. S. VENIERIS, M. E. ANAGNOSTOU, G. I. STASSINOPOULOS and E. N. PROTONOTARIOS

NATIONAL TECHNICAL UNIVERSITY OF ATHENS
ELECTRICAL & COMPUTER ENGINEERING DEPARTMENT
9 HEROON POLYTECHNIOU STR., ZOGRAPHOU, 157 73 ATHENS, GREECE
TEL. + 30 1 772 2551 / FAX. + 30 1 772 2530
E-MAIL: VENIERIS@CS.NTUA.GR

We examine the role of ATM as a provider of efficient remote interworking between LANs. We identify key required functionality and show how this is satisfied by basic ATM capabilities, like label multiplexing and associated flexible bandwidth allocation. We show how the inherently connection oriented nature of ATM networks can be employed to support connectionless data transfer between LANs. Finally we discuss the bandwidth requirements of the traffic, which is generated by the LANs and is injected into the ATM network.

1. INTRODUCTION

The B-ISDN based on the Asynchronous Transfer Mode (ATM) is definitely adopted as the target solution for implementing the future all-purpose integrated services telecommunication network [15], [16], [36]. In its early stage of introduction, the ATM technology will be used both in the private domain in so called ATM Local Area Networks (LANs) [8], [17], [37] as well as in the role of a public Wide Area Network (WAN) to provide connectivity among remote data networks by offering flexible cross connect functions [25]. This fact together with the need to assure interoperability of existing or future networks with ATM can explain the dramatic increase of research interest towards the direction of ATM Interworking Units (AIUs) [11], [12], [13], [14], [18], [21], [22], [39], [41], [42]. The mission of the AIU is to route Protocol Data Units (PDUs) to the final destination across the ATM network, in a format recognisable by the receiver, while preserving the quality of the supported service and exploiting as much as possible ATM network resources.

In this paper we study the interconnection of LANs through ATM networks. Bridges and routers typically interconnect adjacent LANs [33], [9]. To provide for the same functions remotely, Interworking Units (IWUs) are required. Their task is to transparently use the WAN, in our case an ATM based B-ISDN. In other words, problems arising from the heterogeneity of LANs and from the intervening transfer network should be hidden from the user. The flexibility and novel features of ATM deserve particular attention during the specification and design process of AIUs. Factors influencing the AIU design are the speed of the interconnected segments, the number and characteristics of the supported services and the level of compatibility between the protocols of the segments and the ATM protocol stack. The final product should then fulfil user and network operator requirements in terms of Quality of Service (QoS), implementation cost and network resource exploitation.

To accomplish their task AIUs should provide a relay protocol accompanied by functions such as address resolution, bandwidth allocation, and service discrimination policy as shown in Fig. 1.

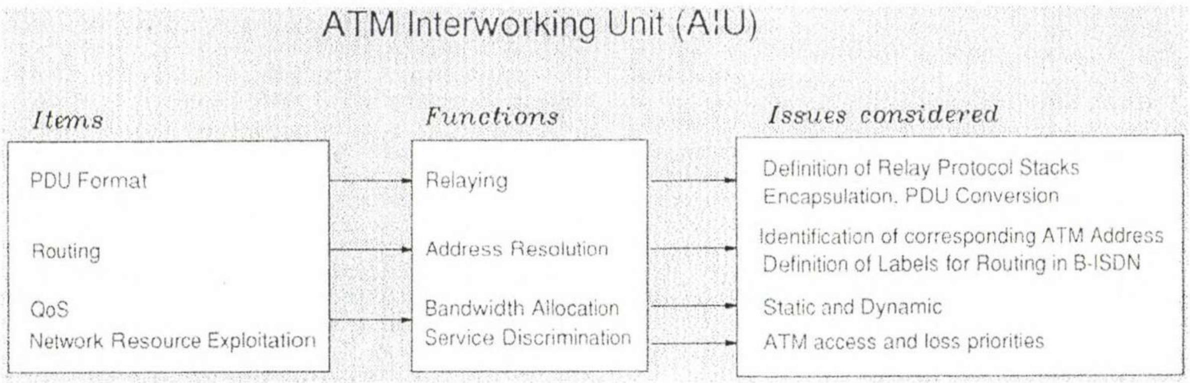

Fig. 1. AIU's scope and functions

Beyond their classical usage as customer premises networks LANs are expected to play different roles in the near future. They will act as more economical means of user access to the B-ISDN and they are also a candidate technical solution for part of the fixed network of the future Universal Mobile Telephony System (UMTS) [24],[27] which in turn will be connected with the ATM network.

UMTS is a third generation mobile system aiming to provide for a unified user access through low-power Mobile Terminals (MTs) usable both for wide-area (cellular) and local area (cordless) applications. The UMTS design should be flexible enough to cater for all the envisaged kinds of environments (e.g. Public, Business, Domestic). The terminal capabilities should vary as well to suit the specific user needs aiming to massive market penetration.

In the current stage of UMTS development the radio access technique (i.e. TDMA or CDMA) is not yet known. At the same time in the fixed network integration with B-ISDN is the primary target. However, in all broadband evolution and deployment scenarios Metropolitan Area Networks (MANs) are playing an important role. Therefore, the potential candidates for the fixed part of the UMTS Access Network (UAN) could be: the B-ISDN User-Network Interface (B-UNI) [43], DQDB based MANs [35] or high speed LANs [37]. In this way the importance of LAN-ATM interworking emerges again.

The paper is organized as follows: In Section 2. we present the general interworking principles for interconnecting heterogeneous non-ATM networks through an ATM WAN. It includes description of the AIU principal functionality and indications of protocol stacks that could accomplish the interworking requirements. Special emphasis is given on the addressing operations of the AIU where we demonstrate the use of ATM labels for routing information among interconnected LANs. Section 3. deals with the application of the interworking principles to LAN interconnection through ATM networks. In Section 4. we address the problem of ATM bandwidth allocation and policing of LAN created traffic and we discuss several alternatives with reference to the bandwidth value and the congestion control method. Section 5. summarizes the conclusions of this study.

2. INTERWORKING ISSUES

2.1. Relay Protocol Stacks

The role of an AIU is to relay information from one LAN to another via the ATM network. Hence the AIU has a dual objective: to restructure PDUs of the source LAN according to the requisites of the destination LAN and to transfer reconstructed PDUs across the ATM network in the form of ATM cells. Each AIU is double faced (Fig. 2). It incorporates a LAN protocol stack, and an ATM stack similar, up to some layer, to that of any endsystem of the interconnecting ATM network. PDU conversion functions are placed on top of this dual stack. Interworking occurs at a layer, where international or de facto standard protocols exist for all LANs, this layer being, so to speak, the common denominator of the different environments. Take Logical Link Control (LLC) as an example: Since this layer is common to all IEEE 802.3-5 LANs [6], relaying functions can extend up to the LLC and the same primitives can be used at both sites for the purpose of interconnecting different Medium Access Control (MAC) sublayers [33]. The higher the level of compatibility of the interconnected networks, the lower is the layer where interworking is possible. In the extreme case, where the interconnected networks are the same, PDU conversion amounts to PDU encapsulation. The latter is necessary for transmission through the ATM based stack.

Converted or merely encapsulated LAN PDUs have to pass through the connecting network in the form of ATM cells by establishing virtual connections between the AIUs. A two level hierarchy of connections is available, Virtual Path Connections (VPCs) multiplexed on physical transmission paths and Virtual Channel Connections (VCCs) multiplexed on VPCs. In both cases the ATM uses label multiplexing, the label being either the VP Identifier (VPI) or the VC Identifier (VCI). Segmentation and reassembly of encapsulated LAN PDUs to and from ATM cells is performed by the Segmentation and Reassembly (SAR) sublayer directly above the ATM layer. Through the use of a Multiplexing Identifier (MID) a third level of multiplexing is provided, this time within the SAR sublayer and in expense of AAL protocol implementation complexity and bandwidth waste [44]. VPIs, VCIs and MIDs can be looked as resources offered by ATM technology to solve addressing and PDU identification issues, as explained below.

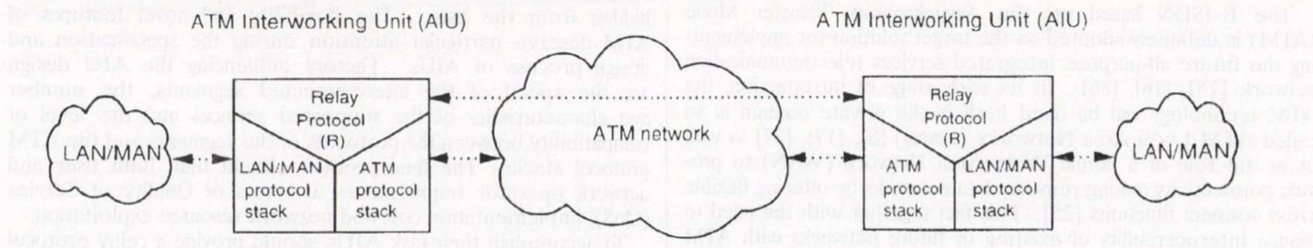

Fig. 2. ATM interworking unit protocol stack overview

In this paper we address interworking principles appropriate for the connectionless (CL) operation of the interconnected LANs. The ATM layer providing interconnection is however inherently connection oriented (CO). This incompatibility has been recognized and resolved not only by special provisions in the ATM Adaptation Layer (AAL) but also through specially devized functions to serve connectionless traffic. Thus ITU-T recommends two, conceptually different, mechanisms for CL service support [1], [2], [3]. The first one uses semi-permanent VPCs between AIUs, on which the segmented PDU is carried in the payload of the corresponding ATM cell stream. CL protocols are terminated at the AIUs featuring as ATM endsystems. In the second mechanism CL protocols are terminated also inside specially configured ATM nodes realising CL Service Functions (CLSFs), and routing decisions are taken by retrieving specific addressing information included in the cell payload. The procedure does not involve PDU reassembly. Everything occurs "on the fly" by interpreting and modifying the part of the ATM payload that corresponds to the Protocol Control Information (PCI) serving the CL protocol. This mechanism sets extra requirements on the AIU functionality, which should take care of CL PCI interpretation and modification at CLSF nodes.

Beyond functional requirements, realization simplicity, and effective use of ATM bandwidth have to be considered. For an elegant AIU design, duplication of functions at different layers should be avoided, so that sensible use of processing resources is effected.

2.2. Addressing

The AIU at the source side has to map LAN addresses to a set of ATM addresses and identifier values (VPI, VCI, MID) employed in the ATM network. The inverse mapping is performed at the other end, provided that the addressing policy is the same in both LANs.

The first action of an AIU is to determine the ATM Network Address (ANA) corresponding to the Destination Address (DA) of the incoming LAN PDU. The ATM based stack then determines the identifier(s) required for routing towards the desired ANA. Provided that the first ITU-T mechanism for CL service support exists, semi-permanent VPCs undertake the transparent transfer to the remote AIUs, so that ANA merely determines an appropriate VPI leading to the desired destination. Given the second ITU-T mechanism, virtual connections issuing from the AIUs can terminate at intermediate CL nodes with resident CL Network Access Protocol (CLNAP) functions. The CLNAP layer sits on top of the AAL3/4 or AAL5 layer and undertakes routing functions based on the CLNAP Destination Address (CDA). Both AAL3/4 and AAL5 protocols arrange that the CDA resides in a fixed octet of the first cell conveying a higher layer PDU. The CDA is inspected and used by CLNAP to determine the VPI towards the next CLSF. All subsequent cells of the same PDU are segmented by AAL3/4 or AAL5 and are routed across the same path. In the AAL3/4 alternative cells belonging to different PDUs may use the same AAL3/4 connection in which case they will appear intermixed in the CLSF. To identify the particular PDU a cell belongs to and hence the proper VPI, the MID field present in all AAL3/4 segments of the PDU will have the same value. Hence upon arrival of the first cell, denoted as BOM (Begin Of Message) the MID value is stored and mapped to the VPI corresponding to CDA. All subsequent cells denoted as COM (Continuation Over Message) or EOM (End Of Message) with the same MID value are allocated the same VPI. In the AAL5 alternative no multiplexing on a segment level is allowed and hence only an indication of the first or the last segment of a PDU is required for the proper routing of cells. This is provided in the PT (Payload Type) field of the header of the last cell which is assigned the value AUU=1 (ATM user-to-ATM user information). With the above organization routing of the segmented PDU to the next CLSF node occurs without reassembly. The ANA is associated to the CDA which is in turn handled by the lower layer resources (MID at AAL3/4 and VPI at VP sublayer) providing end-to-end delivery without reassembly. Notice also that while MID and VPI have local significance, the ANA and CDA are E.164 addresses [7]. The general address mapping functionality of an AIU is given in Fig. 3 for the more demanding case of AAL3/4.

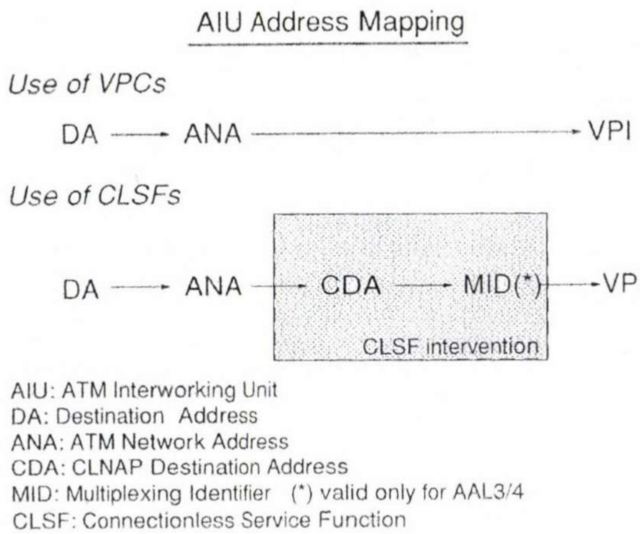

Fig. 3. Address mapping in AUIs

A. VPI allocation

In both ITU-T mechanisms VPCs have to be established to serve communicating AIUs. These VPCs are either point-to-point or point-to-multipoint [25], [26]. The corresponding VPI values are not only useful for the proper switching of cells in the ATM network entities (either cross connects and/or CLSFs) but are also involved in the address mapping functionality of the AIU.

According to the first ITU-T mechanism the desired interconnecting configuration is directly mapped to corresponding VPC set-ups. Since only the VPI field of the ATM cell is interpreted in the ATM cross connects, the leftover VCI field can be used for coding addressing information as required by the AIU protocols (see developments in [13], [8] and [45]). A set of alternatives for a VPC set-up in a point-to-multipoint configuration and the use of the VPI/VCI field for each alternative is illustrated in Fig. 4. In Fig. 4(a) a common VPC is established for all traffic originating from an AIU to all other AIUs (point-to-multipoint VPC). The VPI value is associated to the sending AIU identity. In such a multicast solution the Destination Address is indispensable, e.g the VCI codes the DAbx address of the destination station x in LAN b. In the second alternative of Fig. 4(b) a VPC for each destination AIU is established (multipoint-to-point VPC).

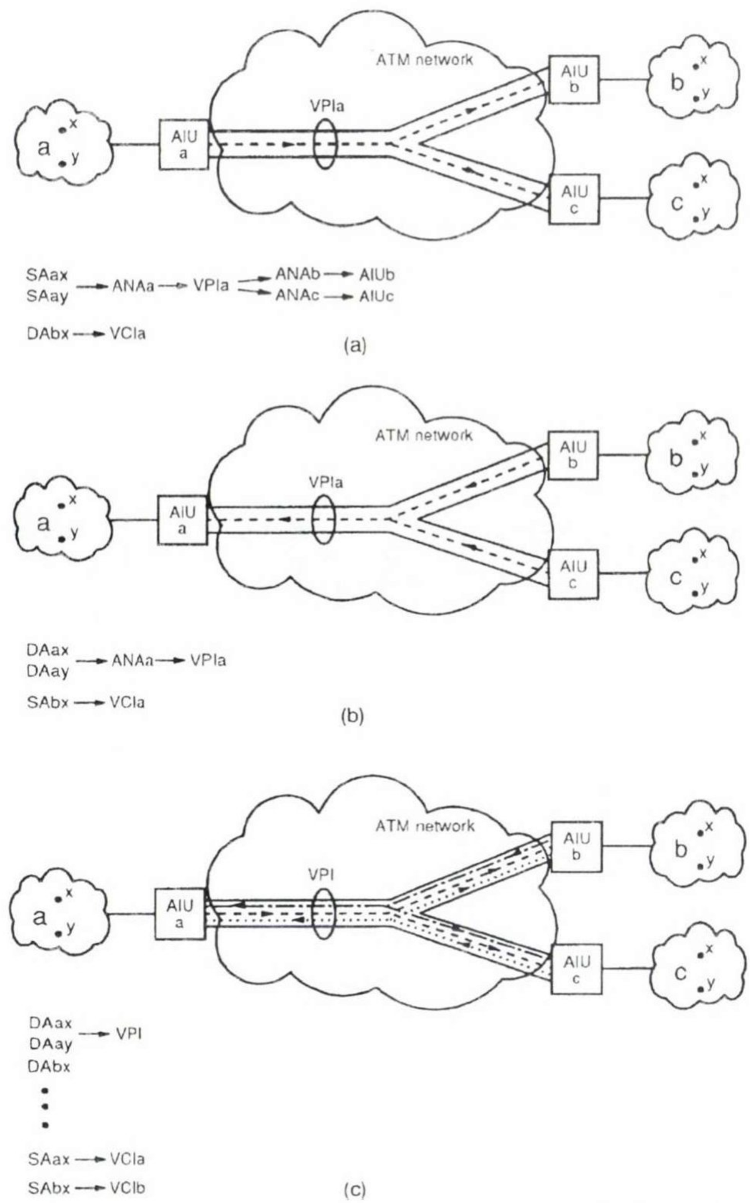

Fig. 4. Configurations and usage of VCIs with the ITU-T mechanism for CL service support

The VPI is now associated to the receiving AIU identity and the VCI can be used to identify the source station x in LAN b and acts as message identifier to the reassembler of the destination AIU, so that interleaving of cells sent by different stations on different AIUs on the same VPC becomes possible. The third alternative shown in Fig. 4(c) assumes that a single VPC is established among all interconnected AIUs (many-to-many VPC). The VPI identifies the association of the interconnected networks and possibly the particular administration authority. In effect the VPI does not contribute to addressing and the VCI undertakes the burden of identifying among other source and destination AIU addresses. Notice that in (a), (b), or (c) the VCI field has no functional significance within the ATM network and is only used at the AIUs to convey the addresses of the attached stations. The above scenarios presume universally administered station addresses. If addresses instead have local significance the VCI should be associated with the ANA of the AIUs, while internal addresses have to be incorporated internally in the relayed PDUs.

According to the second ITU-T mechanism involving CLSF nodes, cases (a), (b), (c) above have analoga, however at the CLNAP layer. VPCs and their identifiers are needed for interconnecting CLSF nodes so that the CDA undertakes the addressing/routing role that the VPI has in the first ITU-T mechanism. Notice also that case (c) is in fact inherently provided by any connectionless protocol. Any message found anywhere in the network is routed to (attracted by) its destination. With a many-to-many VPC the same functionality is provided at a lower layer. In general use of CLSFs according to the second ITU-T mechanism is recommended whenever a large number of LANs has to be interconnected with sparse traffic between the majority of possible source destination pairs. Procedures and cost for setting up and using a large number of dedicated VPCs is avoided and routing functions are provided on a collective basis by CLSF nodes.

In the rest of this paper we apply the above general principles of ATM based interworking in a typical ATM interworking paradigm. It considers LANs following the IEEE 802.3-5 standards [6]. This application covers the most demanding case in terms of protocol relay functionality due to the inherent incompatibility of interconnected sides and interconnecting network.

3. LAN INTERWORKING

According to the principles established above the relay protocol of a LAN AIU (LAIU) has to convert the MAC-PDU of LAN A to a MAC-PDU of LAN B (Fig. 5) and to transfer this PDU across the ATM network with ATM cells. The first objective is analogous to the case of heterogeneous LAN interconnection. However the two operations can be combined towards a more efficient solution in terms of protocol operations. Heterogeneous LAN interconnection is usually resolved by resorting to higher than MAC sublayer resources; for example using the addressing capability of the Internet Protocol or its variances [19]. The specification of a Unified MAC (U-MAC) protocol able to bridge heterogeneous LANs at the MAC layer achieves interworking at a lower layer. This of course means that addressing problems must be properly solved. So we intend to use a relay protocol, which has the ability to code and transfer only those parameters that are considered generic in the sense that all MAC protocols need them. These are the DA, SA and the Frame Control of a MAC-PDU according to the lines established in [9] and [14].

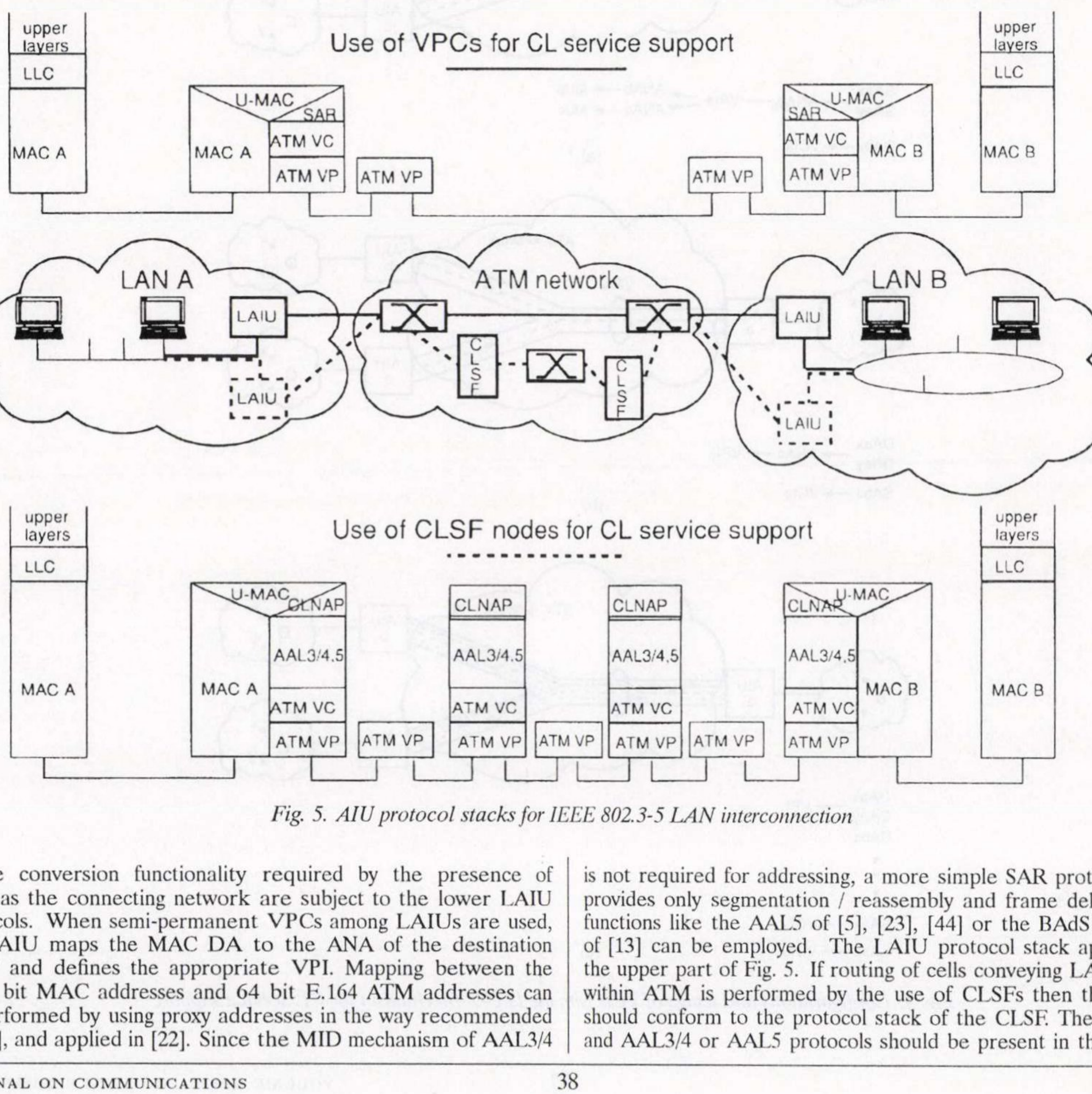

Fig. 5. AIU protocol stacks for IEEE 802.3-5 LAN interconnection

The conversion functionality required by the presence of ATM as the connecting network are subject to the lower LAIU protocols. When semi-permanent VPCs among LAIUs are used, the LAIU maps the MAC DA to the ANA of the destination LAIU and defines the appropriate VPI. Mapping between the 16-48 bit MAC addresses and 64 bit E.164 ATM addresses can be performed by using proxy addresses in the way recommended in [10], and applied in [22]. Since the MID mechanism of AAL3/4 is not required for addressing, a more simple SAR protocol that provides only segmentation / reassembly and frame delimitation functions like the AAL5 of [5], [23], [44] or the BAdS protocol of [13] can be employed. The LAIU protocol stack appears in the upper part of Fig. 5. If routing of cells conveying LAN traffic within ATM is performed by the use of CLSFs then the LAIU should conform to the protocol stack of the CLSF. The CLNAP and AAL3/4 or AAL5 protocols should be present in the LAIU, as appears in the lower part of Fig. 5. AAL is here sublayered into the SAR and Common Part Convergence Sublayer (CPCS) [4].

When interconnecting heterogeneous networks one has to deal separately with each sublayer function and the corresponding field in the MAC frame. Incompatibilities can be best resolved by stripping MAC of all corresponding functions and frame subfields and by providing equivalent functionality on the ATM side. Addressing information can be hosted in the VCI field of ATM cells, which otherwise remain unused as seen above. Frame delimitation and CRC functions are either unnecessary or can be undertaken by SAR functions. This shifting of functionality towards the ATM is well determined in the case of the second ITU-T mechanism for CL service support. Here due to the presence of CLSF nodes SAR type 4, CPCS type 4 and CLNAP are required at endsystems (LAIUs), thus the AAL functionality is given. With the first ITU-T mechanism, since only LAIUs are involved (compare the protocol stacks in Fig. 5) the designer is more free to tune this shift according to its environment. SAR type 5 is a solution, which has achieved standard status [5], but in principle any proprietary SAR protocol is possible provided all involved LANs adhere to it. Moreover a U-MAC and corresponding SAR protocol can be used also in the homogeneous LAN case, if one goes into the trouble of replacing MAC protocol procedures, which anyway can interwork thanks to homogeneity, by potentially more efficient ATM counterparts.

4. ALLOCATION OF BANDWIDTH TO LAN CREATED TRAFFIC

Inside the ATM network sufficient bandwidth should be allocated to support the traffic between the AIUs. The approaches here vary. The most conservative one allocates bandwidth equal to the bit rate of the interconnected networks, while the most dynamic one reserves bandwidth upon the arrival of information in the AIU (see [18]). The latter implies the existence of a protocol among AIUs, AIU and CLSF, CLSF and CLSF, which is activated each time a PDU or a sequence of PDUs arrive at the AIU. It causes a call to be set up for a PDU duration time scale and to be spontaneously cleared without explicit further action after the bulk PDU transfer. This protocol should be very fast, even hardware implementable, and outside the scope of management which is orders of magnitude slower. The emerging advantages of the dynamic reservation in terms of ATM resource exploitation and fair charging can be met only if implementation related issues and delay overhead are properly resolved.

While the dynamic option described in the previous paragraph may not be easy to implement, the conservative one obviously wastes bandwidth, unless the traffic generated by the LAN is exceptionally regular. The charging mechanism of the ATM network will most probably take into account the bandwidth allocated to each user. The ideal mechanism, which defines the bandwidth requested by the LAN has to face a complex bandwidth minimization problem. The factors that influence the outcome are (a) the characteristics of the traffic generated by the LAN, (b) the mechanism of the interworking unit(s), and (c) the policing mechanism of the ATM network.

4.1. LAN Traffic characteristics

Since the birth of LANs and LAN analysis it was a common belief that LAN traffic could be approached by a Poisson distribution. This belief was not totally unfounded as it often happens that the aggregate traffic of a large number of sources is well approached by a Poisson source. Also, it is very confortable in mathematical calculations, and the classical analysis of the ALOHA protocol [30] is based on this assumption. Nevertheless this assumption has not confirmed by experimental data. According to [29] it seems that traffic "spikes" ride on longer term "ripples" that in turn ride on still longer "swells". In [46] it is shown that LAN traffic can be modelled by using self-similar processes. This idea is further developed in [47] where the poisson assumption is critically tested over its accuracy for a number of different service connections and applications.

4.2. LAN Traffic Descriptors and Policing Parameters

Policing has been standardized by the ITU-T [32] and the ATM Forum [28], [34] as the concept that will be used in the future ATM network to preserve the network from user contract violations and mishappenings that could cause serious problems in its operation.

At ITU-T there have been so far two peak cell rate based policing configurations. The ATM Forum has introduced the sustainable cell rate as an additional traffic parameter in the source traffic descriptor. However, it has been realized that an increased number of traffic parameters is difficult to be handled by both the user and the network. The user has to describe his traffic appropriately and the network has to police the traffic accordingly. Policing sustainable cell rates in addition to peak cell rates would approximately double the hardware effort for policing. In order to avoid the excessive complexity the new flexibility in the choice of traffic parameters has been restricted. Thus the resulting additional policing configurations need a hardware effort similar to the peak cell rate based policing configurations.

Traffic parameters describe traffic characteristics of an ATM connection. For a given ATM connection, traffic parameters are grouped into a source traffic descriptor. The set of traffic parameters within a source traffic descriptor can vary from connection to connection [28], [34], [32]. Accordingly, different policing configurations correspond to each possible set of traffic parameters [20].

The Peak Cell Rate (PCR) traffic parameter specifies an upper bound on the traffic that can be submitted on an ATM connection. It is measured in cells per second. The peak cell rate is the inverse of the peak emission interval of the ATM connection. The Peak Emission Interval (PEI) is the minimum interarrival time between two consecutive requests by the source at the physical layer service access point to send an ATM cell [32]. Policing the peak cell rate of a cell flow can be done by a Leaky Bucket. The parameters of a Leaky Bucket policing PCR are uniquely defined by the peak cell rate together with the cell delay variation tolerance. According to the Leaky Bucket algorithm [20] a counter is associated with each source. The counter is incremented whenever the source produces a cell and is decremented periodically. If the counter exceeds an upper limit, the cell, which has produced the counter increase is discarded.

The sustainable cell rate (SCR) traffic parameter is an upper bound on the conforming average rate of an ATM connection. It is measured in cells per second. The sustainable cell rate is a useful traffic parameter only if the realized average cell rate of an ATM connection can be upper bounded to a value below the peak cell rate. The Maximum Burst Size (MBS) traffic parameter is the maximum number of consecutive cells that a connection may transmit at the peak cell rate. It is measured in number of cells. Sustainable cell rate and maximum burst size are optional traffic parameters that always have to be declared jointly in the source traffic descriptor and could be used only additionally to the peak cell rate that has to be specified in any case for every connection. The parameters of a Leaky Bucket policing SCR (together with MBS) are uniquely defined by the sustainable cell rate and the maximum burst size together with the peak cell rate and the cell delay variation tolerance.

All cells have their cell loss priority (CLP) bit set to either 0 or 1. Traffic parameters apply either with respect to the CLP=0 cell flow that is handled with space priority within the ATM network or with respect to the whole CLP=0+1 cell flow of user data of an ATM connection. In [12] we have considered the case where all LAN traffic is transmitted over a single VP. In this case all the user's packets have the same importance and after processed by the AAL, are submitted to the ATM network with the same CLP.

4.3. Bandwidth for LAN Traffic

The obvious issue is how much this bandwidth should be (although the right question to ask would concern the whole contract). This is actually a common issue with all ATM access networks with shared medium due to the interarrival distortions caused by the access control mechanism. Access control resolves contention but alters the characteristics of the traffic generated by the user. Hence, estimations of the required bandwidth cannot be relied upon multiplexed user source traffic models that ignore the jitter introduced by the particular access control mechanism. This remark is very important for heavy bursty data traffic issued by LAN users as it plays an essential role in dimensioning the AIU buffer and estimating the actual bandwidth required for transferring the LAN traffic through ATM. In the following we elaborate on two issues of bandwidth allocation, namely, the development of dynamic congestion control protocols for services similar to the ones provided by LANs and traffic regulation policies that allow the prediction and dimensioning of LAN offered traffic.

A. Dynamic Congestion Control Protocols

Currently a new service category has been recognized, widely known as the ABR (Available Bit Rate) service [34], [32]. The ABR service aims at the cheap support of data traffic in ATM networks. It is especially suitable for LAN traffic not only because of the connectionless and delay insensitive character of such traffic but also due to its bursty character. The latter makes the description of LAN traffic a task hard to perform, which calls for flexible short term bandwidth allocation or traffic regulation at the point of access to the ATM network.

The ABR service support passes through the development of a traffic flow control scheme. At this point two approaches have been recognized as the most prominent candidates [40], [38]. The rate-based congestion control implements a feedback mechanism which uses RM (resource management) cells for notifying the originator to reduce its rate in case congestion is experienced in any element of the route to the receiver. The rate-based congestion control is defined rather as a framework for a family of such mechanisms giving freedom to a number of variances and implementations. It also allows the application of the mechanism locally; i.e., between any neighbouring network elements of the route or in ATM LANs [31]. Bandwidth guarantees for ABR service are defined through the establishment of a minimum rate contract, which makes its possible to be used also for other near real-time applications.

The credit-based congestion control operates on a link by link basis. The originator transmits an ABR cell only if a credit has been sent by the receiver. An important issue of the credit-based congestion control is the total number of credits allocated to a specific connection or in other words the connection available bandwidth in any link of the communication path. The number of credits may be static or dynamically updated. In the latter case buffer space sharing of the receiving node is optimized, however in the expense of a specific protocol for modifying the number of credits according to demand.

B. Regulating LAN-ATM traffic

A simple version of the problem of the "allocation of bandwidth" to LAN traffic entering an ATM network is how to set the values of the contract parameters in order to avoid future contract violations. In simple words, how much "bandwidth" to ask so as to avoid being policed. Asking for the correct amount of bandwidth means that the source will avoid being policed, which in turn means that the network is obliged to deliver all cells to their destination intact and in time. Whether the network is capable to fulfil its obligations is an open problem.

When it comes to the problem of asking the correct amount of bandwidth for LAN generated traffic the influence of the interworking mechanism between the LAN and the ATM cannot be ignored.

The simplest resource management method for LAN interworking applications is to allocate WAN bandwidth equal to the LAN capacity. This mechanism however results in poor utilization of the WAN resources and additionally in unfair charging. The reason is that LAN users are typically high burstiness Variable Bit Rate (VBR) sources.

In [12] we have presented a source model, which can be used to simulate the behaviour of LAN stations, and create traffic similar to the one described in [29]. By using this realistic traffic source we have studied the impact of policing on LAN traffic and the influence of LAN-ATM interworking on the bandwidth required for LAN traffic entering an ATM network.

In our study three alternatives are considered for handling LAN traffic at the LAIU:

No-Buffering, No-Shaping (NB/NS): This alternative reflects the absence of any appreciable processing and buffering delay in the LAIU. It has been used in order to obtain results regarding the amount of ATM resources that would be required for LAN interconnections when LAN traffic passes transparently through the LAIU. In a real system this alternative corresponds to a high-speed implementation of the LAIU protocol functionality. ATM cells generated by the AAL and ATM protocol procedures exercized on each frame are transmitted into the ATM network in time equal to the transmission time of the frame in the LAN. Hence, the LAIU handles LAN traffic without buffering and without inserting delay and cell delay variation at the LAN frame level.

No-Buffering, Shaping (NB/S): The maximum delay one can introduce in the LAIU for traffic shaping without resorting to frame buffering is equal to the minimum interdeparture time of frames in the MAC. For the CSMA/CD LAN this delay is 16 microsec. The shaping functionality of the NB/S scheme becomes more advantageous for short frames where a dramatic increase of the peak rate is experienced due to the significant overhead the CPCS-PCI adds to the frame. This is not the case for long size frames where the CPCS-PCI length is not critical because the available frame buffering time has to be distributed to a big number of cells.

Buffering, Shaping (B/S): The objective in this alternative is to restrict the peak rate of LAN traffic entering the ATM network to a specified value. This could be achieved by adopting a firmware implementation of the LAIU protocol which is characterized by the speed of the processor, and the processes included in the LAIU protocols. The time consumed for a LAIU protocol process may be deterministic or variable. In the latter case, parameters playing an essential role both in the frame processing time and the time per process are the frame length and the specific AAL protocol. The value of the processor speed is selected so that the peak rate of the ATM connection supporting LAN interconnection remains under a specified value.

Here we should put some more intelligence. We should consider that after shaping we have the Network Operator UPC with which we have a traffic contract (parameters) and we know its working algorithm (Leaky Bucket). Therefore in this architecture one should consider not only the restriction of peak rate to a known value but also send the cells according to the agreed contract.

The result of [12] is that for certain low traffic applications where LAIU speed is not a bottleneck, firmware developments can be employed. The trade-off is then between the LAIU buffer size and the ATM bandwidth reserved for LAN interconnection application. It should be stressed however, that for fast LAIUs and under a cell loss objective, the unpredictable peaks of LAN traffic result in much higher bandwidth demand than the expected. This would then necessitate the use of a spacer at the ATM entrance that should be taken into account in the techno-economical evaluation procedure of the implementation alternatives. Hence the problem for interconnection of existing LANs is formulated in the following question, slow LAIUs with buffers or fast IWUs with spacers?

5. CONCLUSIONS

The paper summarizes the issues emerging from LAN interconnection through ATM based WANs. It focused on the protocol functionality of the LAN-ATM Interworking Unit for accommodating PDU conversion, routing and QoS requirements. We have shown that the inherent features of ATM like label multiplexing and dynamic bandwidth allocation are valuable for realising the interworking functionality in a relatively simple and efficient manner.

REFERENCES

[1] ITU-T, "Rec. I. 364 – Support of Broadband Connectionless Data Service on B-ISDN", Geneva, June 1992.

[2] ITU-T, "Rec. I. 211 – B-ISDN Service Aspects", Geneva, June 1992.

[3] ITU-T, "Draft Rec. I. 327 – B-ISDN Functional Architecture", Geneva, June 1992.

[4] ITU-T, "Rec. I. 362,3 – B-ISDN ATM Adaptation Layer (AAL) Functional Description, Specification", Geneva, June 1992.

[5] ITU-T, "Draft Rec. I. 363, section 6 – AAL type 5", Geneva, Jan. 1993.

[6] ANSI/IEEE Standards 802. 2 – Logical Link Control, 802. 3 – Carrier Sense Multiple Access with Collision Detection, 802. 4 – Token-Passing Bus, 802. 5 – Token Ring, 1985.

[7] ITU-T, "Rec. E. 164 – Numbering Plan for the ISDN era", Red Book, Vol. II, Fascicle II. 2, Geneva, 1985.

[8] J. -Y. LeBoudec, E. Port and H. L. Truong: "Flight of the FALCON", *IEEE Communications Magazine*, Vol. 31, No. 2, Feb. 1993, pp. 50-55.

[9] J. A. Berntsen, J. R. Davin, D. A. Pitt and N. G. Sullivan: "MAC Layer Interconnection of IEEE 802 Local Area Networks", *Computer Networks ISDN Systems*, 10(5), 1985, pp. 259-273.

[10] L. Svobodova, P. A. Janson and E. Mumprecht: "Heterogeneity and OSI", *IEEE Journal on Selected Areas in Communications*, Vol. 8, No. 1, Jan. 1990, pp. 67-79.

[11] S. Rao: "Interworking of DQDB MAN and ATM based B-ISDN", in *Proceedings of Interworking 92*, Bern, Nov. 1992.

[12] I. S. Venieris, J. -A. Sanchez-Papaspiliou and M. E. Anagnostou: "Interworking Functions Effect on Bandwidth Allocation for LAN – BISDN Interconnection", *Local Area Network Interconnection*, Eds. R. O. Onvural, A. A. Nilsson, pp. 269-286, Plenum Press, New York, 1993.

[13] G. I. Stassinopoulos, I. S. Venieris and R. Carli: "ATM Adaptation Layer Protocols and LAN Interconnection", in *Proceedings of IEEE 15th LCN*, Mn, Sep. 1990.

[14] I. S. Venieris, E. N. Protonotarios, G. I. Stassinopoulos and R. Carli: "Bridging Remote Connectionless LAN/MANs through Connection Oriented ATM Networks", *Computer Communications*, Vol. 15, No. 7, Sep. 1992, pp. 418-428.

[15] J. -Y. Le Boudec: "The Asynchronous Transfer Mode: A Tutorial", *Computer Networks ISDN Systems*, Vol. 24, No. 4, 1992, pp. 279-309.

[16] M. De Prycker: "*Asychronous Transfer Mode*", 2nd edition, Elis Horwood, Simon & Schuster Int'l. , Chichester, U. K, 1993.

[17] E. Biagioni, E. Cooper and R. Sansom: "Designing a Practical ATM LAN", *IEEE Network Magazine*, Vol. 7, No. 2, Mar. 1993.

[18] M. Gerla, T.-Y. Tai and G. Gallassi: "LAN/MAN Interconnection to ATM: A Simulation Study", in *Proceedings of INFOCOM'92*, Florence, May 1992.

[19] Special issue: "The Future of the Internet Protocol", *IEEE Network Magazine*, Vol. 7, No. 3, May 1993.

[20] E. P. Rathgeb: "Modelling and Performance Comparison of Policing Mechanisms for ATM Networks", *IEEE Journal on Selected Areas in Communications*, Vol. 11, No. 8, Oct. 1993

[21] S. Kapoor, M. M. Buddhikot and G. M. Parulkar: "Design of an ATM-FDDI Gateway", *Internetworking: Research and Experience*, Vol. 4, No. 1, Mar. 1993.

[22] I. S. Venieris, J. D. Angelopoulos and G. I. Stassinopoulos: "Efficient Use of Protocol Stacks for LAN/MAN-ATM Interworking", *IEEE Journal on Selected Areas in Communications*, Vol. 11, No. 8, Oct. 1993.

[23] K. Kerhof and A. VanHalderen: "AAL type 5 to support the Broadband connectionless data bearer service", in *Proceedings of Interworking 92*, Bern, Nov. 1992.

[24] T. Norp and A. J. M. Roovers: "UMTS Integrated with B-ISDN", *IEEE Communications Magazine*, Vol. 32, No. 1, pp. 60-65, Nov. 1994.

[25] M. De Prycker",ATM Switching on Demand", *IEEE Network Magazine*, Vol. 6, No. 2, Mar. 1992.

[26] R. Bubenik, M. Gaddis and J. De Hart: "Communicating with Virtual Paths and Virtual Channels, in *Proceedings of INFOCOM'92*, Florence, May 1992.

[27] E. Kuisch, H. Hegeman and T. Norp: "Network Aspects of UMTS", *Proceedings of ISS'95*, Vol. 1, pp. 421-425, Berlin, April 1995.

[28] ATM Forum: "User Network Interface Specification", Version 3. 1, 1994.

[29] H. J. Fowler and W. E. Leland: "Local Area Network Traffic Characteristics with Implications for Broadband Network Congestion Management", *IEEE Journal on Selected Areas in Communications*, Vol. 9, No. 7, pp. 1139-1149, Sept. 1991.

[30] N. Abramson: "Development of the ALOHANET", *IEEE Transactions on Information Theory*, Vol. IT-31, pp. 119-123, March 1985.

[31] P. Newman: "Traffic Management for ATM Local Area Networks", *IEEE Communications Magazine*, Vol. 32, No. 8, pp. 44-51, Aug. 1994.

[32] ITU-T, "Rec. I. 371 – Traffic Control and Congestion in B-ISDN", (Frozen Issue), Geneva, July 1995.

[33] IEEE 802. 1d, "MAC Bridges", May 1990.

[34] ATM Forum, "Traffic Management Specificiation", Version 4, 1995.

[35] IEEE Std 802. 6 – 1990, IEEE Stnadards for Local and Metropolitan Area Networks: "Distributed Queue Dual Bus (DQDB) Subnetwork of a Metropolitan Area Network (MAN)", 1991.

[36] T. M. Chen and S. S. Liu: "*ATM Switching Systems*", Artech House, Boston, 1995.

[37] Special issue, "ATM LAN's: Implementations and Experiences with an Emerging Technology", *IEEE Journal on Selected Areas in Communications*", Vol. 13, No. 4, May 1995.

[38] H. T. Kung and R. Morris: "Credit-Based Flow Control for ATM Networks", *IEEE Network Magazine*, Vol. 9, No. 2, pp. 40-48, March/April 1995.

[39] A. N. Tantawy and M. Zitterbart: "A Scheme for High-Performance LAN Interconnection Across Public MAN's", *IEEE Journal on Selceted Areas in Communications*, Vol. 11, No. 6, Oct. 1993.

[40] F. Bonomi and K. W. Fendick: "The Rate-Based Flow Control Framework for Available Bit Rate ATM Service", *IEEE Network Magazine*, Vol. 9, No. 2, pp. 25-39, March/April 1995.

[41] K. Kvols, S. Manthrope and I. Norros: "Engineering Guidelines for the Design of an Interworking Unit", *Interoperability in Broadband Networks*, Ed. S. Rao, IOS Press, Amsterdam, 1994.

[42] I. S. Venieris, J. -A. Sanchez-P. and E. N. Tsiotsios: "Architecture and Performance of ATM Interworking Units", *Interoperability in Broadband Networks*, Ed. S. Rao, IOS Press, Amsterdam, 1994.

[43] ITU-T, "Rec. I. 413 – B-ISDN User-Network Interface", Geneva, June 1992. BUNI

[44] T. Suzuki: "ATM Adaptation Layer Protocol", *IEEE Communications Magazine*, Vol. 32, No. 4, pp. 80-83, April 1994.

[45] H. L. Truong, W. W. Ellington Jr., J.-Y. Le Boudec, A. X. Meier and J. W. Pace: "LAN Emulation on an ATM Network", *IEEE Communications Magazine*, Vol. 33, No. 5, pp. 70-85, May 1995.

[46] W. Leland, M. Taqqu, W. Willinger and D. Wilson: "On the self-similar nature of Ethernet Traffic (extended version)", *IEEE/ACM Transactions on Networking*, Vol. 2, No. 1, pp. 1-15, Feb. 1994.

[47] V. Paxson and S. Floyd: "Wide Area Traffic: The Failure of Poisson Modeling", *IEEE/ACM Transactions on Networking*, Vol. 3, No. 3, pp. 226-244, June 1995.

Iakovos S. Venieris received the Dipl. Ing. degree from the University of Patras, Patras, Greece in 1988, and the Ph.D. degree from the National Technical University of Athens (NTUA), Athens, Greece, in 1990, all in electrical and computer engineering. During 1991-1992 he was with the National Defense Research Center, Athens, Greece, performing research in the area of telecommunications electronics for military applications. From 1992-1994 he was a research associate in the Telecommunications Laboratory of NTUA. He is currently an Assistant Professor in the Electrical and Computer Engineering Department of NTUA. His research interests are in the fields of B-ISDN, high speed LAN's and MAN's, all optical networks, internetworking, signalling, resource scheduling and allocation for network management, modelling, performance evaluation and queueing theory. He has over forty publications in the above areas. Dr. Venieris has received several national and international awards for academic achievement. He has been exposed to standardization body work and has contributed to ETSI and ITU-T. He leads NTUA participation in several European Union projects. Dr. Venieris is a member of IEEE and the Technical Chamber of Greece.

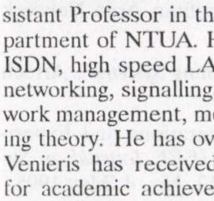

Miltiades E. Anagnostou received the Electrical Engineers Diploma from the National Technical University of Athens (NTUA) in 1981. During the period from 1981 to 1987 he was a teaching assistant at NTUA. In 1987 he received his Ph.D. in the area of computer networks. From 1987 to 1989 he served the Greek army in the Air Force Research and Development Center. From 1989 to 1991 he was a Lecturer, and since 1991 he is an Assistant Professor in the Computer Science Division, Dept. of Electrical and Computer Engineering of the NTUA. He teaches courses on modern telecommunications, formal specification of protocols, stochastic processes, and queueing theory. Since 1981 Dr. Anagnostou has been involved in several research programs both national and international in the areas of ATM based broadband networks. Dr. Anagnostou is author of over 50 scientific papers in the areas of computer networks, protocols, queueing theory, algorithms, mobile telephony, and B-ISDN. He is a member of the Tech. Chamber of Greece and of IEEE.

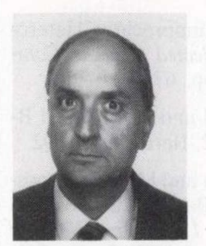

George I. Stassinopoulos received the Degree in Electrical Engineering from the Swiss Federal Institute of Technology (ETH Zuerich) in 1974 and the Ph.D. degree in Automatic Control from the Imperial College, London, Department of Computing and Control in 1977. In 1977 to 1981 he acquired industrial experience in the design and manufacture of micro-processor based industrial controllers. Since 1981 he has been a member of the staff of the National Technical University of Athens (NTUA), Department of Computer Science, where he is currently a professor. His current research interests are in the fields of data communication networks, LANs, MANs, packet circuit and hybrid switching systems, analysis and synthesis of communication networks, routing, flow control and queueing theory. He has over fifty publications in the above areas. He has participated in many national research programs dealing with communication networks as well as in the European Union RACE programme. He is a member of the Technical Chamber of Greece and Chairman of IEEE Section Greece.

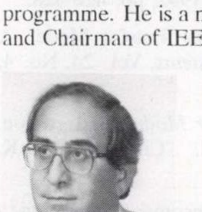

Emannuel N. Protonotarios received the degree in Mechanical and Electrical Engineering (summa cum laude) from the National Technical University of Athens (NTUA), Athens, Greece, in July 1963, and the Ph.D. degree in Electrical Engineering from Columbia University, New York, NY, in 1966. From 1966 to 1968 he worked at Bell Laboratories, Holmdel, NJ, as a member of the Technical Staff in the Digital Transmission Laboratory, doing fundamental work in PCM and DPCM transmission systems. From 1968 to 1973 he was an Assistant Professor and then an Associate Professor of Electrical Engineering at Columbia, where he taught and performed research in digital communication systems. During this period he spent some time as a Visiting Professor of Electrical Engineering at the University of Patras, Patras, Greece. At present he is the Director of the Telecommunications Laboratory of the Electrical and Computer Engineering Department of NTUA. He has been Chairman of the Department of Electrical Engineering, Director of the Computer science Division and Vice Rector for Academic Affairs at NTUA, where he has been a professor since 1973. He has published over 100 scientific papers. Dr. Protonotarios received nine prizes for academic achievement. He serves on many committees for evaluation of research in Greece.

MODIFIED JPEG ALGORITHM FOR HIGHER COMPRESSION RATIOS

D. GY. PÁZMÁNY

TECHNICAL UNIVERSITY OF CLUJ-NAPOCA
STR. BRATIANU 26
3400 CLUJ-NAPOCA, RUMANIA

The paper presents a modification in the standard JEPG algorithm resulting in higher compression ratios with the same subjective quality.

1. INTRODUCTION

The Joint Photographic Expert Group's standard offers an algorithm for compression and decompression of black and white and colour still images. With this technique could be compressed and restored original images with almost imperceptible image degradation at compression ratios to around 20:1.

For achieving this goal the algorithm's baseline system use lossless and lossy compression techniques. Lossless techniques encode input data so that the decoding process can perform an exact reproduction of the original data, but they play a little role in the value of global compression ratio. This is because the reduction of the inherent redundancy in image data can't be proceeded, however, long.

High compression ratios can be achieved by discarding subjective redundancy informations from the original image data, informations that are completely or almost imperceptible for the human viewer. In this manner, lossy compression techniques could have an important role in increasing the compression ratios.

This paper takes into account the possibility of achieving higher compression ratios, by transforming a lossless compression technique from the standard JPEG algorithm in a lossy one by taking in consideration the physiological characteristics of the human visual system and by decreasing the visible artifacts that appear at high compression ratios.

2. THE STRUCTURE OF THE JPEG ALGORITHM

The JPEG algorithm's baseline system includes five essential stages: RGB -> YUV conversion, segmentation and DCT, quantization, zig-zag ordering and RLE, Huffmann coding.

Transforming the image data representation is a lossy procedure that exploits the independence of the luminosity and the chromatic information allowing a higher compression of the second one, due to the characteristics of the human eye. As it is known from the television techniques, the visual system is less sensitive to fine details of chromatic information, than to the same luminance details. For instance, the PAL and the SECAM colour systems are based on that presumed fact that the human eye can't distinguish between the chromatic information on succesive television lines. Many image treating systems and standards are exploiting this possibility to decrease the amount of image data. Starting from the RGB representation with 8 bits for each primary colour component, it is preferable to transform them in a 8:4:4 YUV representation. Such a representation offers a 3:2 compression ratio.

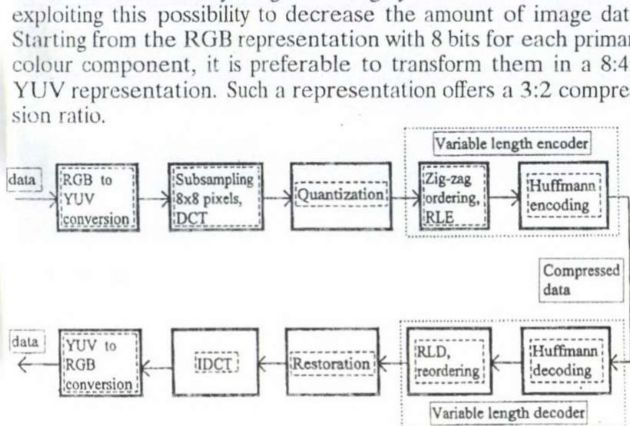

Fig. 1. The JPEG standard algorithm's baseline structure

The discrete cosine transform applied to the 8x8 pixels image blocks decomposes the original piece of image in a sum of 64 basic images in order to reveal the spatial frequencies. The amplitude of each basic image is given by the corresponding DCT coefficient. The transfer of the information from the space domain into the frequency domain is useful in order to discard high frequency components (DCT coefficients), following the low-pass filter characteristic of the human visual system. If the accuracy of the computation is good enough, DCT and IDCT (inverse DCT) form a lossless procedure.

Quantization is another lossy stage in the standard JPEG algorithm. The values of the elements in the quantization matrixes tell us how many low amplitude, high frequency DCT coefficients will be made zero and what degree will the compression achieve. Every DCT coefficient will receive a new value computed according to it's original value. If the quantization step is:

$$qs = c, \qquad [1]$$

where c is the value of the corresponding element from the quantization matrix, then the new value will be n if the DCT coefficient's old value is in the domain:

$$D = [(2n-1) * qs/2; \quad (2n+1) * qs/2]. \qquad [2]$$

The zig-zag ordering followed by run-length encoding cuts those DCT coefficients which values was made zero resulting a smaller size for the data file. The reordering is necessary because these coefficients are grouped in the high frequency corner of the coefficient's matrix. The zig-zag ordering affects only 63 elements from the DCT coefficient's matrix, the DC elements being treated separately. For every DC coefficient only the difference between its value and the value of the DC coefficient from the preceding image segment will be retained. By using this original form, RLE is a lossless procedure.

The statistically Huffmann coding works on the RLE data structure and gives the global compression ratio. It is also a lossless technique.

The reconstruction of the image performs the inverse operations in reversed order.

3. MODIFIED RUN-LENGTH ENCODING

The DCT coefficients, supposing an 8 bits representation for Y, U and V, are represented on 11 bits (-1024 to 1023). Using a "Zero-Pack-Unit" (for instance in CL550) the RLE process gives a variable length code. The code has a fixed length part in form NNNNCCCC, where NNNN signifies the number of zeros before the coded DCT coefficient and CCCC the class of the coefficient's value (the 2 based logarithm plus 1). The variable length part contains the sign bit and the from zero differing low order bits.

NNNN	CCCC	S	Low order bits

NNNN	S	CCC

Fig. 2. Modified run-length code

Accepting that the sensitivity characteristic of the human eye is a logarithmic one, it would be enough to maintain the class of the DCT coefficient's value and cut the variable length part except the sign bit. This could mean a simplified representation of the run-length code.

Moreover, using quantization matrixes with elements greater than 8, the new value of the DCT coefficients will be represented on less then 8 bits (-128 to 127) and so for keeping the class will be enough 3 bits. The fourth bit could be the sign bit.

The experiments denote a very good tolerance of the observer's eyes when a logarithmic scale of amplitudes for the DCT base images is used.

4. ELIMINATING THE ARTIFACTS CAUSED BY THE INCREAZED QUANTIZATION MATRIX ELEMENTS

There are in use some well tested quantization matrixes nowadays. A global characteristic of these matrixes is that they are chosen for the quantization of either the luminosity transform coefficients or the chromatic information carrying transform coefficients, making use of the already mentioned property of the human visual system. Generally speaking, the quantization matrix elements take values between 10 and 120. While the Y quantization matrix's elements values are increasing uniformly from low to high frequencies, the U and V quantization matrixes have very few low values in the low frequency corner and the remaining part of the matrix is filled with elements that have aproximately the same, important values.

Increasing the quantization matrix elements usually means a multiplication of them with the same value. In this case artifacts such as banding, blocking and ringing can appear. By treating the phenomenon as a simple quantization procedure (in fact it's a requantization) all these artifacts can be considered quantization errors.

A well-known method to diminish the quantization error is dithering. It can be presumed that a pseudorandom noise with square probability function would be the best in this case. Because of the difficulty of generating such a noise, a gaussian dither can be added to the reconstructed DCT coefficients before the IDCT procedure. In case of using quantization matrix elements multiplied by a factor of 2, a dither with the amplitude between 1/8 and 1/4 of the value of the corresponding quantization matrix element could make the artifacts nearly invisible.

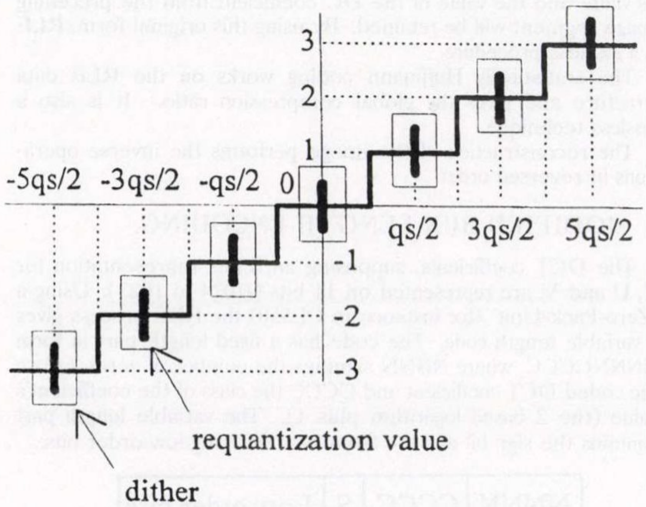

Fig. 3. Requantization with dither

Fig. 4. The original image

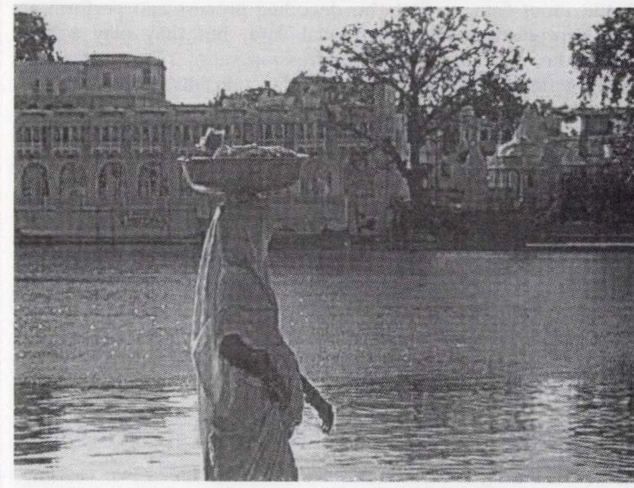

Fig. 5. The restored image with doubled quantization matrix elements

Fig. 6. The restored image after a standard JPEG compression

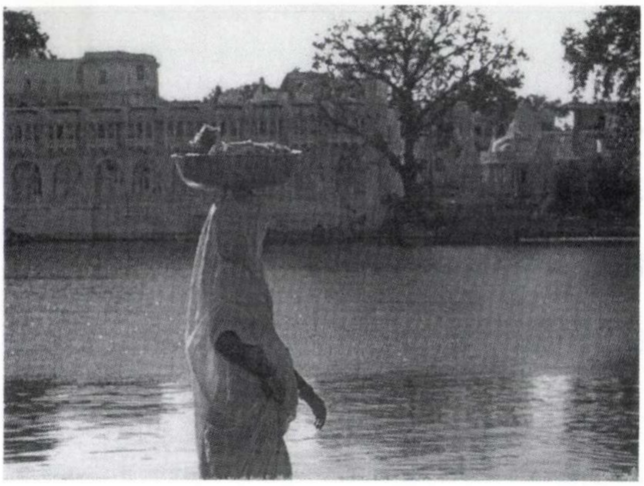

Fig. 7. The restored image with doubled quantization matrix elements after the modified JPEG compression and dithering

5. CONCLUSIONS

By using the mentioned techniques, we could obtain a compression ratio approximately 40:1, with the same subjective quality for the reconstructed image as the quality obtained at the ratio 20:1 when the standard algorithm was used.

An important advantage obtained by using these methods is the simplified and faster algorithm. The modified RLE although changes the initial conditions of the Huffmann coding (instead of 161 possible starting values there will be 255), the global effect is an important reduction of the data's volume.

By modifying the run-length code, this step of the algorithm becomes a lossy technique with regard to the physiological characteristics of the human visual system, allowing us to obtain a higher compression.

Finally, any error that appears due to the lossy steps in the JPEG algorithm can be interpreted as a quantization error and a well-founded dithering can have a good influence on the restored images.

REFERENCES

[1] A. N. Netravali and B. G. Haskell: *"Digital Pictures, Representation and Compression"*, Plenum Press, New York, 1988.

[2] M. Rabbani and P. Jones: *"Digital Image Compression Techniques"*, SPIE Optical Engineering Press, Bellingham, 1991.

[3] G. K. Wallace: "The JPEG picture compression standard", *Comm. ACM.*, Vol. 34, No. 4, pp. 31-44, Apr. 1991.

[4] A. W. Swager: "Image compression lightens storage and transport burdens", *EDN*, July 18, 1991.

[5] M. Leonard: "IC Executes Still-Picture Compression Algorithms", *Electronic Design*, May 23, 1991.

[6] M. Leonard: "Scanning The Options For Image Compression", *Electronic Design*, July 9, 1992.

[7] J. Buck: "Hilfreicher Verlust. Der JPEG-Algorithmus", MC, pp. 94-101, June 1993.

[8] "Grafikkonvertierung unter Windows. Die grose Welt der Grafikformate", *Microsoft System Journal*, Jan./Feb. 1993.

[9] R. A. Quinnell, Technical Editor: "EDN - Special Report: Image Compression", *EDN*, January 21, 1993.

[10] P. Pirsch, N. Demassieux and W. Gehrke: "VLSI Architectures for Video Compression – A Survey", *Proc. IEEE*, Feb. 1995.

Dénes György Pázmány received the Diplom Engineer degree in Electronics and Telecommunications at the Polytechnic Institute, Cluj-Napoca, Romania in 1984. Since 1984 he has worked at the industrial Automation Department of the National Research Institute for Automation (IPA), local office Cluj-Napoca, as development engineer, scientific researcher (1987), senior researcher (1990). Since 1994 he has been with the Communications Department of the Technical University, Cluj-Napoca, as an assistant professor. His research interests are in information theory, digital communications and signal procesing with applications to image coding and transmission.

7TH JOINT EUROPEAN NETWORKING CONFERENCE

May 13 – 16, 1996, Budapest, Hungary

Organized by TERENA, the Trans-European Research and Education Networking Association;

with the **local assitance** of HUNGARNET, the Hungarian Academic and Research Networking Association.

NETWORKING IN THE INFORMATION SOCIETY

Subject areas for the conference:

- User Support and Education
- Policy, Economic and Social Issues
- Network Engineering
- Network Technology
- Application Technology
- Infrastructure developments
- Networking Services

An exhibition will be organized for international and Hungarian companies and institutions to demonstrate their products and services.

Conference proceedings containing full papers will be handed out to the participants.

The traditional pre-conference workshop will be held the week prior to the conference. Travel and tuition support may be available for selected attendees. Additional information from the JENC7 Secretariat at the address below.

Further information

from
JENC7 Secretariat
c/o TERENA Secretariat
Singel 466-468
NL 1017 AW Amsterdam
< jenc7-sec@terena.n1 >
http://www.terena.n1/terena/jenc7/

or
JENC7 Local Organization
c/o MTA SZTAKI
Kende u. 13-17.
H-1111 Budapest
< richter@sztaki.hu >
http://www.iif.hu/jenc/

4TH ICIN'96 INTERNATIONAL CONFERENCE ON INTELLIGENCE IN NETWORKS

November 25 – 28, 1996

at Palais des Congrès, Bordeaux, France

Conference Outline:

Applications and services (Personal Communications, Mobile Communications, Data Services, ISDN, Internet, multimedia, Virtual Private Networks, corporate services, Global Services (GVNS), operator support, screenphone, ADSI, ...).

Architecture (IN evolution, network elements, IN-ISDN-X25-ATM interaction, IN in and supporting mobile telephony, network interworking, distributed processing, open networking, future IN architecture).

Network and Systems Implementations (operators' roll out experiences, IN product implementation, multi-vendor IN configurations, trials, prototypes, network optimization and planning, validation).

Service Specification, Creation and Management (service creation and deployment, management architecture, IN and TMN integration, service interaction, future interworking, service specification using object orientation and formal methods, service creation experience).

Marketing and Regulatory Aspects of IN (customization, ergonomical aspects, promotion of new services, possible new business opportunities, deregulation aspects, operator-service provider partnerships).

Deadlines:

March 15, 1996:	summaries (preferably appr. 1000 words, but not exceeding 2000 words)
June 15, 1996:	acceptance of papers
September 15, 1996:	camera ready papers

Conference Secretariate:

ADERA
ICIN'96
B.P. 196 33608 PESSAC Cedex
Phone: 33 56151151
Fax: 33 56151160

ICOMT '96

INTERNATIONAL CONFERENCE ON MULTIMEDIA TECHNOLOGY AND DIGITAL TELECOMMUNICATIONS SERVICES

October 28–30, 1996, Budapest

The main aim of this conference to bring together people from research, industry, business, government and academia who are interested in problems related to multimedia technology and new telecommunications services.

Conference topics include but not limited to:

- **Signal processing in multimedia systems, standard**
- **Distributed multimedia architectures**
- **Multimedia networking and synchronization**
- **Servers, terminals, storage, data bases**
- **Multimedia applications**
- **Telecommunication services, broadband communications**

Authors are invited to submit 3 copies (original and two copies) or original contributions as full papers or extended summaries on recent applications, developments and research.

Submission of papers or summaries:	**June 30, 1996**
Notification of acceptance:	**August 15, 1996**
Camera-ready papers due:	**September 20, 1996**

Scientific Society for Telecommunication
ICOMT '96 Secretariat
H-1055 Budapest, Kossuth Lajos tér 6-8.
Tel: 36 1 153-1027, Fax: 36 1 153-0451, E-mail: h6084ant@ella.hu